

AD-A128 746

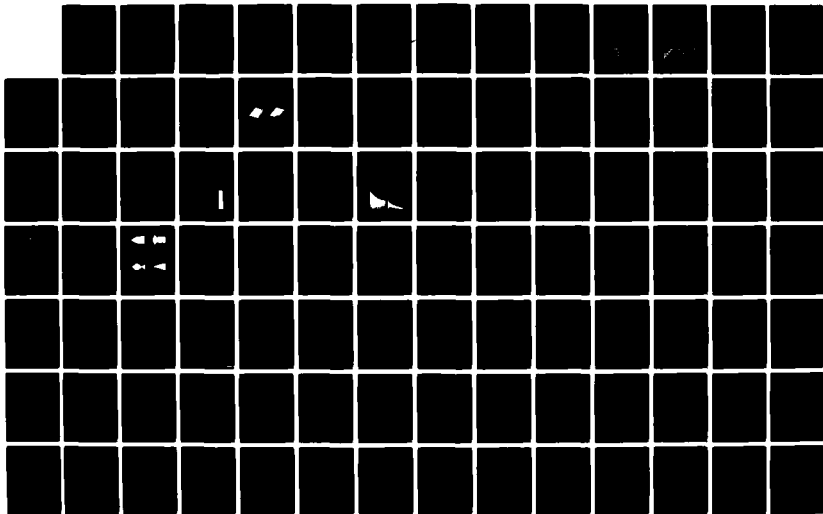
THEORY OF LASER-STIMULATED SURFACE PROCESSES(U)
ROCHESTER UNIV NY DEPT OF CHEMISTRY T F GEORGE ET AL.
MAY 83 UROCHESTER/DC/B3/TR-32 N00014-80-C-0472

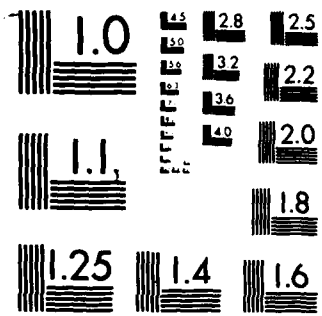
1/2

UNCLASSIFIED

F/G 20/5

NL





MICROCOPY RESOLUTION TEST CHART
NATIONAL BUREAU OF STANDARDS 1963-A

12

OFFICE OF NAVAL RESEARCH
Contract N00014-80-C-0472
Task No. NR 056-749
TECHNICAL REPORT No. 32

AD A 128746

Theory of Laser-Stimulated Surface Processes

by

Thomas F. George, Jui-teng Lin,
A. C. Beri and William C. Murphy

Prepared for Publication

in

Progress in Surface Science

Department of Chemistry
University of Rochester
Rochester, New York 14627

DTIC
JUN 1 1983

May 1983

Reproduction in whole or in part is permitted for any
purpose of the United States Government.

This document has been approved for public release and
sale; its distribution is unlimited.

DTIC FILE COPY

83 05 31 123

Unclassified

SECURITY CLASSIFICATION OF THIS PAGE(When Data Entered)

atom near a metal. In connection with gas-surface interactions, the influence of laser radiation on diffraction patterns and energy transfer in atom-surface scattering is explored. Collisional ionization and ion neutralization in the presence of laser radiation are discussed. The roles of partial pressure and surface coverage in laser-stimulated surface processes are analyzed. Finally, some ideas on surface waves and annealing are presented.

Unclassified

SECURITY CLASSIFICATION OF THIS PAGE(When Data Entered)

THEORY OF LASER-STIMULATED SURFACE PROCESSES

Thomas F. George[†], Jui-teng Lin^{*}, A. C. Beri[†] and William C. Murphy[†]

[†]Department of Chemistry, University of Rochester
Rochester, New York 14627

^{*}Laser Physics Branch, Optical Sciences Division, Naval Research Laboratory
Washington, D.C. 20375

Abstract

Theoretical techniques for describing laser-stimulated surface processes in a vacuum and at a gas-surface interface are presented. For adspecies-surface systems, the laser excitation of vibrational degrees of freedom is considered, and quantum-mechanical and classical models and also an "almost first-principles" treatment of the competition between multiphoton absorption and multiphonon relaxation are discussed. The laser excitation of electronic degrees of freedom is considered with respect to surface states of semiconductors and metals, for the predissociation of diatomic adspecies on metal substrates, for ionization, and for resonance fluorescence of a gaseous atom near a metal. In connection with gas-surface interactions, the influence of laser radiation on diffraction patterns and energy transfer in atom-surface scattering is explored. Collisional ionization and ion neutralization in the presence of laser radiation are discussed. The roles of partial pressure and surface coverage in laser-stimulated surface processes are analyzed. Finally, some ideas on surface waves and annealing are presented.

Contents

1. Introduction
2. Adspecies-Surface Systems
 - A. Vibrational degrees of freedom
 - i. Excitation and relaxation with multiphoton-multiphonon effects
 - ii. Desorption and migration
 - B. Electronic degrees of freedom
 - i. Excitation to surface states and charge transfer
 - ii. Predissociation
 - iii. Ionization - thermionic and photoelectric
 - iv. Resonance fluorescence
3. Gas-Surface Interactions
 - A. Diffraction
 - B. Phonon excitation



Accession For	
ADVIS GRA&I	<input checked="" type="checkbox"/>
ADVIS TAB	<input type="checkbox"/>
ADVIS REPROD	<input type="checkbox"/>
ADVIS DISTRIBUTION	<input type="checkbox"/>
Availability Codes	
Avail and/or	Special
A	

- C. Collisional ionization and neutralization
- D. Partial pressure and surface coverage

4. Surface Waves

5. Annealing

Acknowledgments

References

Abbreviations

AS	Adspecies-Surface
CCGM	Cabrera-Celli-Goodman-Manson
CW	Continuous Wave
FBZ	First Brillouin Zone
FWHM	Full Width at Half Maximum
GLE	Generalized Langevin Equation
HMP	Heisenberg-Markoff Picture
IR	Infrared
IVR	Intramolecular Vibrational Relaxation
LEPS	London-Eyring-Polanyi-Sato
LSSP	Laser-Stimulated Surface Processes
NFE	Nearly-Free Electron
OBE	Optical Bloch Equations
RLV	Reciprocal Lattice Vector
RWA	Rotating-Wave Approximation
SBE	Surface Bloch Equations
SERS	Surface-Enhanced Raman Scattering
SMF	Surface Magnetic Field
SW	Surface Wave
UV	Ultraviolet
1D	One-Dimensional
2D	Two-Dimensional
3D	Three-Dimensional

1. Introduction

While the field of laser-induced chemical and physical processes in the gas phase can now be regarded as well established,¹⁻⁵ the situation with respect to condensed phases, particularly interfaces, is still in its early stages.¹ However, a number of pioneering experiments and theoretical developments have indicated that laser-induced molecular rate processes at a solid surface or at gas-solid or liquid-solid interfaces contain a wealth of new and exciting phenomena. The most visible use of lasers in this regard has come from experiments which suggest new processes in microelectronics.⁶ Lasers have been demonstrated to be efficient in the annealing of semiconductors⁷ and in stimulating deposition and etching on the dimensions of a micrometer.⁸⁻¹⁰ Since the basic mechanisms underlying the observations of the experiments on deposition and etching are associated with molecular dynamics, including energy transfer and reactions, this represents a frontier in

the general area of laser-induced chemistry and physics as well as in micro-electronics.

Perhaps the first type of dynamical process to be seriously considered in a laser-surface experiment was desorption.¹¹⁻¹⁵ While the laser is generally believed to stimulate desorption through heating effects, it is possible that selective, nonthermal mechanisms play an important role in some instances, which will be explored further in this article. Experimental work has also been carried out in connection with laser-stimulated migration, decomposition and chemical reactions.¹⁶⁻²⁰

Theoretical developments of laser-stimulated surface processes (LSSP) have occurred at Rochester and elsewhere.²¹⁻²⁷ In this review article we shall focus on our own theoretical work at Rochester, touching on other work as it might relate to ours. Our work so far has considered dynamical rate processes where the laser plays the role of a stimulator rather than a probe. We shall therefore be ignoring a host of spectroscopic processes which generally give information on the static properties of surface systems. We include in such processes surface-enhanced Raman scattering (SERS), although one should bear in mind that some of the mechanisms responsible for SERS may play a role in LSSP.^{25,28} We should also emphasize that our theoretical analyses always assume the stimulator to be laser radiation, rather than an incoherent source such as electrons or ions. However, much of our formalism would be readily applicable to processes resembling LSSP, such as electron-stimulated desorption.

A review of our work on LSSP was written about three years ago,²⁹ and this present review article will incorporate aspects of that review with our progress made during the past three years. We shall restrict ourselves to surface processes occurring either in a vacuum or at a gas-solid interface. Our presentation is organized as follows: In Sec. 2 we consider adspecies-surface systems, first discussing the excitation of vibrational degrees of freedom by IR laser radiation. We develop both quantum-mechanical and classical models and also an "almost first-principles" treatment to describe the competition and interplay between multiphoton absorption and multiphonon relaxation. We then explore how laser-excited vibrations can lead to desorption and migration. Proceeding to the excitation of electronic degrees of freedom by near-IR, visible or UV laser radiation, we analyze how the promotion of electrons into surface states in semiconductors and metals can enhance the charge distribution at the surface, leading to desorption or other dynamical processes. We then present a semiclassical theory of laser-induced predissociation of a diatomic adspecies on a metal, where we include the effects of the surface magnetic field along with the phonon "continuum". We also look at laser-induced ionization of an adspecies and

competing roles of thermionic and photoelectric effects. Finally, we examine resonance fluorescence of an atom near a metal surface.

In Sec. 3 we turn to gas-surface interactions, considering first the influence of laser radiation on the diffraction patterns of atoms scattering off a surface, and then treating the energy transfer between an atom and a surface as mediated by the laser excitation of a surface phonon. We present models of both collisional ionization and ion neutralization at a surface as influenced by laser radiation, where the latter is an extension of the discussion in Sec. 2 on the laser excitation of electronic surface states. The roles of partial pressure and surface coverage in LSSP are also analyzed. We end the review article with some ideas associated with surface waves and annealing.

2. Adspecies-Surface Systems

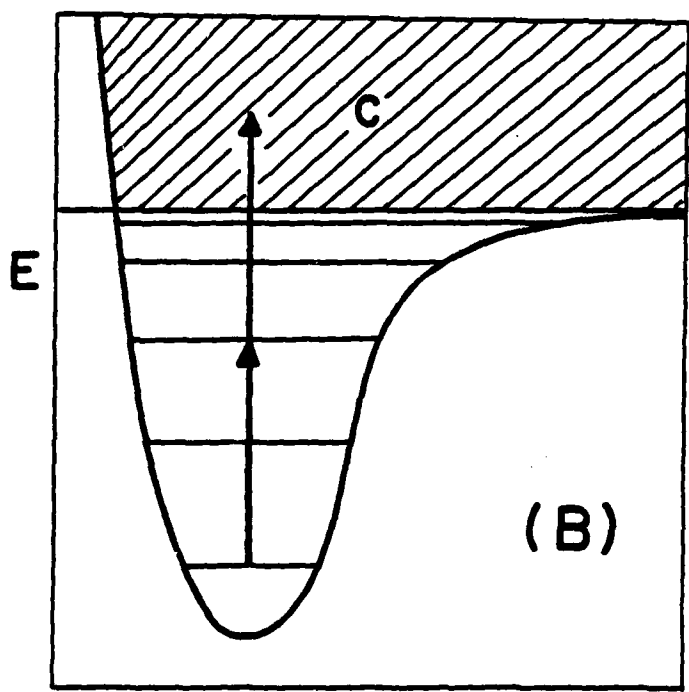
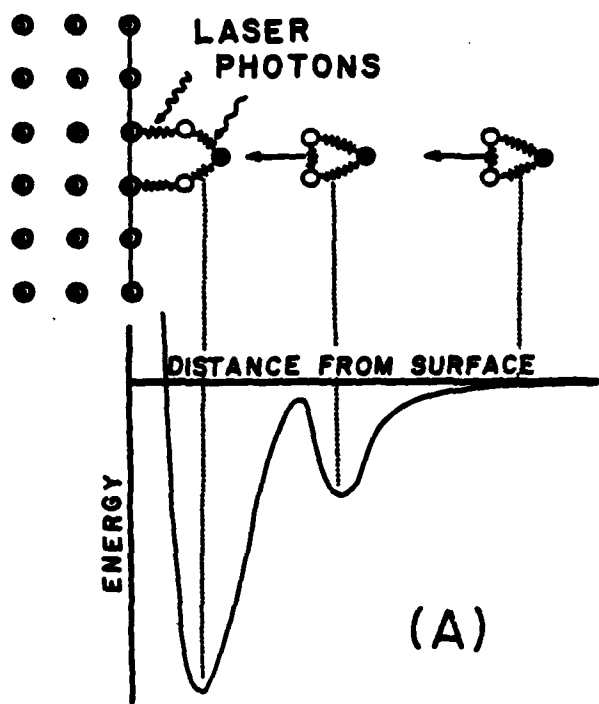
Laser photochemistry has the unique capability of providing us the means to very selectively control chemical reactions. In particular, in conjunction with a solid surface, catalytic reactions can be channeled along specific pathways by utilizing the coherence and monochromaticity of laser radiation to resonantly (or quasiresonantly) excite specific degrees of freedom while leaving others unaffected. In Fig. 1 we present a variety of situations which illustrate selective LSSP, each briefly described in the caption.

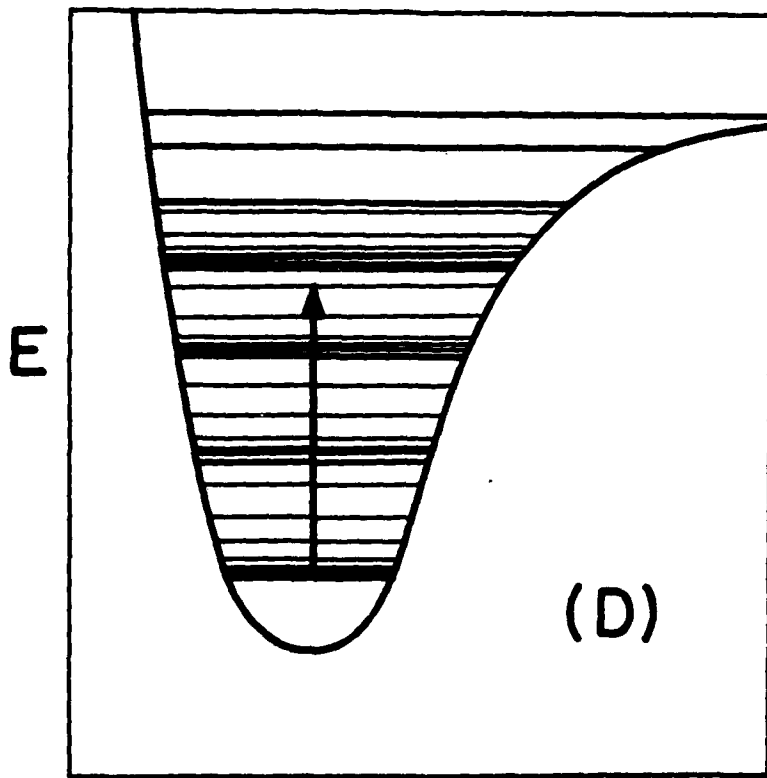
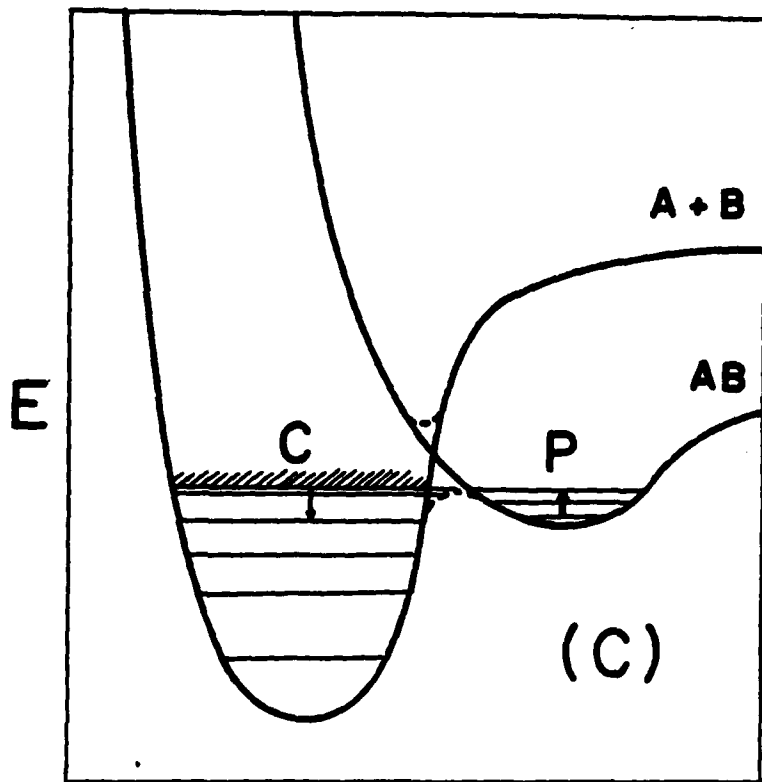
Each figure represents the degree of freedom selectively chosen by the laser frequency which we call the active, A, mode. Other degrees of freedom will be involved in the chemical process either as direct competitors for the laser energy or indirectly as an energy sink, and are referred to as bath, B, modes. The overall energy transfer can be described in terms of the couplings between the laser field, the A mode and the B modes.

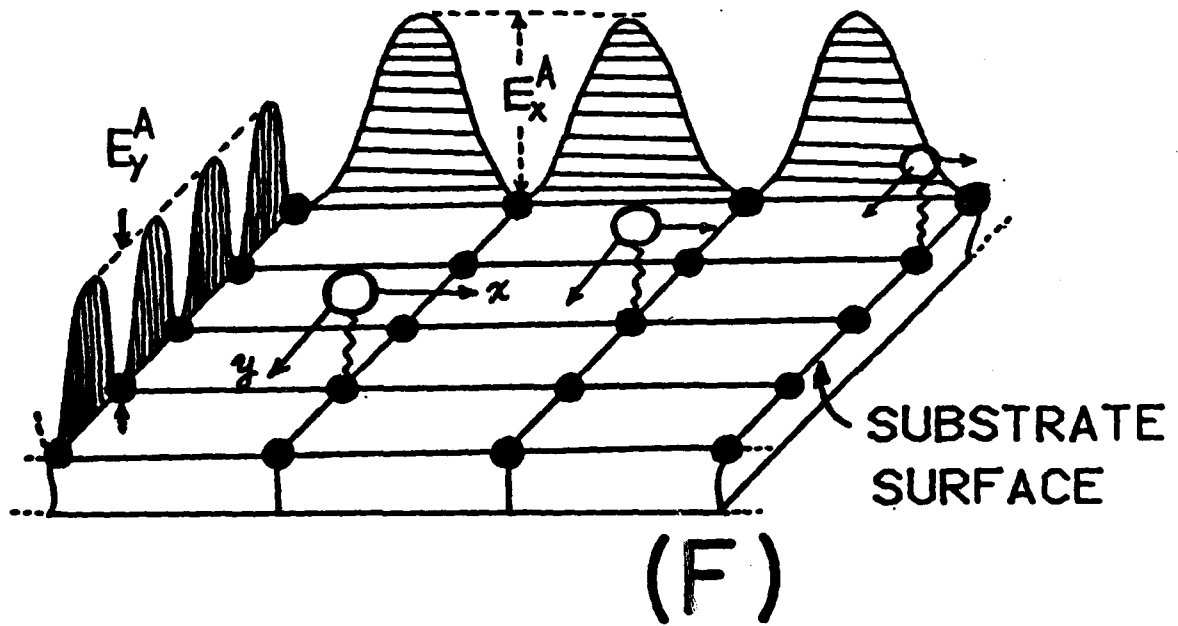
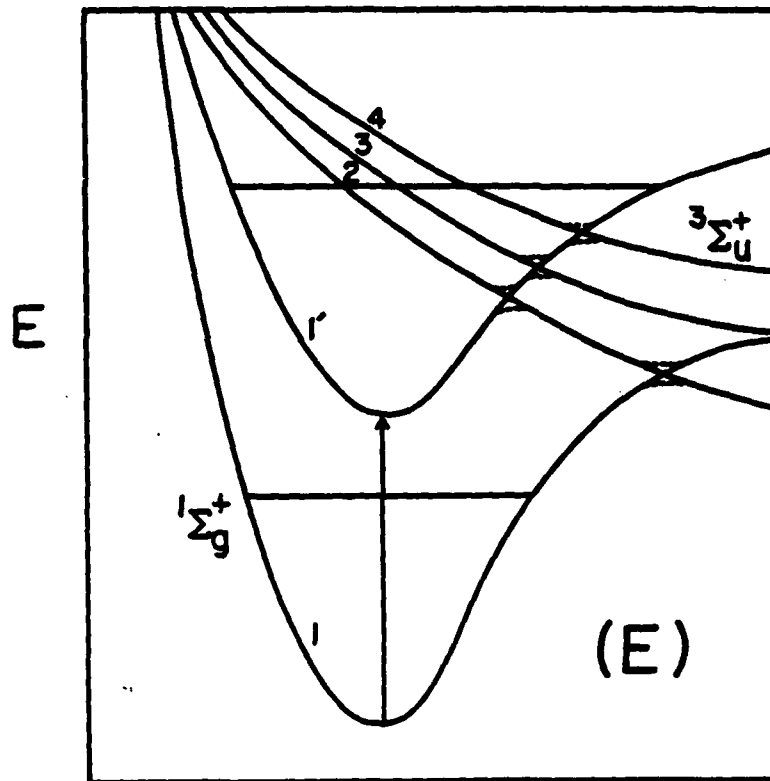
The processes in Fig. 1 can be classified as involving vibrational and/or electronic degrees of freedom. The former include IR LSSP and form the subject of Sec. 2.A, while the latter includes visible or UV LSSP and are treated in Sec. 2.B.

A. Vibrational degrees of freedom

For processes involving vibrational degrees of freedom of the adspecies-surface system one needs laser radiation in the infrared range. The overall dynamics consists of resonant or near-resonant absorption of laser photons by IR-active modes of the system and relaxation to other available channels, leading to excitation, desorption, migration and subsequent chemical reactions. We begin by discussing the general process of excitation accompanied by relaxation from a quantum and classical model point of view, as well as from a first-principles







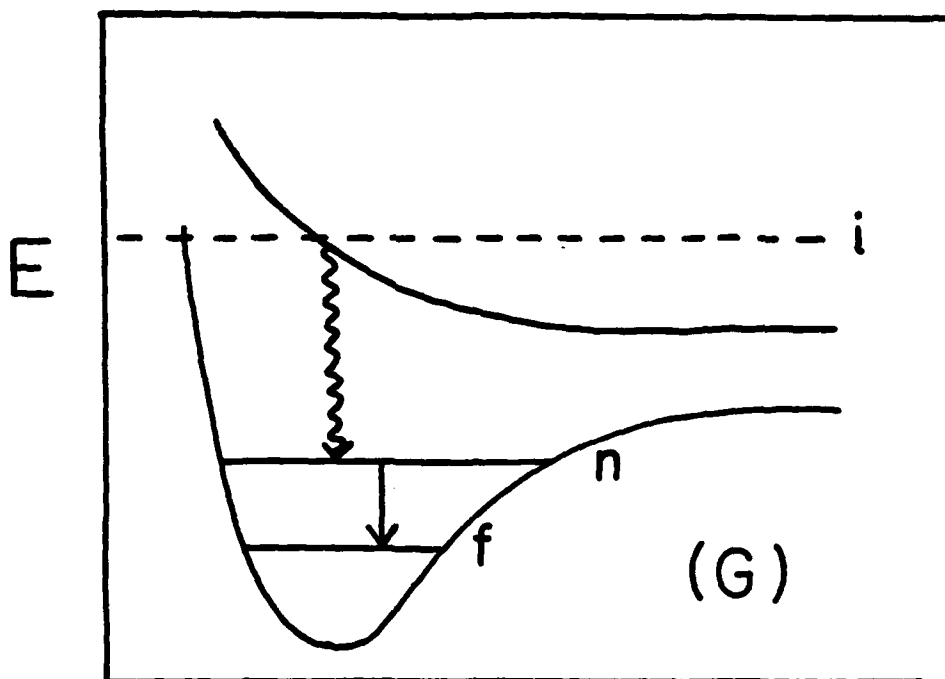


Fig. 1. Schematic representations of a potpourri of laser-stimulated surface processes. The energy E of the adspecies-solid system is shown along the vertical axes as a function of distance from the surface in (A)-(E) & (G) and as a function of position along the surface in (F).

(A) A typical case of molecular adsorption. The shallow well admits a precursor physisorbed state, with the molecule retaining its original identity. The deeper well corresponds to chemisorption with major chemical changes in structure and bonding. Possible selective excitations by laser photons are suggested.

(B) A case of desorption. Resonant adsorption of one laser photon is followed by passage to the continuum C of the adspecies-surface potential by another photon.

(C) Dissociative adsorption. This is a specific case of (A) for a diatomic species AB . Laser pumping of the internal modes of AB or the adsorptive bond in the physisorbed state P promotes penetration of the barrier to the chemisorbed state C , where the system can be stabilized by energy transfer to vibrational or electronic degrees of freedom of the solid. Note that in the chemisorbed state the adspecies looks more like individual atoms than a diatomic molecule.

(D) Rotational excitation of an adspecies. While rotation is often hindered by adsorption, certain situations allow high rotational excitations.

(E) The intense surface magnetic field at a metal surface can break the spin degeneracy of the electronic states of an adspecies. Here the upper triplet state of H_2 is split into three states labeled 2, 3 and 4. The ground singlet and its "photon-dressed" representation are labeled 1 and 1'. The avoided crossings generated by the intersections of 1' with 2, 3 and 4 lead to enhancement of the predissociation rate relative to the laser-induced gas-phase rate.

(F) Selective migration on a surface. For the case of different barriers to migration $E_x^A > E_y^A$ along the surface, migration rates can be selectively enhanced in the x - or y -direction by a judicious choice of radiation frequency.

(G) Laser-induced curve switching leading to adsorption. Transition from an initial unbound state i by stimulated emission to a bound state n is followed by a phonon-stimulated (stabilizing) transition to a lower bound state f .

purely quantum viewpoint in Sec. 2.A.i. The models developed are used in a description of the dynamics of adsorption and migration in Sec. 2.A.ii.

(i) Excitation and relaxation with multiphoton-multiphonon effects.

(a) Quantum-mechanical models. We first study the dynamics of excitation and relaxation of an adspecies-surface system by means of quantum-mechanical models in which microscopic Hamiltonians for both single-phonon relaxation and multiphonon relaxation are investigated within the Heisenberg picture.²⁹⁻³¹ The photon energy population is studied via a master equation. The selective nature of laser-stimulated surface processes is studied numerically for a multilevel system within the Schrödinger picture.^{32,33} Finally, the isotopic separation of adsorbed species is studied via the Heisenberg equation of motion.^{34,35}

Laser excitation with single-phonon relaxation. Consider a heterogeneous system of atoms or molecules adsorbed on a uniform solid surface and subjected to infrared laser radiation. The vibrational degrees of freedom of the adspecies-surface system can be divided into two groups, namely, the pump-mode (resonant infrared-active vibrational mode of the selectively driven adspecies) and the bath-mode (all other modes including adspecies inactive modes and the surface phonon modes). The radiation feeds energy into the pump-mode, and the heat bath provides a relaxation mechanism. The microscopic model Hamiltonian describing this relaxation dynamics can be written in the following second-quantized form.²⁹⁻³¹

$$H = H_A + H_B + H_{AB} + H'(t) , \quad (2.1a)$$

$$H_A = \hbar\omega_A a^\dagger a + \sum_{p=3} \hbar\beta_p (a^\dagger + a)^p , \quad (2.1b)$$

$$H_B = \sum_j \hbar\omega_j b_j^\dagger b_j , \quad (2.1c)$$

$$H_{AB} = \sum_j \hbar(K_j a^\dagger b_j + K_j^* a b_j^\dagger) , \quad (2.1d)$$

$$H'(t) = \hbar v(t) (a^\dagger + a) , \quad (2.1e)$$

$$v(t) = (2\hbar m_A \omega_A)^{-\frac{1}{2}} \mu'(0) E \cos(\theta) \cos(\omega t) . \quad (2.1f)$$

H_A and H_B are the unperturbed Hamiltonian (vibrational energy) of the pump-mode and the bath-mode respectively; H_{AB} is the interaction Hamiltonian coupling the pump-mode and the bath-mode; and $H'(t)$ is the adspecies-field effective interaction Hamiltonian. The operators a^\dagger, a and b_j^\dagger, b_j are the usual harmonic vibrational ladder operators (with fundamental frequencies ω_A and ω_j) of the pump-mode and the bath-mode respectively. β_p is the anharmonicity of the nonlinear quantum

oscillator (pump-mode); $\mu'(0)$ is the derivative of the effective dipole moment of the pump-mode evaluated at the equilibrium point; E is the electric field of the radiation with frequency ω , linearly polarized at an angle θ with respect to the effective dipole moment; and m_A is the reduced mass associated with the active mode. In Eq. (2.1d), K_j represents the coupling between the active mode and the j th bath mode.

The equation of motion for an operator $\hat{O}(t)$ in the Heisenberg picture,

$$\hat{O}(t) = \exp(iHt/\hbar) \hat{O} \exp(-iHt/\hbar), \quad (2.2)$$

where the time-independent operator \hat{O} is defined in the Schrödinger picture, is

$$\frac{d\hat{O}(t)}{dt} = \frac{1}{i\hbar} [\hat{O}(t), H]. \quad (2.3)$$

Employing the operator algebra³⁶

$$[a(t), H] = \partial H / \partial a^\dagger(t), \quad (2.4a)$$

$$[b(t), H] = \partial H / \partial b^\dagger(t), \quad (2.4b)$$

We obtain the following set of coupled equations:

$$\dot{a}(t) = i\omega_{\text{eff}} a(t) - i \sum_j K_j b_j(t) - i v(t), \quad (2.5a)$$

$$\dot{b}_j(t) = -i\omega_j b_j(t) - iK_j^* b_j(t), \quad (2.5b)$$

where ω_{eff} is the effective frequency obtained by the contact transformation,³⁰ including anharmonicity up to fourth order, Eq. (2.1b),

$$\omega_{\text{eff}}(t) = \omega_A - 2\varepsilon^* a^\dagger(t) a(t), \quad (2.6a)$$

$$\varepsilon^* = 30\beta_3^2 / \omega_A - 6\beta_4. \quad (2.6b)$$

We solve for the phonon operators $b_j(t)$ by formally integrating Eq. (2.5b) to obtain

$$b_j(t) = b_j(0) \exp(-i\omega_j t) - iK_j^* \int_0^t dt' a(t') \exp[-i\omega_j(t-t')]. \quad (2.7)$$

Substituting Eq. (2.7) in Eq. (2.5a), we get

$$\dot{a}(t) = -i\omega_{\text{eff}}(t) a(t) + A_1(t) + A_2(t) - i v \cos(\omega t) \quad (2.8a)$$

where

$$A_1(t) = -i \sum_j K_j^* b_j(0) \exp(-i\omega_j t), \quad (2.8b)$$

$$A_2(t) = - \sum_j |K_j|^2 \int_0^t d\tau a(t-\tau) \exp(-i\omega_j \tau), \quad (2.8c)$$

$$V = (2\pi m_A \omega_A)^{-1/2} \mu'(0) E \cos(\theta) . \quad (2.8d)$$

Note that $A_2(t)$ contains the kernel function which will be investigated by the following two techniques.

We first use a Markoff approximation in which the characteristic time of the phonon operators is much smaller than the time over which significant phase and amplitude modulation of $a(t)$ take place.³⁶ Hence we may use the phonon-free solution of Eq. (2.8a), $a(t-\tau) = a(t)\exp(-i\omega_A\tau)$, to evaluate the integral $A_2(t)$, extending the upper limit t to ∞ ,

$$A_2(t) \approx -a(t) \int_0^\infty d\tau \sum_j |K_j|^2 \exp[i(\omega_A - \omega_j)\tau] = -(\gamma_1/2 + i\delta\omega) a(t) , \quad (2.9)$$

where the damping factor, γ_1 , and the frequency shift, $\delta\omega$, are given by

$$\gamma_1 = 2\pi |K(\omega_A)|^2 \rho(\omega_A) , \quad (2.10a)$$

$$\delta\omega = P \left[\sum_j |K_j|^2 / (\omega_A - \omega_j) \right] , \quad (2.10b)$$

where P stands for "principal part." In deriving Eq. (2.10), we assumed a continuum spectrum for the phonon modes with a density of states ρ . Note that both K and ρ are evaluated at the active mode frequency ω_A since

$$\int_0^\infty d\tau \exp[i(\omega_A - \omega_j)\tau] = \pi \delta(\omega_A - \omega_j) + iP[1/(\omega_A - \omega_j)] . \quad (2.11)$$

For an alternate method to decouple the many-mode equations of motion, we can evaluate $A_2(t)$ by assuming a continuum phonon spectrum, without using a Markoff approximation, to obtain

$$A_2(t) = - \int_0^\infty d\tau a(t-\tau) \int_0^\infty d\omega_j |K(\omega_j)|^2 \rho(\omega_j) \exp[i(\omega_A - \omega_j)\tau] . \quad (2.12)$$

This yields the same result as Eq. (9) if we assume that $|K(\omega_j)|^2 \rho(\omega_j) \approx |K(\omega_A)|^2 \rho(\omega_A)$, i.e., a slowly varying function of ω_j peaked at $\omega_j = \omega_A$. This can be easily seen by recalling that

$$\int_0^\infty d\omega_j \exp[i(\omega_A - \omega_j)\tau] = \pi \delta(\tau) + iP(1/\tau) . \quad (2.13)$$

Substituting Eq. (2.9) into Eq. (2.8a) we obtain the decoupled equation

$$\dot{a}(t) = -i(\omega_{\text{eff}} + \delta\omega - i\gamma_1/2)a(t) + A_1(t) - iV \cos(\omega t) . \quad (2.14)$$

The effects of the phonon modes have thus been incorporated into a damping factor, γ_1 , and a frequency shift, $\delta\omega$, of the active mode. There are some other alternate techniques to treat the multimode phonon effects, e.g., the Wigner-Weisskoff single-pole approximation which we shall discuss later when dealing with multiphonon relaxation processes.

We now calculate the ensemble-averaged excitation of the active mode, $\langle n(t) \rangle \equiv \langle \langle a^\dagger(t)a(t) \rangle \rangle$, where $\langle \langle \dots \rangle \rangle$ denotes an ensemble average over the phonon (bath) modes and the active mode coordinate. In order to use the rotating-wave approximation (RWA), i.e., neglecting highly oscillating terms $[\exp(\pm 2i\omega t)]$, we transform the operator into a rotating frame defined by

$$\langle \tilde{a}(t) \rangle = \langle a(t) \rangle \exp(i\omega t) , \quad (2.15)$$

which, combined with a "white noise" assumption for the phonon modes, $\langle A_1(t) \rangle = 0$, transforms Eq. (2.14) into

$$\langle \dot{\tilde{a}}(t) \rangle = - \left[i(\Delta - 2\varepsilon^* \langle a^\dagger(t)a(t) \rangle) + \gamma_1/2 \right] \langle \tilde{a}(t) \rangle - iV/2 , \quad (2.16a)$$

$$\langle \dot{n}(t) \rangle = -(iV/2) \langle \langle \tilde{a}^\dagger(t) - \tilde{a}(t) \rangle \rangle - \gamma_1 (\langle n(t) \rangle - \bar{n}) , \quad (2.16b)$$

where $\Delta = \omega_A + \delta\omega - \omega$ is the detuning and where \bar{n} is the steady-state occupation number given by the Bose function

$$\bar{n} = (\exp[\hbar\omega_A/kT] - 1)^{-1} . \quad (2.16c)$$

The above equations are coupled via the anharmonic term $2\varepsilon^* \langle a^\dagger(t)a(t) \rangle$ and cannot be solved analytically. However, for low excitation, we may ignore the anharmonicity and solve Eq. (2.16) to obtain the average excitation for the harmonic case with $\varepsilon^* = 0$,

$$\langle n(t) \rangle = \left[\frac{(V/2)^2}{\Delta^2 + (\gamma_1/2)^2} \right] \left(1 + e^{-\gamma_1 t} - 2e^{-\gamma_1 t/2} \cos(\Delta t) \right) + \bar{n} \left(1 - e^{-\gamma_1 t} \right) . \quad (2.17)$$

In this case the steady-state excitation is linearly proportional to the laser intensity (or $(V)^2$) and is characterized by a Lorentzian with $\text{FWHM} = \gamma_1$. For $\Delta \neq 0$, the transient excitation oscillates between the two exponential curves $[1 + \exp(-\gamma_1/2)]$ and $[1 - \exp(-\gamma_1/2)]$. For $\gamma_1 = 0$, $\langle n(t) \rangle \approx \sin^2(\Delta t/2)/\Delta^2$ which has the same functional form as that of the excited-state population for a two-level system obtained from perturbation theory. For high excitations, the average excitation requires numerical integration due to the nonlinear coupling $2\varepsilon^* \langle a^\dagger(t)a(t) \rangle$. However, the steady-state excitation $X \equiv \langle n(t) \rangle_{\text{s.s.}}$ is given by a cubic equation

$$X = \frac{AI}{(\Delta - 2\varepsilon^*X)^2 + (\gamma_1/2)^2}, \quad (2.18)$$

where $A = (\hbar/2m_A \omega_A) (V/2\hbar)^2 (8\pi/c)^2$ and I is the laser intensity $I = E^2/(8\pi/c)$ in cgs units.

So far we have discussed only the situation where the damping, or level width of the excitation is governed by the so-called T_1 (energy) relaxation rate, γ_1 . To include the effects of T_2 (phase) relaxation on the excitation, we investigate the ensemble average (over the phonon bath coordinates) equation of motion for the active mode operator, $\hat{O}(t) = a(t)$ or $a^\dagger(t)a(t)$, in the Heisenberg-Markoff picture (HMP),³⁶

$$\begin{aligned} \frac{d\langle \hat{O}(t) \rangle}{dt} = & \left\langle \left[iV(t)/\hbar \left[\frac{\partial \hat{O}(t)}{\partial a^\dagger(t)} - \frac{\partial \hat{O}(t)}{\partial a(t)} \right] - (\gamma_1/2) \left[\frac{\partial \hat{O}(t)}{\partial a(t)} a(t) \right. \right. \right. \\ & \left. \left. \left. + a^\dagger \frac{\partial \hat{O}(t)}{\partial a^\dagger(t)} \right] \right\rangle + \gamma_1 \bar{n} \frac{\partial^2 \hat{O}(t)}{\partial a(t) \partial a^\dagger(t)} + \left\langle \frac{d\hat{O}(t)}{dt} \right\rangle_{T_2}. \end{aligned} \quad (2.19)$$

The last term involving the dephasing (T_2 processes) is characterized by the dephasing-induced broadening factor γ_2 as follows:

$$\left\langle \frac{d\hat{O}}{dt} \right\rangle_{T_2} = \gamma_2 \left\langle \left[a^\dagger(t)a(t), \hat{O}(t) \right] a^\dagger(t)a(t) - a^\dagger(t)a(t) \left[a^\dagger(t)a(t), \hat{O}(t) \right] \right\rangle, \quad (2.20)$$

which is mathematically constructed such that, for $\hat{O}(t) = a(t)$ and $a^\dagger(t)a(t)$,

$$\left\langle \frac{da(t)}{dt} \right\rangle_{T_2} = -\gamma_2 a(t), \quad \left\langle \frac{d[a^\dagger(t)a(t)]}{dt} \right\rangle_{T_2} = 0. \quad (2.21)$$

This assures that the T_2 dephasing changes only the phase of the active mode without changing its vibrational energy. By analogy with the above phenomena, in collisional phenomena the T_1 and T_2 relaxation correspond to inelastic and elastic scattering, respectively, and the overall collisional broadening is then given by $\gamma_1 + \gamma_2$.

By using Eq. (19) and RWA, the ensemble-averaged equations of motion in HMP are found to be

$$\langle \dot{\hat{a}}(t) \rangle = - [i(\Delta - 2\varepsilon^* \langle a^\dagger(t)a(t) \rangle) + (\gamma_1 + \gamma_2)/2] \langle \tilde{a}(t) \rangle - iV/2, \quad (2.22a)$$

$$\langle \dot{\hat{n}}(t) \rangle = (iV/2) \langle \langle \tilde{a}^\dagger(t) - \tilde{a}(t) \rangle \rangle - \gamma_1 (\langle n(t) \rangle - \bar{n}), \quad (2.22b)$$

which are different from Eq. (2.16) by the total broadening $(\gamma_1 + \gamma_2)$ in Eq. (2.22a). For the harmonic case, $\varepsilon^* = 0$, the exact solution for the average excitation is³⁵

$$\langle n(t) \rangle = L(\Delta) \left[\frac{\Gamma_+}{\Gamma_1} \left(1 - e^{-\Gamma_1 t} \right) + \frac{\Gamma_+ \Gamma_- / 2}{\Delta^2 + (\Gamma_- / 2)^2} \left(e^{-\Gamma_1 t} - e^{-\Gamma_+ t / 2} \cos(\Delta t) \right) \right] + \bar{n} (1 - e^{-\Gamma_1 t}) \quad (2.23a)$$

$$L(\Delta) = (v/2\hbar)^2 / [\Delta^2 + (\Gamma_+ / 2)^2], \quad (2.23b)$$

$$\Gamma_{\pm} = \gamma_1 \pm \gamma_2, \quad (2.23c)$$

which reduces to Eq. (2.17) for $\gamma_2=0$ as it should. For fast dephasing $\gamma_2 \gg \gamma_1$, Eq. (2.23) becomes

$$\langle n(t) \rangle = L(\Delta) \left[\frac{\gamma_2}{\gamma_1} \left(1 - e^{-\gamma_1 t} \right) + 2e^{-\gamma_2 t / 2} \cos(\Delta t) \right] + \bar{n} \left(1 - e^{-\gamma_1 t} \right). \quad (2.24)$$

The transient excitation profiles of Eq. (2.23) and (2.24) are shown in Figs. 2(A) and (B), respectively. We see that the excitation profile for the $\gamma_2=0$ case is quite different from the $\gamma_1=0$ case.

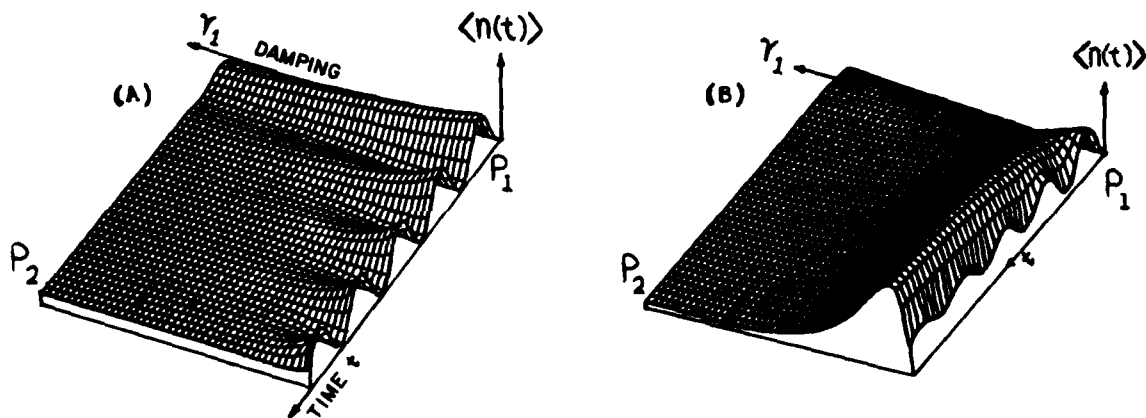


Fig. 2. Excitation profiles in $(\gamma_1, t, \langle n(t) \rangle)$ space for $(\Delta, V) = (5, 5)$ and the ratio $\gamma_2/\gamma_1 =$ (A) 0 and (B) 10. The values of the points P_1 and P_2 are $(0.05, 0, 0)$ and $(4.25, 6, X)$, respectively, where X is the steady-state excitation.

For high excitations with $\epsilon^* \neq 0$, the coupled equations can only be solved numerically, and the results for the transient average excitations are shown in Fig. 3. We note that the saturation of the average excitation is due to the energy relaxation as well as the anharmonicity of the active mode.²⁹ In order to reach high excitation, one requires a higher pumping rate compared to the energy relaxation rate. We shall come back to this feature when we discuss the selectivity of these processes.

The steady-state average excitation, X , for a cold surface (i.e., \bar{n} negligible) can be easily found by setting $\dot{\bar{n}}(t) = \langle \dot{\bar{n}}(t) \rangle = 0$ in Eq. (2.22), which gives the cubic equation

$$X = \frac{(V/2)^2 (\Gamma_+ / \gamma_1)}{(\Delta - 2\epsilon^* X)^2 + (\Gamma_+ / 2)^2} \quad (2.25)$$

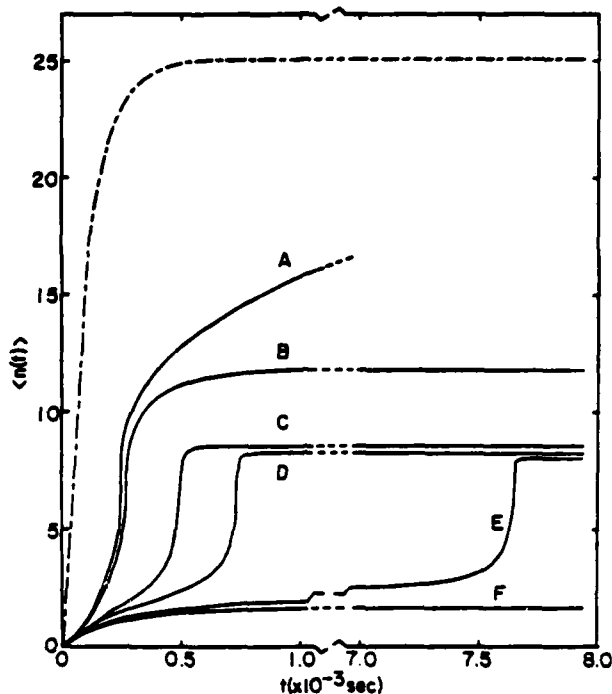


Fig. 3. The average excitation as a function of time with $\gamma_2=10 \text{ cm}^{-1}$ and $I=10 \text{ W/cm}^2$. The solid-dashed curve represents $\epsilon^*=\Delta=0$ and lifetime $\tau=\gamma_1^{-1}=10^{-4}$ sec. The solid curves correspond to $\epsilon^*=2 \text{ cm}^{-1}$ and $\Delta=24.9 \text{ cm}^{-1}$ for (A) lossless system with very long lifetime, (B) $\tau=10^{-3}$ sec, (C) $\tau=1.5 \times 10^{-4}$ sec, (D) $\tau=1.2 \times 10^{-4}$ sec, (E) $\tau=10^{-4}$ sec, and (F) $\tau=9.5 \times 10^{-5}$ sec.

The optimal detuning then occurs at the maximum ($dX/d\Delta = 0$) and is given by $\Delta^* = 2\epsilon^*X^*$ (note - the single asterisk which was already attached to ϵ does not signify an optimal condition as it does for Δ and X). At the other extreme where $dX/d\Delta \rightarrow \infty$, we obtain a quadratic equation for the detuning, whose two roots correspond to a "bistability" in X as a function of Δ . By equating the two roots, we obtain the critical pumping rate $|V^*|^2 = \gamma_1 \Gamma_+^2 / (2\epsilon^*)$, implying that the existence of the bistability is a consequence of the condition $V > V^*$. For a fixed laser intensity, which is proportional to V^2 (or the pumping rate), the bistability criterion may also be stated in terms of the anharmonicity as $\epsilon^* > \epsilon^{**} = (\gamma_1/2) (\Gamma_+/V)$. This "bistability" feature of the steady-state excitation is shown in Fig. 4. It is seen that when the anharmonicity ϵ^* is larger than the critical value, ϵ^{**} , the excitation profile shows the bistable transition from P to Q as the detuning increases, and from R to S as the detuning decreases. We note that the maximum excitation is red-shifted to $\Delta^* > 0$, which is a general property of any nonlinear

oscillator with $\epsilon^* > 0$. A classical analogy of this nonlinear quantum oscillator has been known for some time.³⁷

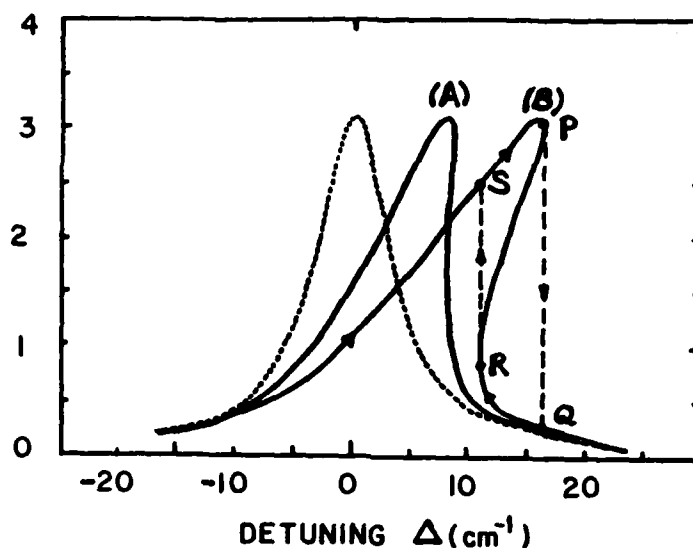


Fig. 4. Anharmonic steady-state excitations showing the bistability feature for $(\gamma_1, \gamma_2, \nu) = (4, 4, 10)$ and (A) at the critical value of $\epsilon^* = \epsilon^{**} = 1.28$ and (B) above the critical value, $\epsilon^* = 2.56 > \epsilon^{**}$. The bistable points are shown by P, Q, R, and S. The harmonic steady-state excitation (dotted curve) is a Lorentzian.³⁴

Laser excitation with multiphonon relaxation. We have derived the single phonon relaxation rate given by Eq. (2.10) which is proportional to the coupling strength and the phonon density of states, both evaluated at the active mode frequency, a result of integration over a delta function, Eq. (2.11). It is easy to see that if $\omega_A > \omega_j$ the single phonon rate is zero and the only contribution to the energy relaxation is that due to multiphonon coupling. This is not strictly true if one includes the finite lifetime of the phonon mode due to intramode anharmonic coupling. Mathematically, this implies that the delta function in Eq. (2.11) should be replaced by a Lorentzian with $\text{FWHM} = 2\gamma_B$, where γ_B is the phonon decay rate. The corrected single-phonon relaxation rate including the effects of finite phonon lifetime is then found to be

$$\begin{aligned} \gamma_1 &= \text{Re} \int_0^\infty d\omega_j |K(\omega_j)|^2 \rho(\omega_j) \int_0^\infty d\tau \exp[-i(\omega_j - \omega_A) - \gamma_B/2] \tau \\ &= \int_0^\infty d\omega_j |K(\omega_j)|^2 \rho(\omega_j) (\gamma_B/2) / [(\omega_j - \omega_A)^2 + (\gamma_B/2)^2], \end{aligned} \quad (2.26)$$

where Re is the real part. The rate, δ_1 , is significant even if $\omega_A - \omega_j$ does not exceed γ_B by an order of magnitude. Therefore the finite-lifetime phonon always

gives a large single-phonon rate even for a system with frequency spectrum $\omega_A > \omega_j$ while the infinite-lifetime model ($\gamma_B = 0$) gives a zero single-phonon rate. However, for an IR active adspecies-surface system the active mode frequency usually is much higher than that of the phonon modes, i.e., we have the situation $(\omega_A - \omega_j) \gg \gamma_B$ (e.g., for CO/Ni $\omega_A \sim 1000 \text{ cm}^{-1}$, $\omega_j \sim 300 \text{ cm}^{-1}$ and $\gamma_B \sim 50 \text{ cm}^{-1}$) which results in a very small single phonon rate. For systems with a big energy gap between the active and phonon modes we shall go beyond the single-phonon relaxation model and study the multiphonon rate.

The microscopic Hamiltonian describing an adspecies surface system with $\omega_A > \omega_j$ subjected to infrared radiation accompanied by multiphonon relaxation may be expressed as³¹

$$H = H_A + H_B + H_{AB} + H'(t), \quad (2.27)$$

which is the same as that of the single phonon except that the interaction Hamiltonian H_{AB} describing multiphonon relaxation is now given by

$$H_{AB} = \sum_{j_1, j_2, \dots, j_N} \left[\kappa G_{j_1, j_2, \dots, j_N} b_{j_1} b_{j_2} \dots b_{j_N} a^\dagger + \kappa G_{j_1, j_2, \dots, j_N}^* b_{j_1}^\dagger b_{j_2}^\dagger \dots b_{j_N}^\dagger a \right] \\ \equiv \sum_V (\kappa G_V B_V a^\dagger + \kappa G_V^* B_V^\dagger a), \quad (2.28)$$

where we define a multiphonon operator

$$B_V \equiv \prod_{j_1, j_2, \dots, j_N} b_{j_1} b_{j_2} \dots b_{j_N}, \quad (2.29)$$

and G_V is the coupling strength. It is seen that H_{AB} reduces to Eq. (2.1d) and describes single phonon relaxation when $N=1$ and $G_V = K_j$. The Heisenberg equations of motion are

$$\dot{a}(t) = i[\omega_{\text{eff}}(t) + \tilde{\omega}(t)]a(t) - i \sum_V G_V B_V(t) - iV \cos(\omega t), \quad (2.30a)$$

$$\dot{B}_V(t) = -i\Omega_V B_V(t) - iN_V G_V^* a(t), \quad (2.30b)$$

where

$$\Omega_V = [B_V(t), H_B] = \sum_{j=j_1}^{j_N} \omega_j, \quad (2.31a)$$

$$N_V = [B_V(t), H_{AB}] = \prod_{j=j_1}^{j_N} (B_V(t) B_V(t) - B_V^\dagger(t) B_V^\dagger(t)), \quad (2.31b)$$

and $\omega(t)$ is a stochastic frequency modulation which accounts for dephasing effects.

By employing the Markoff approximation as used in the single phonon case, Eq. (2.30) is decoupled and results in the ensemble-averaged equations of motion in the HMP^{31,36}

$$\langle \dot{\tilde{a}}(t) \rangle = -[i(\Delta - 2\varepsilon^* \langle a^\dagger(t) a(t) \rangle) + (\gamma_1 + \gamma_2)/2] \langle \tilde{a}(t) \rangle - iV/2, \quad (2.32a)$$

$$\langle \dot{\tilde{n}}(t) \rangle = -iV/2 \langle \langle \tilde{a}^\dagger(t) - \tilde{a}(t) \rangle \rangle - \gamma_1 (\langle n(t) \rangle - \bar{N}), \quad (2.32b)$$

which have the same structure as that for the single phonon case [Eq. (2.22)] except that here the multiphonon equilibrium occupation $\bar{N} = \prod_j \bar{n}_j$ and the relaxation factor is given by,

$$\gamma_1 = 2\pi \sum_V |G_V|^2 \bar{N}_V \delta(\omega_A - \Omega_V), \quad (2.33a)$$

where

$$\bar{N}_V = \prod_{j=j_1}^{j_N} (\bar{n}_j + 1) - \prod_{j=j_1}^{j_N} \bar{n}_j. \quad (2.33b)$$

In deriving Eq. (2.33), the phonon-induced frequency shift is neglected and we assume that the stochastic frequency obeys the simple correlation $\langle \tilde{\omega}(t) \tilde{\omega}(t') \rangle = \gamma_2 \delta(t-t')$. We note that the significant difference between single-phonon and multiphonon processes lies in the nature of the relaxation factor, γ_1 , which is temperature independent [Eq. (2.10)] for single-phonon relaxation but is strongly temperature dependent for multiphonon relaxation. For example, for an Einstein spectrum with $\rho(\omega_j) = \delta(\omega_j - \omega_E)$ and $\Omega_V = p\omega_E$ (p-phonon processes), we find that

$$\gamma_1 = 2\pi \left[|G(\omega_j)|^2 \bar{n}_j^p \right]_{\omega_j = \omega_E} \left(\exp[p\hbar\omega_E/kT] - 1 \right) \quad (2.34)$$

Multiphonon processes with a multimode laser. In the previous discussion classical single-mode laser radiation was considered. We now investigate the effects of a multimode laser with finite bandwidth γ_0 on the average excitation of the active mode, $\langle n(t) \rangle$, by means of a second-quantized laser field such that, instead of Eq. (2.1e), we have

$$H' = \hbar \sum_k V_k (c_k^\dagger + c_k), \quad (2.35)$$

where c_k^\dagger and c_k are the harmonic ladder operators for the k-th mode of the quantized field and V_k is proportional to the electric field due to radiation and may be referred to as the Rabi frequency of the excitation. The Heisenberg equations of motion, previously given by, Eq. (2.30), now become

$$\dot{a}(t) = -i\omega_{\text{eff}}(t)a(t) - i \sum_{\nu} G_{\nu} B_{\nu}(t) - i \sum_{k} V_k c_k(t), \quad (2.36)$$

$$\dot{B}_{\nu}(t) = -i\Omega_{\nu} B_{\nu}(t) - iN_{\nu} G_{\nu}^* a(t), \quad (2.37)$$

$$\dot{c}_k(t) = -i\omega_k c_k(t) - iV_k a(t). \quad (2.38)$$

The above coupled equations can be solved by using the Markoff approximation to include the many-body effects due to the phonon modes and the laser modes as developed in the previous sections. Here we shall present an alternative technique.

Taking the Laplace transform of Eq. (2.35), we get

$$a(s) = U(s)a(s) + \sum_{\nu} V_{\nu}(s)B_{\nu}(s) + \sum_k W_k(s)c_k(s), \quad (2.39)$$

where $a(s)$, $B_{\nu}(s)$ and $c_k(s)$ are the Laplace transforms of $a(t)$, $B_{\nu}(t)$ and $c_k(t)$, respectively, and

$$U(s) = \left[s+i\omega_A + f_1(s) + f_2(s) \right]^{-1}, \quad (2.40)$$

$$V_{\nu}(s) = -iG_{\nu} \left[(s+i\Omega_{\nu}) \left[s+i\omega_A + f_1(s) + f_2(s) \right] \right]^{-1} \quad (2.41)$$

$$W_k(s) = -iV_k \left[(s+i\omega_k) \left[s+i\omega_A + f_1(s) + f_2(s) \right] \right]^{-1}, \quad (2.42)$$

$$f_1(s) = \sum_{\nu} |G_{\nu}|^2 N_{\nu} / (s+i\Omega_{\nu}), \quad (2.43a)$$

$$f_2(s) = \sum_k |V_k|^2 / (s+i\omega_k). \quad (2.43b)$$

Employing the Wigner-Weisskopf single-pole approximation, i.e., $s \approx 0$ in Eq. (2.39), we obtain the inverse Laplace transforms of Eqs. (2.40)-(2.42) leading to

$$a(t) = U(t)a(0) + \sum_{\nu} V_{\nu}(t)B_{\nu}(0) + \sum_k W_k(t)c_k(0), \quad (2.44)$$

which readily gives us the average excitation

$$\begin{aligned} \langle n(t) \rangle &= \langle \langle a^{\dagger}(t)a(t) \rangle \rangle \\ &= |U(t)|^2 \bar{n}(0) + \sum_{\nu} |V_{\nu}(t)|^2 \langle \langle B_{\nu}^{\dagger}(0)B_{\nu}(0) \rangle \rangle + \sum_k |W_k(t)|^2 \langle \langle c_k^{\dagger}(0)c_k(0) \rangle \rangle \\ &= \sum_{\nu} \left[\frac{|G_{\nu}|^2}{\Delta_{\nu}^2 + (\Gamma/2)^2} \right] \left[1 + e^{-\Gamma t} - 2e^{-\Gamma t/2} \cos(\Delta_{\nu} t) \right] \bar{n}_{\nu}(0) \end{aligned}$$

$$+ \sum \left[\frac{|V_k|^2}{\Delta_k^2 + (\Gamma/2)^2} \right] \left[1 + e^{-\Gamma t} - 2e^{-\Gamma t/2} \cos(\Delta_k t) \right] \bar{n}_k(0), \quad (2.45)$$

where $\bar{n}(0)$, $\bar{n}_j(0)$ and $\bar{n}_k(0)$ are the initial occupation numbers of the active, phonon and photon modes, respectively, defined by a Bose function with the same temperature but at a different frequency. The detunings are defined by $\Delta_V = \omega_A - \Omega_V$ and $\Delta_k = \omega_A - \omega_k$, where Ω_V is the multiphonon frequency and ω_k is the k-th mode laser frequency. Finally $\Gamma = \gamma_1 + \gamma_0$ is the total damping factor describing the effects of the parallel nonradiative (phonon) and radiative (photon) relaxation of the quantum oscillator into two independent, noninteracting multimode baths. We note that the multiphonon rate γ_1 has a temperature dependence given by Eq. (2.33) or (2.34), while γ_2 is independent of temperature since we consider dipole transitions of the active mode, i.e., the interaction Hamiltonian H' , Eq. (2.35), contains only linear coupling terms in the resonance excitation with frequency $\omega_k \approx \omega_A$. For an Einstein spectrum, $\gamma_1 \approx 2\pi |G_E|^2 \rho_E \bar{N}_E$ and $\gamma_0 \approx 2\pi |V_F|^2 \rho_F \bar{n}_F$, and the average excitation at resonance, $\Delta_V = \Delta_k = 0$, becomes a simple exponential decaying function

$$\langle n(t) \rangle = \left(\frac{2}{\pi \Gamma^2} \right) \left(|G_E|^2 \rho_E \bar{N}_E + |V_F|^2 \rho_F \bar{n}_F \right) \left(1 - e^{-\Gamma t/2} \right)^2, \quad (2.46)$$

which is characterized by the incoherent phonon field and the coherent laser field with initial occupation $\rho_E \bar{N}_E$ and $\rho_F \bar{n}_F$, respectively.

Energy feedback effects on the laser excitation. The above discussion assumed no direct phonon excitation via laser radiation and, that during the excitation of the active mode, the phonon modes are assumed to be still cold enough that there is no significant energy feedback from the laser-heated substrate. For the case of strong phonon coupling, i.e., a short lifetime for the active mode, the laser photon energy absorbed by the active mode may be rapidly transferred to the phonon modes and these thermal phonons may provide significant feedback energy to thermally perturb the active mode.³⁸ A rigorous calculation to include energy feedback effects due to the heated substrate involves the numerical solution of a non-equilibrium system in which, instead of assuming a constant equilibrium occupation number of the phonon modes, $\bar{n}_j(t) \approx n_j(0)$, one studies the transient occupation $\bar{n}_j(t)$ by solving the heat diffusion equation³⁵

$$\frac{\partial T}{\partial t} = \nabla \cdot (D \nabla T) + \frac{\theta}{C_V} \gamma_1(t). \quad (2.47)$$

T is the laser-heated temperature of the system with diffusivity D and heat capacity C_V , and heat (excitation of the active mode) diffuses according to the gradient, ∇ , in the direction of energy flow. θ is a coverage factor obtained

from the knowledge of the number of active modes and the total absorption cross section. The above equation is highly nonlinear because of the complicated temperature dependence of the relaxation rate, $\gamma_1(t)$, which is now also time dependent via the transient phonon occupation $\bar{n}_j(t)$.

To demonstrate the feedback effects of the thermal phonons on the excitation of the active mode, we analyze a simplified situation based on the microscopic coupled Heisenberg equations rather than attempting a numerical solution of the heat diffusion equation, which is a macroscopic description. We investigate the multiphonon system where Eqs. (2.36)-(2.38) are iteratively solved to second order in the active mode operator, $a(t)$. The average excitation of the active mode including the feedback energy from the thermal phonons is found to be

$$\langle n(t) \rangle = \langle n(t) \rangle^{(1)} + \langle n(t) \rangle^{(2)}, \quad (2.48a)$$

where the first-order excitation $\langle n(t) \rangle^{(1)}$ is given by Eq. (2.39) and the second-order excitation $\langle n(t) \rangle^{(2)}$ at resonance, $\Delta_v = \Delta_k = 0$, is given by

$$\langle n(t) \rangle^{(2)} = \sum_v \left[G_{vj}^3 \bar{n}_j (\gamma_1/2)^2 \right]^2 \left[t^2 - \frac{4t}{\gamma_1} \left(1 - e^{-\gamma_1 t} \right) + \left(\frac{1 - e^{-\gamma_1 t/2}}{\gamma_1/2} \right)^2 \right], \quad (2.48b)$$

which is proportional to the time-dependent quantity $|G_v|^6 (\bar{n}_j t)^2$ and provides the feedback energy.

Master equation and energy population. The master equation describing the photon energy population in the energy (n) space can be written as²⁹

$$\frac{dP_n}{dt} = -(I\sigma_n/\hbar\omega) [P_n - (g_n/g_{n+1})P_{n+1}] + (I\sigma_{n-1}/\hbar\omega) [P_{n-1} - (g_{n-1}/g_n)P_n]. \quad (2.49)$$

P_n is the population (adspecies/cm²) of the level of energy $n\hbar\omega$ (i.e., absorbing n laser quanta, and g_n is the degeneracy of the n -th level, related to the number of vibrational modes S participating in the processes by

$$g_n = g_0 (n+1)^{S-1}. \quad (2.50)$$

σ_n is the quantal absorption cross section of the adspecies (as a whole) for a transition from energy level n to $n+1$. By investigating the structure of the absorption cross section given by Eq. (2.49), we may in general express the cross section in the form

$$\sigma_n = (n+1)^\alpha \sigma^*, \quad (2.51)$$

where σ^* and α are correlated parameters depending on the relative magnitudes of the anharmonicity and the bandwidth. For example, by Eq. (2.51): $\alpha=1$ and $\sigma^* = B\Gamma_0/[\Delta^2 + \Gamma_0^2]$, for $\epsilon^*=0$ (harmonic oscillator) and $\bar{\Gamma}_n = \Gamma_0$ (constant bandwidth); $\alpha=-1$ and $\sigma^* = B\Gamma_0/(2\epsilon^*)^2$, for anharmonic oscillator, $\bar{\Gamma}_n = \Gamma_0 < 2\epsilon^*(n+1/2)$ and $\Delta = -\epsilon^*$;

$\alpha=0$ and $\sigma^*=B/\Gamma_0$ for $\varepsilon^*=\Delta=0$ and $\bar{\Gamma}_n=(n+1)\Gamma_0$; B depends on the dipole derivative.²⁹

The exact solution of the quantal master equation for general forms of σ_n and g_n is not available. However, we shall discuss two limiting cases which are physically interesting and can be analytically solved.

(1) $\alpha=S=1$ (single-mode harmonic oscillator). The master equation, Eq. (2.49), for this case becomes

$$\frac{dP_n}{dt} = - (I\sigma^*/\hbar\omega) [(n+1)P_{n+1} + nP_{n-1} - (2n+1)P_n] . \quad (2.52)$$

By using the initial condition

$$P_n(t=0) = N_0 \delta(n) , \quad (2.53)$$

and the normalization

$$\sum_{n=0}^{\infty} P_n = N_0 , \quad (2.54)$$

where N_0 is the total number of adspecies/cm², the solution of Eq. (2.52) gives the population function

$$P_n(t) = N_0 W^n(t) / [1+W(t)]^{n+1} , \quad (2.55a)$$

$$W(t) = \sigma^* \phi / \hbar\omega , \quad (2.55b)$$

$$\phi = \int_0^t dt I = \text{laser fluence (J/cm}^2\text{)} . \quad (2.55c)$$

The corresponding average excitation (quanta/adspecies) is

$$\langle n(t) \rangle = \frac{1}{N_0} \sum n P_n = W \propto \phi . \quad (2.56)$$

(2) $\alpha=0$ (constant cross section), $S=1$. For this case the master equation, Eq. (2.49), becomes

$$\frac{dP_n}{dn} = - (I\sigma^*/\hbar\omega) [2P_n - P_{n+1} - P_{n-1}] . \quad (2.57)$$

With the same initial condition Eq. (2.53) and by using the recurrence relation of the modified Bessel function, we obtain the population function

$$P_n(t) = NN_0 \exp(-2W) I_n(2W) , \quad (2.58)$$

where N is the normalization constant given by Eq. (2.54), I_n is the modified Bessel function, and W is again given by Eq. (2.55).

The corresponding average excitation for this population is

$$\langle n(t) \rangle = 2(W/\pi)^{1/2} \propto \phi^{1/2} . \quad (2.59)$$

We note that the average excitation is linearly proportional to the laser fluence,

$\langle n(t) \rangle \propto \phi$, in case (1), while $\langle n(t) \rangle \propto \phi^{1/2}$ in case (2). For the general expression of $\sigma_n = (n+1)^\alpha \sigma^*$, we shall find a general form for the average excitation given by $\langle n(t) \rangle \propto \phi^{1/(2-\alpha)}$ by using the diffusion approximation as follows. As mentioned previously, the exact solutions of the quantal master equation are not available for the general forms of σ_n and g_n . We shall now assume that the population P_n , the degeneracy g_n and the cross section σ_n are smooth functions in the n -space. The quantal master equation, under this quasicontinuum assumption, is then converted into the classical diffusion equation

$$\frac{\partial P_n}{\partial t} = \frac{1}{\hbar\omega} \frac{\partial}{\partial n} [\sigma_n g_n \frac{\partial}{\partial n} (P_n/g_n)] . \quad (2.60)$$

Substituting Eqs. (2.50) and (2.51) into Eq. (2.60), a particular solution of Eq. (2.60) consistent with the initial condition, Eq. (2.53) is

$$P_n(t) = NN_0 g_n \exp[n^\beta / (\beta^2 W)] , \quad (2.61a)$$

$$N = (\beta/g_0) (\beta^2 W)^{-S/\beta} / \Gamma(S/\beta) , \quad (2.61b)$$

$$\beta = 2 - \alpha , \quad (2.61c)$$

where W is again given by Eq. (2.55b) and N is the normalization factor. The average excitation (quanta/adspecies) for this classical population function can then be calculated as

$$\langle n(t) \rangle = N_0^{-1} \int_0^\infty dn P_n = (\beta^2 W)^{1/\beta} \Gamma[(S-1)/\beta] \Gamma(S/\beta) , \quad (2.62)$$

which is proportional to $\sigma^{1/\beta}$ (since $W \propto \phi$) and consistent with the quantal results Eqs. (2.56) and (2.59), for $\beta = 1$ ($\alpha=1$) and $\beta = 2$ ($\alpha=0$). It is worth noting that for $\alpha = -1$ (anharmonic oscillator) $\langle n(t) \rangle \propto \phi^{1/3}$ in this classical diffusion model, whereas the steady-state excitation $\langle n(t) \rangle_{s.s.} \propto I^{1/3}$ in the quantal Heisenberg-Markoff model [Eq. (2.18)]. Combining Eqs. (2.50) and (2.51), we may express the population function in terms of the average excitation

$$P_n = \frac{N_0 \beta}{\Gamma(S)} \left(\frac{F(S)}{\langle n(t) \rangle} \right)^S n^{S-1} \exp[-(\frac{nF(S)}{\langle n(t) \rangle})^\beta] , \quad (2.63a)$$

$$F(S) = \Gamma[(S+1)/\beta] \Gamma(S/\beta) . \quad (2.63b)$$

For a comparison with the above classical diffusion model, we now consider a Boltzmann thermal distribution $P_n^*(t)$ which is characterized by the effective temperature T_{eff} and the quantal degeneracy g_n^* [g_n in Eq. (2.50) is a classical degeneracy] as follows:

$$P_n^*(t) = NN_0 g_n^* \exp[-n\hbar\omega/kT_{\text{eff}}] , \quad (2.64)$$

where

$$N = \left[\sum_{n=0}^{\infty} P_n^*/N \right]^{-1} = [1 - \exp(\hbar\omega/kT_{\text{eff}})]^S, \quad (2.65a)$$

$$g_N^* = (n+S-1)!/[n!(S-1)!], \quad (2.65b)$$

and the effective temperature T_{eff} is defined as the average excitation energy per vibrational mode and is governed by energy conservation as

$$\hbar\omega\bar{n} = \hbar\omega\langle n(t) \rangle/S, \quad (2.66a)$$

$$\bar{n} = [\exp(\hbar\omega/kT_{\text{eff}}) - 1]^{-1}. \quad (2.66b)$$

For a multiphoton process ($\langle n(t) \rangle \gg 1$), we obtain the high effective temperature limit ($kT_{\text{eff}} \gg \hbar\omega$), and for $n \gg S$, Eqs. (2.65) and (2.66) reduce to

$$\bar{n} \approx kT_{\text{eff}}/\hbar\omega, \quad kT_{\text{eff}} = \hbar\omega\langle n(t) \rangle/S, \quad (2.67a)$$

$$N \approx (kT_{\text{eff}}/\hbar\omega)^S, \quad (2.67b)$$

$$g_n^* \approx n^{S-1}/(S-1)! = g_n. \quad (2.67c)$$

The population function reduces to

$$P_n^*(t) = \left[\frac{N_0 n^{S-1}}{(S-1)! (\langle n(t) \rangle/S)^S} \right] \exp\left(-\frac{nS}{\langle n(t) \rangle}\right), \quad (2.68)$$

which is identical to the result of the classical diffusion equation, Eq. (2.63a) for the case $\alpha = 1$ (harmonic oscillator).

The distribution function given by Eq. (2.68) is shown in Fig. 5 with a Poisson function which is obtained from a Schrödinger equation as follows. Denoting the time-dependent wave function by

$$|\psi(t)\rangle = \sum_{n=0}^{\infty} C_n(t) \exp(-iE_n t/\hbar) |M\rangle, \quad (2.69)$$

the probability amplitudes $C_n(t)$ satisfy the RWA Schrödinger equation

$$i\hbar \frac{dC_n(t)}{dt} = v_{n,n-1}(t)C_{n-1}(t) + v_{n,n+1}(t)C_{n+1}(t), \quad (2.70)$$

where $v_{n,n-1}(t)$ and $v_{n,n+1}(t)$ are the matrix elements of the interaction Hamiltonian $H(t)$, Eq. (2.1e), given by

$$v_{n,n-1}(t) = \langle n | V \cos(\omega t) (a^\dagger + a) | n-1 \rangle \exp(i\omega_{n,n-1} t) = \sqrt{n} V \cos(\omega t) \exp(i\omega_{n,n-1} t), \quad (2.71)$$

$$v_{n,n+1}(t) = \sqrt{n+1} V \cos(\omega t) \exp(i\omega_{n,n+1} t), \quad (2.72)$$

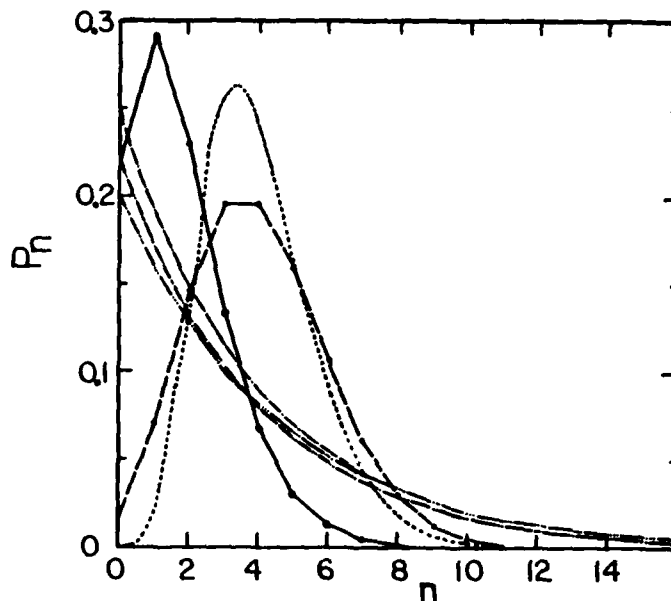


Fig. 5. The distribution functions of four-photon excitations ($\langle n(t) \rangle = 4$), for Poisson population (---), diffusion model population with $S=1$ (-.-) and $S=6$ (.....), Boltzmann population with $S=1$ (-.-.-) and $S=6$ (—), and quantal population with $S = \alpha = 1$ (-.-.-).²⁹

$$\omega_{n,n-1} = (E_n - E_{n-1})/\hbar, \quad (2.73)$$

$$E_n = \hbar(\omega_A - \epsilon^* n - i\gamma_1/2)n, \quad (2.74)$$

and V is proportional to the Rabi frequency given in Eq. (2.1f).

The analytic solution of Eq. (2.70) with the initial condition $|\Psi(0)\rangle = |0\rangle$, (i.e., for cold surface, the adspecies is initially in the ground state) for the harmonic case ($\epsilon^* = 0$) can be shown to be

$$C_n(t) = [(-iW)^n/n!]^{1/2} \exp(-W/2), \quad (2.75)$$

where W is the energy absorbed by the active-mode given by

$$W = \frac{AI}{\Delta^2 + (\gamma_1/2)^2} [1 + e^{-\gamma_1 t} - 2e^{-\gamma_1 t/2} \cos(\Delta t)]. \quad (2.76)$$

namely, a Lorentzian form. The probability of finding the active mode in the level $|n\rangle$ is given by a Poisson distribution³⁰

$$P_n(t) = |C_n(t)|^2 = (W^n/n!) \exp(-W). \quad (2.77)$$

The average excitation (for $\epsilon^* = 0$) is then given by

$$\langle n(t) \rangle_0 = \sum_{n=0}^{\infty} n P_n = W, \quad (2.78)$$

which is identical to the energy absorbed by the active mode for each adspecies W and is equal to the average number of photons absorbed per adspecies.

Selective versus nonselective excitation. From the steady-state excitation of the active mode [Eq. (2.25)], we see that in order to achieve a higher excitation the laser field detuning should be red-shifted to the optimal value, $\Delta=2\varepsilon^*X$, which is due to the nonlinearity of the cubic equation. We also notice that the active-mode excitation is characterized by the pumping rate, V , the energy relaxation rate, γ_1 , and the phase relaxation rate, γ_2 . At optimal detuning, the steady-state excitation [Eq. (2.25)] reduces to the simple expression

$$X = \frac{R}{\gamma_1} + \bar{n} \quad (2.79a)$$

$$R = \frac{|V|^2}{\gamma_1 + \gamma_2} \quad (2.79b)$$

From the above expression we readily see that the excitation is governed by the ratio between the pumping rate and the overall relaxation rate, R , for a fixed surface temperature which defines the occupation number at thermal equilibrium, \bar{n} . For a large ratio, R , we shall expect a high active-mode excitation which means a highly selective excitation process. For a small ratio, which is the strong phonon coupling case with the energy relaxation rate, γ_1 , characterized by a single phonon or a few phonons, nonselective thermal heating of the system is expected.

To investigate the above selective and nonselective features of laser-stimulated processes more rigorously, we study a multilevel system with the vibrational frequency spectrum shown in Fig. 6 and the energy level diagrams shown in Fig. 7. The total Hamiltonian of the multilevel system (N levels in the A mode, M levels in each B mode and L levels in each C mode) can be written as follows:³³

$$H = H_0 + H_{AB} + H_{BC} + H_{AF} \quad (2.80)$$

$$H_0 = S_N \sum_i \hbar \omega_{a_i} a_i^\dagger a_i + S_M \sum_j \hbar \omega_{b_j} b_j^\dagger b_j + S_L \sum_k \hbar \omega_{c_k} c_k^\dagger c_k \quad (2.81a)$$

$$H_{AB} = S_N S_M \sum_j \hbar g_{ij} a_i b_j^\dagger + S_N S_M \sum_j \hbar g_{ij} a_i^\dagger b_j + hc \quad (2.81b)$$

$$H_{BC} = S_M S_L \sum_j \sum_k \hbar \bar{K}_{jk} b_j c_k^\dagger + S_M S_L \sum_j \sum_k \hbar K_{jk} b_j^\dagger c_k + hc \quad (2.81c)$$

$$H_{AF}(t) = \sum_{i \neq f} \hbar v_{if}(t) a_i^\dagger a_f + hc \quad (2.81d)$$

S 's denote the summations

$$S_N = \sum_{j=1}^N, \quad S_M = \sum_{j_1, j_2, \dots, j_m}^M, \quad S_L = \sum_{k_1, k_2, \dots, k_n}^L, \quad S_j = \sum_{j=j_1}^{j_m}, \quad S_k = \sum_{k=k_1}^{k_{2-m-1}} \quad (2.82)$$

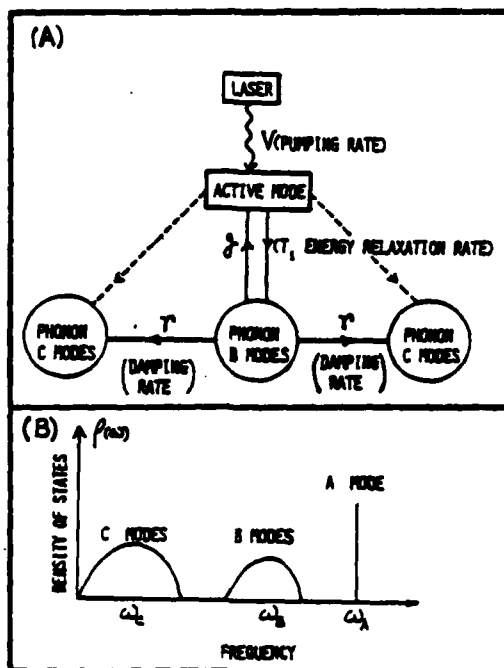


Fig. 6. (A) Schematic diagram of energy transfer processes among the laser photon, the active mode (A) and the phonon modes (B and C); (B) Schematic diagram of the density of states of the system.

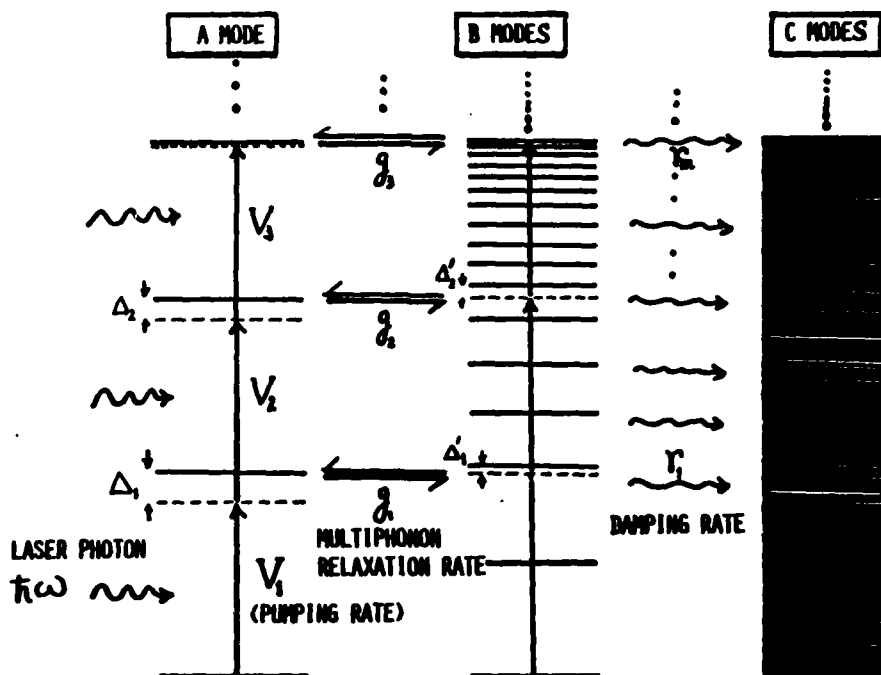


Fig. 7. Schematic energy level diagrams for the A, B and C modes, where V_i are the pumping rates between the i -th and the $(i+1)$ -th vibrational level of the active mode, coupled to the B mode via multiphonon coupling with the coupling factor g_i ; γ_m denotes the energy relaxation of the m -th level of the B mode due to its coupling to the C modes which are condensed modes with density of states ρ .

$$\omega_i = \omega_A - \epsilon_A^* a_i^\dagger a_i, \quad \omega_j = \omega_B - \epsilon_B^* b_j^\dagger b_j, \quad \omega_k = \omega_C - \epsilon_C^* c_k^\dagger c_k, \quad (2.83)$$

where ω_A , ω_B and ω_C are the fundamental frequencies (with anharmonicities ϵ_A^* , ϵ_B^* and ϵ_C^*) of the A, B and C modes, respectively; $v_{if}(t)$ is the pumping rate for a transition from state i to the state f of the pumped A mode; \bar{g} , \bar{K} and g , K are the coupling factors of A-B modes and B-C modes for single-phonon and multiphonon processes, respectively; and hc stands for Hermitian conjugate.

The equations of motion of the Bose operators for the system are found to be

$$i \frac{da_i(t)}{dt} = \omega_i a_i(t) + \sum_{f \neq i} v_{if}(t) a_f(t) + \sum_V g_{iV} B_V(t), \quad (2.84a)$$

$$i \frac{dB_V(t)}{dt} = \Omega_V B_V(t) + \sum_{i=1}^N g_{iV} a_i(t) + \langle [B_V(t), H_{BC}] \rangle, \quad (2.84b)$$

$$i \frac{dC_V(t)}{dt} = \bar{\Omega}_V C_V(t) + \langle [C_V(t), H_{BC}] \rangle, \quad (2.84c)$$

where

$$\Omega_V = \sum_j \omega_j, \quad \bar{\Omega}_V = \sum_k \omega_k, \quad (2.85a)$$

$$N_V = \prod_{j=1}^V (\bar{n}_j + 1) - \prod_{j=1}^V \bar{n}_j, \quad (2.85b)$$

$$\bar{n}_j = \left(e^{\hbar\omega_j/kT} - 1 \right)^{-1}, \quad (2.85c)$$

and the multiphonon operators are given by

$$B_V(t) = \prod_j^V b_j(t), \quad C_V(t) = \prod_k^V c_k(t). \quad (2.86)$$

The above coupled equations [Eq. (2.84)], describing a multilevel system subjected to laser radiation with the accompanying multiphonon relaxations, are not analytically solvable not only due to the many-body effects of the interaction Hamiltonian, H_{BC} , but also due to the large number of couplings when several energy levels are considered. To overcome the difficulty caused by the many-body effects, we shall use the Markoff approximation and treat the C modes as condensed states where the summation over all the C modes may be replaced by an integral over the associated density of states. These procedures enable us to approximate the many-level system as a few-level system.

To demonstrate the selectivity for different pumping rates and multiphonon relaxation rates, we examine a multiphonon process in which the A mode is

described by a three-level system and is coupled to the m -th and the $2m$ -th level of a decaying B mode via m -phonon coupling. Using Eq. (2.84) for the system operators for the two-photon multiphonon process and employing the Markoff and rotating-wave approximations, we obtain

$$\dot{a}_1(t) = -iV_1 a_2(t) \exp(-i\Delta t) , \quad (2.87a)$$

$$\dot{a}_2(t) = -iV_1 a_1(t) \exp(i\Delta_1 t) - ig_1 B_1(t) \exp(-i\Delta'_1 t) - iV_2 a_3(t) \exp(-i\Delta_2 t) , \quad (2.87b)$$

$$\dot{a}_3(t) = -iV_2 a_2(t) \exp(-i\Delta_2 t) - ig_2 B_2(t) \exp(-i\Delta'_2 t) , \quad (2.87c)$$

$$\dot{B}_1(t) = -ig_1^* a_2(t) \exp(i\Delta'_1 t) - (\gamma_1/2) B_1(t) , \quad (2.87d)$$

$$\dot{B}_2(t) = -ig_2^* a_3(t) \exp(i\Delta'_2 t) - (\gamma_2/2) B_2(t) , \quad (2.87e)$$

where $\Delta_1 = \omega_A - \omega$, $\Delta_2 = \Delta_1 - 2\varepsilon^*$, $\Delta'_1 = m\omega_B - \omega_A$, $\Delta'_2 = m\omega_B + 2\varepsilon^* - \omega_A$, ε^* is the anharmonicity of the A mode and V , g , γ are the pumping rates, coupling factors and the damping rates for the related levels, respectively. The above coupled equations are again numerically solved to obtain the level populations:

$$P_1 = |a_1(t)|^2, \quad P_A = |a_2(t)|^2 + |a_3(t)|^2 \quad \text{and} \quad P_B = |B_1(t)|^2 + |B_2(t)|^2 .$$

Therefore P_A and P_B describe the population dynamics of the photon energy deposited in the A and B modes, respectively, while $P_C = 1 - (P_1 + P_A + P_B)$ describes the population loss of the (A+B) modes and represents thermal heating, i.e., the portion of the photon energy randomized in the phonon bath C modes. The energy populations are shown in Fig. 8(A) for selective excitation of the A mode with $(V, g, \gamma) = (4, 0.1, 0.4)$ and in Fig 8(B) for nonselective heating of the C modes with $(V, g, \gamma) = (4, 1, 1)$. We see that for fixed laser pumping rates, $V_1 = V_2 = V$, the selective excitation of the active mode (A) requires a small multiphonon coupling factor, g , and small energy leakage rates, $\gamma_1 = \gamma_2 = \gamma$, out of the B mode, while appreciable nonselective thermal heating of the bath modes (C) is achieved when the coupling factor and the damping rate are comparable to the pumping rate.

Isotope separation of adspecies.³⁵ Isotope separation of species in the gas phase has been successfully studied both experimentally and theoretically. However, for a heterogeneous system, the separation of isotopic species adsorbed on a solid surface has not been experimentally investigated extensively due to the complexity of the technique, involving as it does a combination of surface physics, molecular dynamics and laser optics. We illustrate some possible mechanisms for isotope separation of adspecies using a model based on previously developed theory. The ensemble-averaged equations of motion in HMP for a system consisting of a mixture of two isotopic adspecies may be obtained by extending those for the

single-species case [Eq. (2.22)] as follows:

$$\dot{a}(t) = \left[\omega_{\text{eff}}^A(t) - \omega \right] a(t) + V_A/2 + Db(t) , \quad (2.88a)$$

$$\dot{b}(t) = \left[\omega_{\text{eff}}^B(t) - \omega \right] b(t) + V_B/2 + Da(t) , \quad (2.88b)$$

$$\langle \dot{n}_A(t) \rangle = -V_A \langle \text{Im}[a(t)] \rangle - 2D \langle \text{Im}[a(t)b^\dagger(t)] \rangle - \gamma_1^A \left(\langle n_A(t) \rangle - n_C/2 \right) , \quad (2.88c)$$

$$\langle \dot{n}_B(t) \rangle = -V_B \langle \text{Im}[b(t)] \rangle + 2D \langle \text{Im}[a(t)b^\dagger(t)] \rangle - \gamma_1^B \left(\langle n_B(t) \rangle - n_C/2 \right) , \quad (2.88d)$$

where V_A and V_B are the pumping rates for the A and B modes, n_C is the Bose-Einstein distribution for the C modes, Im denotes the imaginary part and D is the coupling strength between the isotopic adspecies A and B with the effective frequencies ω_{eff}^A and ω_{eff}^B , respectively, whose ensemble averages are given by

$$\langle \langle \omega_{\text{eff}}^{A,B} \rangle \rangle = \omega_{A,B} - 2\epsilon_{A,B}^* \langle n_{A,B}(t) \rangle - i\Gamma_{A,B}/2 , \quad (2.89a)$$

$$\Gamma_{A,B} = \gamma_1^{A,B} + \gamma_2^{A,B} . \quad (2.89b)$$

We note that both of the isotopic frequencies ω_A and ω_B are nearly resonant with the laser frequency. $\langle n_{A,B}(t) \rangle$ denote the average excitations of the A and B species, respectively.

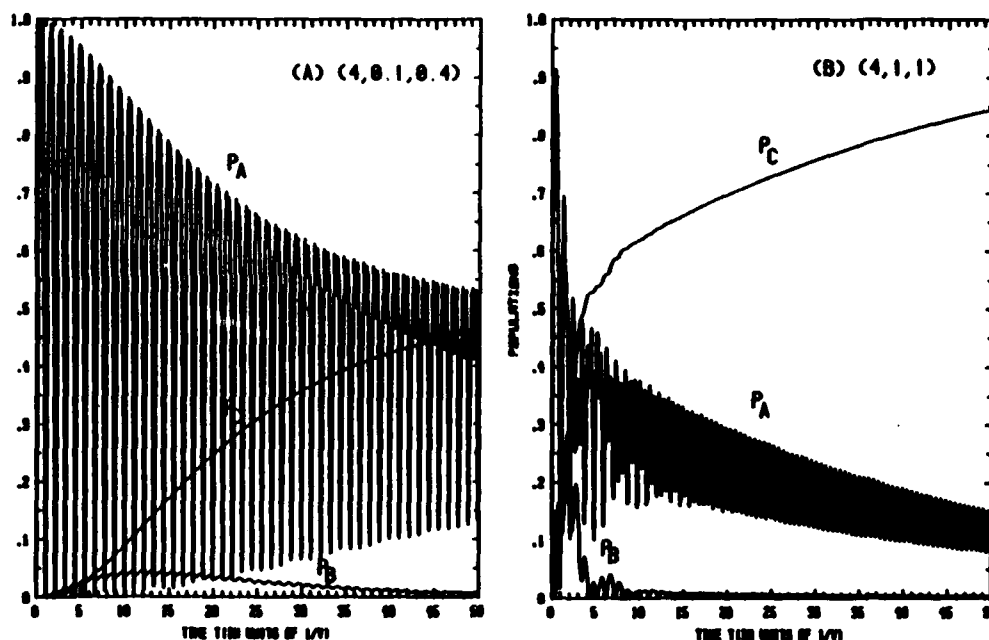


Fig. 8. Energy populations of A, B and C modes of two-photon multiphonon processes, given by P_A , P_B and P_C , respectively, for (pumping rate, coupling factor, damping rate) = $(V, g, \gamma) =$ (A) (4,0.1,0.4): selective excitation; (B) (4,1,1): nonselective thermal heating.³³

The coupled equations [Eq. (2.88)], which are highly nonlinear due to the anharmonic corrections $2\epsilon^* \langle n_{A,B}(t) \rangle$ and the isotope coupling strength D , can only be solved numerically. However, one can obtain the steady-state excitations for the weak-coupling case, $D \approx 0$,

$$\langle n_{A,B}(t) \rangle = \frac{\left[\frac{V_{A,B}}{2} \right]^2 \left[\frac{\Gamma_{A,B}}{\gamma_1^{A,B}} \right]}{\left[\langle \omega_{\text{eff}}^{A,B} \rangle - \omega \right]^2 + \left[\frac{\Gamma_{A,B}}{2} \right]^2}, \quad (2.90)$$

which show that one of the adspecies may be selectively excited without significant excitation of the other when the laser frequency, ω , is tuned to one of the optimal value, i.e., $\Delta_{\text{eff}}^{A,B} \equiv \langle \omega_{\text{eff}}^{A,B} \rangle - \omega = 0$, for either adspecies A or B.

To demonstrate the effect of the coupling strength, D , on the dynamics and the steady-state excitations, we plot the numerical solutions of Eq. (2.88) for the harmonic case ($\epsilon_{A,B}^* = 0$) in Fig. 9. It is seen that $\langle n_A(t) \rangle$ is higher than $\langle n_B(t) \rangle$ for $\Delta_A < \Delta_B$, where $\Delta_{A,B} = \omega_{A,B} - \omega$, with $D=0$ [Fig. 9(A)]. As D increases, both excitations decrease [Fig. 9(B)]. Increasing the coupling strength to the transition value, i.e., $D = D^* = (\Delta_B + \Delta_A)/2$, causes the steady-state excitations to become identical [Fig. 9(C)]. For large coupling strength, $D > D^*$, both excitations are low and $\langle n_B(t) \rangle$ is higher than $\langle n_A(t) \rangle$ [Fig. 9(D)]. These numerical results for the steady-state excitations are seen to be in accord with analytical results. Defining the "difference excitation" $N_L \equiv X - Y$, where X and Y are the steady-state excitations of the adspecies A and B, respectively, we obtain, from Eq. (2.88), for $\epsilon_{A,B}^* = 0$, $V_A = V_B = V$, $\gamma_1^A = \gamma_1^B = \gamma_1$ and $\Gamma_A = \Gamma_B = \Gamma$,

$$N_L = V^2 \Gamma \Omega_+ (\Omega_+ - 2D) / \left[4\gamma_1 \left(z_1^2 + z_2^2 \right) \right], \quad (2.91a)$$

$$z_1 = \Delta_A \Delta_B - D^2 - (\Gamma/2)^2, \quad (2.91b)$$

$$z_2 = \Gamma \Omega_+ / 2, \quad (2.91c)$$

$$\Omega_{\pm} = \Delta_B \pm \Delta_A, \quad (2.91d)$$

$$\Delta_{A,B} = \omega_{A,B} - \omega. \quad (2.91e)$$

The above expression for the steady-state "difference excitation" N_L displays the following important features: (i) isotopic selectivity increases with decreasing coupling strength; (ii) when the coupling strength reaches the transition value $D = D^* = \Omega_+$, there is zero selectivity, i.e., $N_L = 0$ as shown in Fig. 9(C).

(b) Classical models. In the previous sections we have treated the adspecies-surface system as a quantum-mechanical system subject to laser radiation

either as a classical field or as a quantized multimode field. We shall now consider fully classical models, starting with a single-body system³⁹ and then extending the treatments to a many-body system.⁴⁰⁻⁴³ The energy-transfer dynamics is reexamined via the generalized Langevin equation where the memory effects, represented by a damping kernel and a dephasing kernel, are discussed.^{40,41} Multiphonon relaxation processes and possible selective excitation of a specific bond are investigated in terms of the internal resonance condition.⁴¹ Cooperative excitations using several lasers with optimum detunings are investigated. Finally, the results of fully classical models are compared to those of the quantum-mechanical models.

Single-body system. Considering the active-mode of the adspecies as a classical anharmonic oscillator and the remaining modes (inactive modes plus surface phonon modes) as the heat bath, the normal-mode coordinate of the damped nonlinear oscillator, x , satisfies the classical equation of motion³⁹

$$\ddot{x} + 2\gamma\dot{x} + \omega_A^2 x + \lambda_1 x^2 + \lambda_2 x^3 = f(t)/m, \quad (2.92)$$

where γ is the generalized damping factor (the overall absorption line broadening), λ_1 and λ_2 are the small anharmonic coefficients, m is the reduced mass of the adspecies, and the driving radiation field $f(t)$ is given by

$$f(t) = eE \cos(\theta) \cos(\omega t). \quad (2.93)$$

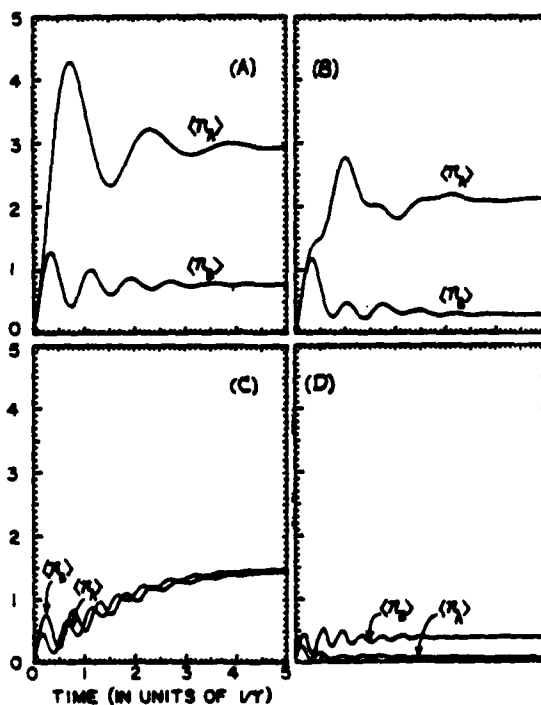


Fig. 9. Time-dependent excitations $\langle n_{A,B}(t) \rangle$ of the active modes for the harmonic case, i.e., $\epsilon^* = 0$ with $(V, \gamma, \Delta_A, \Delta_B) = (10, 1, 4, 8)$ and $D = (A)0, (B)2, (C)D^*,$ and $(D)10$. $D^* = (\Delta_A + \Delta_B)/2 = 6$ is the transition value where $N_- = 0$.³⁵

Here, e is the classical effective charge and θ is the angle between the linearly polarized electric field, E , and the direction of the pumped normal-mode coordinate. The laser frequency ω is tuned to be near resonant to the active-mode frequency ω_A .

By the harmonic balance method, Eq. (2.92) can be linearized to second order in λ_1 and first order in λ_2 :

$$\ddot{x} + 2\gamma\dot{x} + \omega_{\text{eff}}^2 x = f(t)/m, \quad (2.94)$$

where the effective frequency ω_{eff} is related to the amplitude of the classical oscillator A and the classical anharmonicity K^* by

$$\omega_{\text{eff}} = \omega_A - K^* A^2, \quad (2.95a)$$

$$K^* = 5\lambda_1^2/12\omega_A^3 - 3\lambda_2/8\omega_A. \quad (2.95b)$$

The steady-state solution of Eq. (2.95) is straightforward:

$$x_{\text{s.s.}}(t) = A_1 \sin(\omega t) + A_2 \cos(\omega t), \quad (2.96a)$$

where

$$A_1 = 2(eE/m) (\gamma\omega/Z) \cos(\theta), \quad (2.96b)$$

$$A_2 = (eE/m) \left[\omega_{\text{eff}}^2 - \omega^2 \right] / Z \cos(\theta), \quad (2.96c)$$

$$Z = \left[\omega_{\text{eff}}^2 - \omega^2 \right]^2 + (2\omega\gamma)^2, \quad (2.96d)$$

and

$$A^2 = A_1^2 + A_2^2. \quad (2.96e)$$

Combining Eq. (2.93) and the time derivative of Eq. (2.96) we obtain the instantaneous steady-state power absorption of the oscillator

$$p(t) = f(t)\dot{x}_{\text{s.s.}}(t) = eE\omega A_1 \cos^2(\omega t) - (eE\omega A_2/2) \sin(2\omega t). \quad (2.97)$$

Since the second term of Eq. (2.97) vanishes as a result of time averaging, we obtain the time-averaged steady-state power absorption for near-resonant excitations,

$$\overline{p(t)} = \left(\frac{e^2 E^2}{4m} \right) \left[\frac{\gamma}{\left[\Delta - K^* A^2 \right]^2 + \gamma^2} \right] \cos^2(\theta). \quad (2.98)$$

The classical steady-state excitation energy defined by $\mathcal{E} = m\omega_A^2/2 = \overline{p(t)}/\gamma$ results in a cubic equation for the square of the amplitude, $X \equiv A^2$,

$$x = \frac{\left(\frac{eE}{2m}\right)^2 / \omega_A^2}{(\Delta - K^*x)^2 + \gamma^2} \quad (2.99)$$

Generalized Langevin equation.⁴¹ Equation (2.92), describing the motion of a forced anharmonic oscillator, contains only the energy relaxation rate γ and hence cannot completely describe the overall energy-transfer dynamics which, in general, should be characterized by both the energy and the phase relaxation factors as we have shown in the quantum models. As an extension of Eq. (2.92), we investigate the generalized Langevin equation (GLE):

$$\ddot{x}(t) + \int_0^t dt' K_1(t-t') \dot{x}(t') + \omega_{\text{eff}}^2 \int_0^t dt' K_2(t-t') \dot{x}(t') = [f(t) + f_R(t)]/m \quad (2.100)$$

where $f(t)$ and $f_R(t)$ are the driving force due to the laser field and the substrate-induced random force, respectively; K_1 and K_2 are the kernel functions for the energy and phase relaxation, respectively. The major mechanisms which cause the T_1 and T_2 relaxations are: (i) vibration-induced lattice-site transition (migration) of the adspecies; (ii) anharmonic coupling of the phonon bath modes; (iii) the inter- and intraspecies interactions; (iv) the substrate-induced thermal fluctuations of the effective dipole of the adspecies and the effective electric field at the adspecies; and (v) charge transfer and coupling among vibrational degrees of freedom and other degrees of freedom, e.g., librations of the adspecies.^{30,31,40,41} We note that the damping kernel (K_1) characterizes the dynamics of the energy relaxation of the excited adspecies while the dephasing kernel (K_2) only governs the phasing information without causing any change of the energy population.

Employing linear response theory and time-dependent perturbation theory, we may express the averaged energy absorption rate as follows:⁴¹

$$\left\langle \frac{d\mathcal{E}}{dt} \right\rangle = \frac{(eE)^2}{2\hbar\omega} [1 - \exp(-\beta\hbar\omega)] (\text{Re}F[\omega]) \quad (2.101)$$

with $\beta = (kT_0)^{-1}$ and Re denoting the real part of the Laplace-Fourier transform of the velocity correlation function,⁴⁴

$$F[\omega] = \int_0^\infty dt \exp(i\omega t) F(t) \quad (2.102a)$$

$$F(t) = \langle \dot{x}(t) \dot{x}(0) \rangle \quad (2.102b)$$

where the velocity autocorrelation function, $F(t)$, is governed by the GLE in the absence of the laser field. Multiplying both sides of Eq. (2.100) by $\dot{x}(0)$ and performing the ensemble average over the initial conditions, we obtain the

equation of motion for the velocity autocorrelation function

$$\dot{F}(t) + \int_0^t dt' K_1(t-t')F(t') + \omega_{\text{eff}}^2 \int_0^t dt' K_2(t-t')F(t') = \langle \dot{X}(0) f_R(t) \rangle / m \quad (2.103)$$

Taking the Laplace-Fourier transform of Eq. (2.103), we find

$$F[\omega] = \left(\frac{kT_0}{m} \right) \left[\frac{1}{i\omega + K_1[\omega] + \omega_{\text{eff}}^2 K_2[\omega]} \right] \quad (2.104)$$

where $K_1[\omega]$ and $K_2[\omega]$ are the Laplace-Fourier transforms of the kernel functions. In obtaining Eq. (2.104), we have used the initial equilibrium average, $F(0) \equiv \langle \dot{X}(0)\dot{X}(0) \rangle = kT_0/m$, and the convolution theorem for the Laplace-Fourier transform,

$$\mathcal{L}\{g_1^* g_2\} \equiv \int_0^\infty dt e^{-i\omega t} \int_0^t dt' g_1(t-t')g_2(t') = \mathcal{L}(g_1)\mathcal{L}(g_2) \quad (2.105)$$

For given forms of the kernel functions $K_1(t)$ and $K_2(t)$, we can find the associated Laplace-Fourier transforms $K_{1,2}[\omega]$ and compute the average energy absorption rate from the real part of $F[\omega]$. In using the convolution theorem, the kernel functions $K_{1,2}(t)$ and the velocity autocorrelation function $F(t)$ must be well behaved, i.e., $K_{1,2}(t), F(t) \rightarrow 0$, as $t \rightarrow \infty$. Keeping this in mind, we consider a Markoff process where the damping kernel is given by a Dirac delta function,

$$K_1(t) = 2\gamma_1 \delta(t) \quad (2.106)$$

where γ_1 is a constant damping factor. Furthermore, the T_2 dephasing kernel, $K_2(t)$, which destroys the coherent nature of the excitation phase but does not change the energy population of the excited adspecies, is chosen to be an exponential form,

$$K_2(t) = \exp(-2\gamma_2 t) \quad (2.107)$$

where γ_2 is a constant dephasing rate related to the phase correlation time by $2\gamma_2 = \tau_c^{-1}$. Working out the Laplace-Fourier transform of the kernel functions $K_{1,2}[\omega]$ from Eqs. (2.106) and (2.107) and substituting the results into Eq. (2.104), we obtain, from the real part of $F[\omega]$ and Eq. (2.101), the averaged energy absorption rate

$$\left\langle \frac{d\mathcal{E}}{dt} \right\rangle = (eE)^2 P(T_0) \left[\frac{\gamma_2 C + \omega D}{C^2 + D^2} \right] \quad (2.108a)$$

$$P(T_0) = (2\hbar\omega)^{-1} (kT_0/m) [1 - \exp(-\hbar\omega/kT_0)] \quad (2.108b)$$

$$C = \omega_{\text{eff}}^2 - \omega^2 + \gamma_1 \gamma_2, \quad (2.108c)$$

$$D = \omega(\gamma_1 + \gamma_2). \quad (2.108d)$$

The important features of the above equation are: (i) for low temperature ($kT_0 \ll \hbar\omega$), $P(T_0) \propto T_0$, and when the overall broadening ($\gamma_1 + \gamma_2$) is weakly temperature-dependent (for single-phonon relaxation processes), Eq. (2.108) reduces to $\langle d\mathcal{E}/dt \rangle \propto T_0$; however, for multiphonon processes and/or high temperature temperatures, $P(T_0) \propto T_0 \exp(\hbar\omega/kT_0)$, $\langle d\mathcal{E}/dt \rangle$ is strongly temperature-dependent; (ii) for $\Delta = \omega_{\text{eff}} - \omega \ll \omega$ and $\gamma_1 \gamma_2 \ll \omega^2$, Eq. (2.108) reduces to a Lorentzian with $\text{FWHM} = 2(\gamma_1 + \gamma_2)$,

$$\left\langle \frac{d\mathcal{E}}{dt} \right\rangle = \left(\frac{eE}{2} \right)^2 P(T_0) \left[\frac{(\gamma_1 + \gamma_2)}{\Delta^2 + (\gamma_1 + \gamma_2)^2} \right], \quad (2.109)$$

which, except for the temperature-dependent factor, reduces to Eq. (2.98) when $\gamma_2 = 0$.

Stochastic processes. In the previous stochastic quantum model, the many-body effects of the phonon bath were accounted for by defining an effective Hamiltonian in which the active-mode frequency had a complex stochastic component [Eq. (2.74d)]. The latter was obtained as a result of an ensemble average over the stochastic process.³⁰ We shall now investigate the stochastic effects of the laser field,

$$f(t) = eE \cos[\omega t + \tilde{\phi}(t)], \quad (2.110)$$

where $\tilde{\phi}(t)$ is a stochastic random phase factor. For a Markoff process with the phase correlation function $\langle \tilde{\phi}(t) \tilde{\phi}(t') \rangle = 2\gamma_0 \delta(t-t')$, the ensemble average of the field Eq. (2.110) becomes

$$\langle f(t) \rangle = eE \cos(\omega t) e^{-\gamma_0 t}, \quad (2.111)$$

namely a Lorentzian electric field for which γ_0 is the frequency bandwidth and γ_0^{-1} describes the exponential decay of the field envelope at a point in space. Employing the exponentially decaying laser field $f(t)$ in Eq. (2.94), we obtain the average energy stored in the pumped adspecies,

$$\langle \mathcal{E}(t) \rangle = \mathcal{E}_0 \left[e^{-\gamma_0 t} + e^{-\gamma t} - 2e^{-(\gamma_0 + \gamma)t/2} \cos(\Delta t) \right], \quad (2.112a)$$

$$\mathcal{E}_0 = \left(\frac{e^2 E^2}{4m} \right) \left[\frac{1}{[\Delta - \kappa^* A^2]^2 + [\gamma - \gamma_0]^2} \right] \cos(\theta). \quad (2.112b)$$

A novel feature of the above result is that due to the frequency width of the decaying electric field, γ_0 , the ensemble-averaged energy absorption of the adspecies is governed by a total decay rate, $\gamma_0 + \gamma$, but the width of the steady-state energy absorption profile is reduced, i.e., $\text{FWHM} = \gamma_0 - \gamma$. The time that it takes the system to absorb the photon energy is determined by γ_0 or γ , depending on which is larger.

Many-body system. We consider a model system (as shown in Fig. 10) with a diatomic molecule adsorbed on a solid surface and subjected to infrared radiation. The classical Lagrangian may be written as⁴³

$$\mathcal{L} = \mathcal{L}_0 + \sum_i x_i f_i(t) \quad , \quad (2.113a)$$

$$\begin{aligned} \mathcal{L}_0 = & \sum_{i=1,2} m_i \left[\frac{1}{2} (\dot{x}_i^2 - \omega_i^2 x_i^2) - \epsilon_{1i} x_i^3 - \epsilon_{2i} x_i^4 \right] + \frac{1}{2} \sum_{j=3} m_j (\dot{x}_j^2 - \omega_j^2 x_j^2) + \frac{1}{2} \sum_{i>j} \lambda_{ij} x_i x_j + \\ & \sum_{p=2} \sum_{i>j} \frac{1}{(p+1)!} \lambda_{ij}^{(p)} x_i x_j^p + \dots \quad , \quad (2.113b) \end{aligned}$$

where m_i , x_i , ω_i ($i=1,2,3,\dots$) are the mass, the displacement, and the frequency of the i th atoms, respectively, and the interaction terms with coupling constants λ_{ij} and $\lambda_{ij}^{(p)}$ (between the i th and j th atoms) are referred to as the single-phonon (linear) coupling and the p -phonon (nonlinear) coupling, respectively. Here the admolecule is treated as an anharmonic oscillator (up to the quartic terms) while the surface atoms are treated harmonically. The anharmonicities ϵ_{1i} , ϵ_{2i} and the coupling constant λ_{12} are related to the derivatives of the potential energies and e.g., for a Morse potential

$$V(x_1, x_2) = D_e \left[1 - \exp[-a(x_1 - x_2 - x^0)] \right]^2 \quad (2.114)$$

we have $\epsilon_{11} = -a^3 D_e$, $\epsilon_{12} = \frac{7}{12} a^4 D_e$, and $\lambda_{12} = 2a^2 D_e$. Similarly, the coupling constants λ_{ij} and $\lambda_{ij}^{(p)}$ are related to the pair potential energy between the i th and j th atoms by

$$\lambda_{ij} = \left(\frac{\partial^2 V(x_i, x_j)}{\partial x_i \partial x_j} \right)_0 \quad , \quad \lambda_{ij}^{(p)} = \left(\frac{\partial^{p+1} V(x_i, x_j)}{\partial x_i \partial x_j^p} \right)_0 \quad , \quad (2.115)$$

where the subscript zero means evaluation at the minimum of $V(x_1, x_2)$. The second term in Eq. (2.113a) is the interaction energy between the admolecule-surface system and the laser field,

$$f_i(t) = q_i E_i \cos(\omega t) \cos(\theta_i) \quad , \quad (2.116)$$

where q_i is the classical effective charge of the atoms, and θ_i is the angle

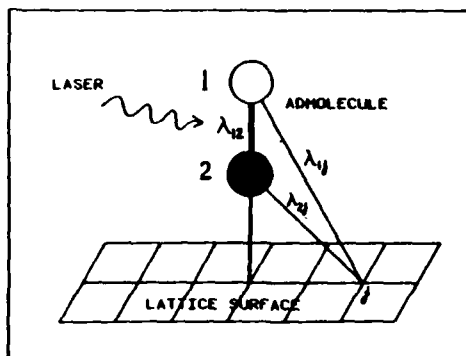


Fig. 10. Diatomic molecule chemisorbed on a solid surface. The coupling constants between adatoms 1 and 2 and among the adatoms and the surface atoms are given by λ_{12} , λ_{1j} , and λ_{2j} , respectively.⁴²

between the linearly polarized electric field E_i (with frequency ω) and the coordinate vector for the optical active mode(s) of the system. Direct numerical analysis of the equation of motion is not tractable due to the complicated many-body effects of the surface atoms. To obtain analytical results, we shall con-

sider a less general Lagrangian, namely one where no explicit interactions are assumed between the surface atoms. Furthermore, the interactions between the admolecule and the surface atoms will be taken into account by introducing damping factors. As an example, we consider CO adsorbed on a nickel surface and subject to IR laser radiation with field frequency near resonance to the stretching frequency of CO. Restricting ourselves to a truncated five-atom chain O-C-Ni-Ni-Ni, with the oxygen atom labeled 1 and so on, the coupled Newton's equation of motion describing this system are⁴²

$$m_1 \ddot{x}_1 = -k_{12}(x_1 - x_2) - \gamma \dot{x}_1 - f(t) \quad , \quad (2.117a)$$

$$m_2 \ddot{x}_2 = -k_{12}(x_2 - x_1) - k_{23}(x_2 - x_3) - \gamma \dot{x}_2 + f(t) \quad , \quad (2.117b)$$

$$m_s \ddot{x}_3 = -k_{23}(x_3 - x_2) - k_s(x_3 - x_4) - \gamma \dot{x}_3 \quad , \quad (2.117c)$$

$$m_s \ddot{x}_4 = -k_s(x_4 - x_3) - k_s(x_4 - x_5) - \gamma \dot{x}_4 \quad , \quad (2.117d)$$

$$m_s \ddot{x}_5 = -k_s(x_5 - x_4) - \gamma \dot{x}_5 \quad , \quad (2.117e)$$

where k and γ are the force constant and damping factor, and $f(t) = qE \sin(\omega t)$ is the laser driving force. The force constants used here are: $k_{12} = 16.8$, $k_{23} = 2.6$ and $k_s = 0.24$ (in units of mdyne/Å), and the atom masses are $m_1 = 16$, $m_2 = 12$, and $m_s = 58.71$ (amu), where $k_s = k_{34} = k_{45}$, and $m_s = m_3 = m_4 = m_5$.

These five coupled second-order differential equations are equivalent to a set of ten coupled first-order differential equations, which were numerically solved

by the Runge-Kutta method. In addition to the amplitudes of the chain atoms, we can compute the energies

$$E_A = \sum_{i=1}^2 \frac{1}{2} m_i \dot{x}_i^2 + \frac{1}{2} k_{12} (x_1 - x_2)^2, \quad (2.118a)$$

$$E_B = \frac{1}{2} m_s \dot{x}_3^2 + \frac{1}{2} k_{23} (x_2 - x_3)^2, \quad (2.118b)$$

$$E_C = \sum_{i=4}^5 \frac{1}{2} m_s \dot{x}_i^2 + \frac{1}{2} k_s [(x_3 - x_4)^2 + (x_4 - x_5)^2], \quad (2.118c)$$

where E_A represents the energy of the adsorbed CO molecule, E_B is the "energy" of the surface, namely the outermost nickel atom, and E_C is the energy of the rest of the solid (chain nickel atoms, 4 and 5).

The numerical results for the amplitudes of the atoms and the energy profiles E_A , E_B and E_C are plotted in Fig. 11 for different sets of values of the damping factor γ and the detuning $\Delta = \omega_0 - \omega$. Fig. 11(A) shows the exact resonance case ($\Delta=0$) with $\gamma=100 \text{ cm}^{-1}$. The near-resonance cases are shown in Fig. 11(B) with $\gamma=100 \text{ cm}^{-1}$ and $\Delta=20 \text{ cm}^{-1}$, Fig. 11(C) with $\gamma=\Delta=10 \text{ cm}^{-1}$, and Fig. 11(D) with $\gamma=\Delta=0$. It is seen that the decaying and oscillating features of the energy profiles are characterized by the damping factor and the detuning, respectively. We note that the amplitudes of the excited CO molecule are much higher than those of the Ni atoms due to the mass differences (atom-2 has the highest amplitude). The energy profiles shown in Fig. 11 are generated for a high-power laser with intensity $I=10^{12} \text{ W/cm}^2$ (hence short computation times, in contrast to the situation of a low-power laser). Due to the high frequency of the field $\omega \approx 10^{14} \text{ sec}^{-1}$, we require time steps on the order of 10^{-15} sec in using the Runge Kutta method. For an actual system of low-power excitation LSSP (with laser intensity $I \approx 10\text{-}100 \text{ W/cm}^2$), we expect similar energy profiles as shown in the high-power cases. This stems from the fact that the energy profiles shown in Fig. 11 are "universal" for any range of laser power, provided the proper time scales (in units of the reciprocal of the pumping rate) are chosen.

For a long-lived adspecies excited by low-power laser radiation, the time scales of the energy profiles lie in the range 10^{-3} to 10^{-6} sec , which are much longer than the time period of the field ($\omega^{-1} \sim 10^{-14} \text{ sec}$). The necessity of using a mesh size of the order of the latter makes for very large computation times for this case. To overcome these difficulties, particularly for low-power excitation processes, we present a method which utilizes the concept of the rotating-wave approximation borrowed from quantum mechanics.³⁶ Consider a model system consisting of adatoms 1 and 2 chemisorbed on a solid surface and subject to

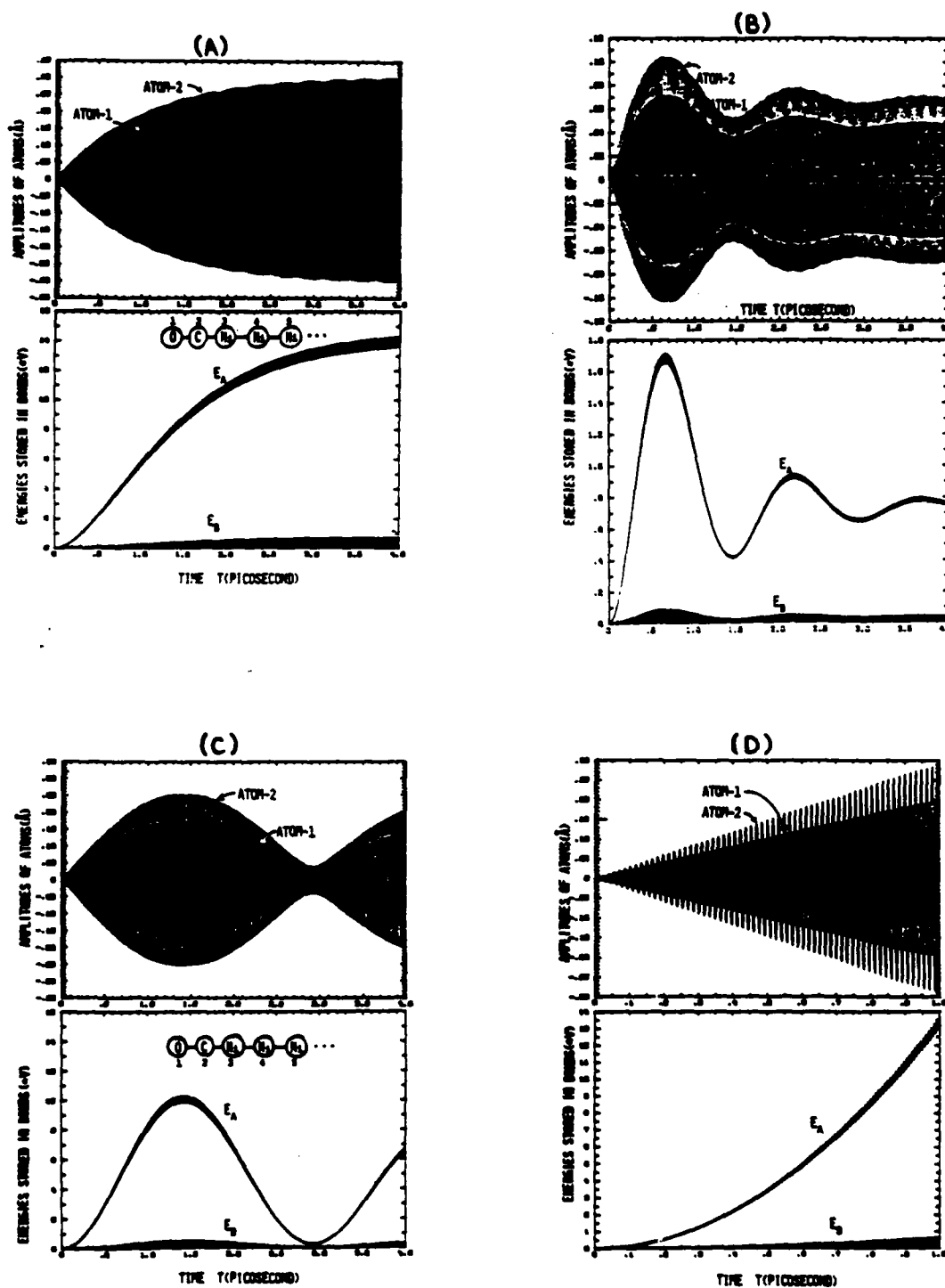


Fig. 11. Amplitudes of atoms and energy profiles for different bonds of the CO/Ni system, subject to a high-power laser with intensity $I = 10^{12} \text{ W/cm}^2$, for different sets of the damping factor (γ) and the detuning (Δ): (A) $\gamma = 100 \text{ cm}^{-1}$ for exact resonance $\Delta = 0$, (B) $\gamma = 100 \text{ cm}^{-1}$, $\Delta = 20 \text{ cm}^{-1}$, (C) $\gamma = \Delta = 10 \text{ cm}^{-1}$, (D) $\gamma = \Delta = 0$.

an external field $[V_i \sin(\omega t)]$, described by a set of coupled equations (for nearest neighbor interactions):⁴³

$$m_1 \ddot{x}_1 = - \frac{\partial v_{12}(x_1, x_2)}{\partial x_1} - m_1 \gamma_1 \dot{x}_1 + V_1 \sin(\omega t) , \quad (2.119a)$$

$$m_2 \ddot{x}_2 = - \frac{\partial v_{12}(x_1, x_2)}{\partial x_2} - \frac{\partial v_{23}(x_2, x_3)}{\partial x_2} - m_2 \gamma_2 \dot{x}_2 + V_2 \sin(\omega t) , \quad (2.119b)$$

$$m_s \ddot{x}_j = - \frac{\partial v_{j-1,j}(x_{j-1}, x_j)}{\partial x_j} - \frac{\partial v_{j,j+1}(x_j, x_{j+1})}{\partial x_j} - m_s \gamma_j \dot{x}_j + V_j \sin(\omega t) , \quad j \geq 3 , \quad (2.119c)$$

where x_i ($i=1,2,3,\dots$) is the coordinate of the i th atom for the longitudinal motion, and the damping terms $m_i \gamma_i \dot{x}_i$ are included to take into account the lateral interactions between the atoms of one row with those of another. The damping factors γ_i ($i=1,2$) for the adatoms simulate the surface effects of the solid crystal, and the damping factors γ_j ($j \geq 3$) of the solid atoms simulate the effect of the bulk of the lattice in representing the free translational motion of the one-dimensional linear chain. This is the significant difference of Eq. (2.119) from that of the usual one-dimensional chain model, where the latter loses all the many-body surface effects of the adatoms and the many-body bulk effects of the solid atoms. By using the rotating frame

$$y_i(t) = x_i(t) \exp(i\omega_0 t) ,$$

where ω_0 is the frequency of the optically-active mode of the adspecies-surface system, we shall consider the near-resonant excitation with the detuning $\Delta = \omega_0 - \omega \approx 0$ (for the harmonic model) or $\Delta = \omega_0 - K^*A^2 - \omega \approx 0$ [for the anharmonic model — see Eq. (2.95)]. The coupled equations of motion Eq. (2.119) become

$$m_1 \ddot{y}_1 = - \frac{\partial v_{12}}{\partial y_1} + m_1 \omega_0^2 y_1 - m_1 \gamma_1 (\dot{y}_1 + i\omega_0 y_1) + \frac{1}{2} V_1 e^{i\Delta t} , \quad (2.120a)$$

$$m_2 \ddot{y}_2 = - \frac{\partial v_{12}}{\partial y_2} - \frac{\partial v_{23}}{\partial y_2} + m_2 \omega_0^2 y_2 - m_2 \gamma_2 (\dot{y}_2 + i\omega_0 y_2) + \frac{1}{2} V_2 e^{-i\Delta t} , \quad (2.120b)$$

$$m_s \ddot{y}_j = - \frac{\partial v_{j-1,j}}{\partial y_j} - \frac{\partial v_{j,j+1}}{\partial y_j} + m_s \omega_0^2 y_j - m_s \gamma_j (\dot{y}_j + i\omega_0 y_j) + \frac{1}{2} V_j e^{-i\Delta t} \quad j \geq 3 , \quad (2.120c)$$

where $\Delta \equiv \omega_0 - \omega$ is the detuning. In obtaining Eq. (2.120) we have used the RWA, that is, we have neglected the fast oscillating terms $\exp[\pm i(\omega_0 + \omega)t]$. The important features of the new equations of motion are: (i) due to the complex

coefficients, the j coupled equations are in fact $2j$ real equations (equivalent to $4j$ first-order differential equations which must be numerically solved); (ii) the time-dependent field with the very fast sinusoidal function $\sin(\omega t)$ is eliminated in the rotating frame by the RWA, and the coupled equations are characterized by the detuning Δ which leads to a much slower oscillating function, $\exp(-i\Delta t)$, compared to the driving force $V_1 \sin(\omega t)$ shown in the original equations of motion [Eq. (2.119)].

Reduction of the many-body problem and universal energy profiles. For tractable results, we shall reduce the many-body problem described by Eq. (2.113) to a few-body problem. For this purpose, we employ the orthogonal transform⁴³

$$x_1 = \frac{1}{\left(\lambda_{1j}^2 + \lambda_{2j}^2\right)^{\frac{1}{2}}} (\lambda_{1j} Q_2 + \lambda_{2j} Q_1) , \quad (2.121a)$$

$$x_2 = \frac{1}{\left(\lambda_{1j}^2 + \lambda_{2j}^2\right)^{\frac{1}{2}}} (\lambda_{2j} Q_2 - \lambda_{1j} Q_1) , \quad (2.121b)$$

$$x_j \equiv Q_j , \quad j \geq 3 . \quad (2.121c)$$

The Lagrangian of the model system becomes, in the transformed normal mode coordinates Q_i ($i=1,2,3,\dots$),

$$\begin{aligned} \mathcal{L}(Q_1, Q_2, \dots, Q_j, \dots) = & \sum_{i=1,2} M_i \left(\frac{1}{2} \dot{Q}_i^2 - \frac{1}{2} \Omega_i^2 Q_i^2 - \frac{1}{3} K_i Q_i^3 - \frac{1}{4} K_i' Q_i^4 \right) \\ & + \frac{1}{2} M_s \sum_{j=3} \left(\dot{Q}_j^2 - \Omega_j^2 Q_j^2 \right) + \Lambda Q_1 Q_2 + Q_2 \sum_{j=3} \lambda_j Q_j + Q_1 \sum_{j=3} \sum_{p=2} \bar{\lambda}_j^{(p)} Q_j^p + \\ & Q_2 \sum_{j=3} \sum_{p=2} \lambda_j^{(p)} Q_j^p + M_1^{-1} \dot{Q}_1 \dot{Q}_2 + \sum_i f_i Q_i , \end{aligned} \quad (2.122)$$

where the transformed frequencies are given by

$$\Omega_{1,2}^2 = \frac{m_1 \lambda_{2j,1j}^2 \omega_1^2 + m_2 \lambda_{1j,2j}^2 \omega_2^2 \pm \lambda_{12} \lambda_{1j} \lambda_{2j}}{M_{1,2} \lambda_j^2} , \quad (2.123a)$$

$$\Omega_j \equiv \omega_j , \quad j \geq 3 , \quad (2.123b)$$

the transformed masses by

$$M_{1,2} = \left(m_1 \lambda_{1j,2j}^2 + m_2 \lambda_{2j,1j}^2 \right) / \lambda_j^2 , \quad (2.124a)$$

$$M_s \equiv m_j , \quad j \geq 3 , \quad (2.124b)$$

$$M^- = \lambda_{1j} \lambda_{2j} (m_1 - m_2) / \lambda_j^2, \quad (2.124c)$$

the transformed new anharmonicities by

$$K_{1,2} = \frac{3[(\epsilon_{11} \lambda_{2j,1j}^3 \mp \epsilon_{12} \lambda_{1j,2j}^3) + \lambda_{12}^{(2)} (\lambda_{2j} \lambda_{1j}^2 \mp \lambda_{1j} \lambda_{2j}^2)]}{\lambda_j^3} \quad (2.125a)$$

$$K'_{1,2} = \frac{\epsilon_{21} \lambda_{2j,1j}^4 + \epsilon_{22} \lambda_{1j,2j}^4}{\lambda_j^4}, \quad (2.125b)$$

and the transformed generalized forces by

$$f_{1,2}(t) = (\lambda_{2j,1j} F_1 \mp \lambda_{1j,2j} F_2) / \lambda_j, \quad (2.126a)$$

$$f_j(t) = F_j(t), \quad j \geq 3. \quad (2.126b)$$

The new coupling constants (note - these are surface-atom site dependent) are defined by

$$\Lambda = \frac{\lambda_{12}}{2\lambda_j^2} \left((\lambda_{2j}^2 - \lambda_{1j}^2) - \frac{2\lambda_{1j} \lambda_{2j}}{\lambda_{12}} (m_1 \omega_2^2 - m_2 \omega_1^2) \right), \quad (2.127a)$$

$$\lambda_j = (\lambda_{1j}^2 + \lambda_{2j}^2)^{\frac{1}{2}}, \quad (2.127b)$$

$$\lambda_j^{(p)} = \frac{\lambda_{1j}^{(p)} \lambda_{1j} + \lambda_{2j}^{(p)} \lambda_{2j}}{(p+1)!}, \quad (2.127c)$$

$$\bar{\lambda}_j^{(p)} = \frac{\lambda_{1j}^{(p)} \lambda_{2j} - \lambda_{2j}^{(p)} \lambda_{1j}}{(p+1)!}. \quad (2.127d)$$

In deriving Eq. (2.122), we have neglected the high-order anharmonic terms (Q_i^n , $n > 4$) and considered the linear coupling terms between Q_1 and Q_2 while keeping the high-order couplings among the adatoms and the surface atoms. Moreover, the couplings among the surface atoms ($Q_i Q_j$, $i, j > 2$), which gives rise to an infinite number of coupled equations of motion, are effectively absorbed into the site-dependent coupling constants ($\lambda_{1j}, \lambda_{2j}$) and the frequency dispersion of the surface-phonon modes.

The corresponding equations of motion in the transformed normal coordinates are

$$\frac{d}{dt} \left(\frac{\partial \mathcal{L}}{\partial \dot{Q}_i} \right) - \frac{\partial \mathcal{L}}{\partial Q_i} = 0, \quad i = 1, 2, 3, \dots \quad (2.128)$$

Substituting from Eq. (2.122), we obtain equations of motion, which are complicated and will not be shown here.⁴³ We shall consider the situation $m_1 \approx m_2 \ll M_s$ and near-resonance excitation $\omega \approx \Omega_{1,2}$, namely no direct laser excitation of the substrate atoms. Under these conditions and employing the asymptotic (or harmonic balance) method,^{37,39} we obtain the linearized equation of motion, from Eq. (2.122) or (2.128) with no multiphonon coupling terms, i.e., neglecting $Q_2 \sum_j \lambda_j^{(p)} Q_j^p$ for $j \geq 3$, $p \geq 2$,

$$\ddot{Q}_1 + \bar{\Omega}_1^2 Q_1 = [\Lambda Q_2 + f_1(t)]/M_1, \quad (2.129a)$$

$$\ddot{Q}_2 + \bar{\Omega}_2^2 Q_2 = \left[\Lambda Q_1 + \sum_{j=3} \lambda_j Q_j + f_2(t) \right]/M_2, \quad (2.129b)$$

$$\ddot{Q}_j + \Omega_j^2 Q_j = \lambda_j Q_2/M_s, \quad j \geq 3. \quad (2.129c)$$

We have introduced the effective frequencies $\bar{\Omega}_1$ and $\bar{\Omega}_2$ which are approximately related to the anharmonicities ($K_{1,2}^*$) and the steady-state amplitudes of the modes (A_1, A_2) by

$$\bar{\Omega}_{1,2} = \Omega_{1,2} - K_{1,2}^* A_{1,2}^2, \quad (2.130a)$$

where

$$K_{1,2}^* = \frac{5K_{1,2}}{12\Omega_{1,2}^3} - \frac{3K_{1,2}'}{8\Omega_{1,2}}. \quad (2.130b)$$

To further reduce the above many-body system, we shall use an iterative scheme starting with the homogenous zero-order solution of Eq. (2.129b)

$$Q_2^{(0)}(t) = B_0 \cos(\bar{\Omega}_2 t). \quad (2.131)$$

From Eq. (2.131) we obtain the first-order solution of Eq. (2.129c) which results in the ensemble-averaged equation of motion for the first-order solution of $Q_2(t)$,

$$\langle \ddot{Q}_2 \rangle + \gamma \langle \dot{Q}_2 \rangle + (\bar{\Omega}_2^2 - \delta\omega) \langle Q_2 \rangle = \left[\Lambda \langle Q_1 \rangle + f_2(t) + \langle f_s(t) \rangle \right]/M_2, \quad (2.132)$$

where $\langle \dots \rangle$ denotes the ensemble average over the surface temperature, and $\langle f_s \rangle$ is the surface fluctuation force given by

$$\langle f_s(t) \rangle = \left\langle \sum_{j=3} \lambda_j A_j \cos(\Omega_j t) \right\rangle. \quad (2.133)$$

γ and $\delta\omega$, the damping factor and frequency shift, respectively, are related to the coupling constant λ_j and the phonon density of states ρ by

$$\gamma = \frac{\pi}{2} \frac{\lambda_j^2(\bar{\Omega}_2)}{M_2 M_s \bar{\Omega}_2^2} \rho(\bar{\Omega}_2) , \quad (2.134a)$$

$$\delta\omega = \frac{1}{M_s} \int_0^\infty d\Omega_j \frac{\lambda_j^2(\Omega_j)}{M_2} \frac{\rho(\Omega_j)}{\Omega_j^2 - \bar{\Omega}_2^2} . \quad (2.134b)$$

In deriving Eqs. (2.132) - (2.134), we have used a Wigner-Weisskopf-type approximation and replaced the sum over the phonon modes by an integral over the associated phonon mode density of states $\rho(\Omega_j)$. The above classical results [Eq. (2.134)] are in exact agreement with our previous quantum-mechanical results where the level broadening and the level shift correspond to the damping factor and the frequency shift, respectively. It is important to note that, in Eq. (2.134), both the coupling constant $\lambda_j(\bar{\Omega}_2)$ and the phonon mode density $\rho(\bar{\Omega}_2)$ are evaluated at the frequency of the Ω_2 mode which is coupled to the surface phonon modes. For a Debye model spectrum $\rho(\Omega_j) = 3\Omega_j^2/\Omega_D$ with the cutoff frequency Ω_D , we obtain

$$\gamma = 3\pi\lambda_j^2(\bar{\Omega}_2) / (2M_2 M_s \Omega_D^3) , \quad (2.135a)$$

$$\delta\omega = \frac{3\lambda_j^2(\bar{\Omega}_2)}{M_2 M_s \Omega_D^2} \left[1 - \frac{\bar{\Omega}_2}{2\Omega_D} \ln \left| \frac{\Omega_D + \bar{\Omega}_2}{\Omega_D - \bar{\Omega}_2} \right| \right] . \quad (2.135b)$$

So far, we have reduced the many-body problem to a two-body problem described by the equations of motion (2.132) and (2.129b), where the surface-induced damping factor and frequency shift of the Ω_2 mode are introduced through the Langevin equation. We shall now further reduce the two-body system to a single-body system where the energy absorption profile may be exactly calculated. For this purpose, we consider the situation where only one of the normal modes is nearly resonant with the field and is strongly excited, namely $\bar{\Omega}_2 \approx \omega$. We further assume that mode 2 (with frequency $\bar{\Omega}_2$) is weakly coupled to mode 1 (with frequency $\bar{\Omega}_1 > \bar{\Omega}_2$) but is strongly coupled to the surface phonon modes via the single-phonon relaxation factor γ . The Langevin equation [Eq. (2.129)] reduces to a single-body equation of motion

$$\langle \ddot{Q}_2(t) \rangle + \gamma \langle \dot{Q}_2(t) \rangle + \bar{\Omega}_2^2 \langle Q_2(t) \rangle = v_2 \cos(\omega t) , \quad (2.136)$$

where we have assumed a "white noise" such that the surface fluctuating force has a zero ensemble average, i.e., $\langle f_s(t) \rangle = 0$, and the pumping rate v_2 is defined by the generalized laser driving force $f_2(t) = M_2 v_2 \cos(\omega t)$. The complete solution of Eq. (2.136) is found to be

$$\langle Q_2(t) \rangle = A_{ab} \sin(\omega t) + A_{el} \cos(\omega t) + e^{-\gamma t/2} [A_0 \cos(\omega'_2 t) + B_0 \sin(\omega'_2 t)] \quad (2.137)$$

with the initial values

$$A_0 = \langle Q_2(0) \rangle, \quad (2.138a)$$

$$B_0 = [\langle \dot{Q}_2(0) \rangle + \frac{1}{2}\gamma \langle Q_2(0) \rangle] / \omega'_2, \quad (2.138b)$$

where

$$\omega'_2 = \left[\bar{\Omega}_2^2 - (\frac{1}{2}\gamma)^2 \right]^{\frac{1}{2}}, \quad (2.138c)$$

$$A_{ab} = \gamma \bar{\Omega}_2^2 v_2 / Z, \quad (2.138d)$$

$$A_{el} = \left(\bar{\Omega}_2^2 - \omega^2 \right) v_2 / Z, \quad (2.138e)$$

$$Z = \left(\bar{\Omega}_2^2 - \omega^2 \right)^2 + (\gamma \omega)^2, \quad (2.138f)$$

$$\bar{\Omega}_2^2 = \Omega_2^2 - \delta \omega. \quad (2.138g)$$

The constants A_{ab} and A_{el} are referred to as the absorptive and the elastic amplitudes because the time-averaged power absorption is entirely due to the out-of-phase displacement $A_{ab} \sin(\omega t)$ [which leads to an in-phase velocity with respect to the driving field $v_2 \cos(\omega t)$]. The corresponding stored energy in the pumped mode is

$$\mathcal{E}(t) = E_0 \left[1 + e^{-\gamma t} - 2e^{-\gamma t/2} \cos [(\omega'_2 - \omega)t] \right] \quad (2.139a)$$

where E_0 is the steady-state energy given by

$$E_0 = \frac{e^2}{32M_2} E_{eff}^2 \left(\frac{\gamma}{\Delta_{opt}^2 + (\frac{1}{2}\gamma)^2} \right)^2. \quad (2.139b)$$

Here we have introduced an effective electric field acting on the mode 2 [see Eq. (2.126a)], for the classical effective charge $e = q_1 = -q_2$,

$$E_{eff} = \frac{\lambda_{2j} E_2 \cos(\theta_2) - \lambda_{1j} E_1 \cos(\theta_1)}{\left(\lambda_{1j}^2 + \lambda_{2j}^2 \right)^{\frac{1}{2}}}, \quad (2.140a)$$

and the optimum detuning

$$\Delta_{opt} = \Delta - K_2^* \left(A_{ab}^2 + A_{el}^2 \right) \quad (2.140b)$$

which is laser intensity dependent [see Eq. (2.138)]. By writing the laser intensity I as $E_{eff}^2 / (8\pi/c)$, the steady-state energy may be expressed in a

conventional form

$$E_0 = (2.5 \times 10^{-7}) \left(\frac{e^2 I}{M_2} \right) \left(\frac{\gamma}{\Delta_{\text{opt}}^2 + (\frac{1}{2}\gamma)^2} \right)^2, \quad (2.141)$$

where the units used are E_0 (eV), I (W/cm²), M_2 (amu), e (4.8 x 10⁻¹⁰ esu), and both the detuning and damping factor are in units of cm⁻¹.

To demonstrate the analogy between the quantum and the classical results, we investigate some of the limiting features of $\langle Q_2(t) \rangle$ and $\mathcal{E}(t)$ for $\gamma=0$ and $\Delta=0$. For the free-oscillator case, i.e., $\gamma=0$, the solution of Eq. (2.132) becomes

$$\langle Q_2(t) \rangle = \frac{2e}{M_2 \Delta_{\text{opt}}} E_{\text{eff}} \cos\left(\frac{1}{2}\Delta_{\text{opt}} t\right) \cos\left[\frac{1}{2}(\omega_2' + \omega)t\right], \quad (2.142)$$

and the energy absorption of the pumped mode is given by

$$\mathcal{E}(t) = \left(2\pi e^2 / c M_2 \right) E_{\text{eff}}^2 \left(\frac{1 - \cos(\Delta_{\text{opt}} t)}{\Delta_{\text{opt}}^2} \right), \quad (2.143)$$

which is an oscillatory function since the available energy, for the isolated B mode, will be necessarily transferred back and forth between the pumped mode and the laser field (via absorption and stimulated emission, in quantum-mechanical language). Note that Eq. (2.143) reduces to

$$\mathcal{E}(t) = \left(\pi e^2 / c M_2 \right) I t^2 \quad (2.144)$$

which is proportional to t^2 for the exact resonance case, i.e., $\Delta_{\text{opt}} = 0$.

The energy absorption given by Eq. (2.139) is shown in Fig. 12 for different sets of the optimum detuning Δ_{opt} and the damping factor γ . It is important to note that these energy absorption profiles are universal for all ranges of the laser intensity ($I = 1 - 10^{12}$ W/cm²) if the associated time scales are in units of γ^{-1} . For a comparison of the energy absorption profiles given by the reduced single-body Langevin equation [Eq. (2.131)] and those of a set of coupled equations for a many-body system [Eq. (2.118)], one may compare Fig. 11(C) with Fig. 12 and also Fig. 11(D) with the results shown in Eqs. (2.143) and (2.144).

Excitation with several lasers. We now extend the excitation of a single-body system by a single laser to the situation where several lasers of different frequencies are used. Recent experiments have demonstrated the advantage of using two lasers for the excitation of species in the gas phase, and recent quantum theoretical calculations support the experimental results.⁴⁵ We shall show that the results of the following classical treatment are identical to that of the

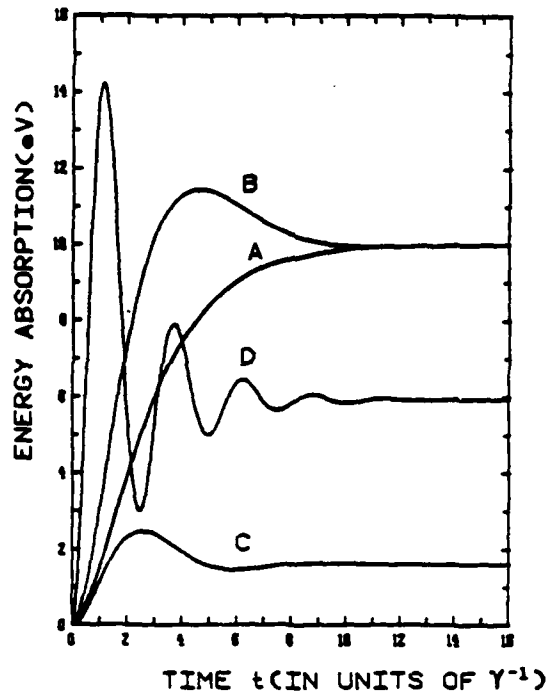


Fig. 12. Universal energy absorption profiles of the pumped mode for different sets of the optimum detuning Δ_{opt} and the damping factor (in units of cm^{-1}): curve A - $\Delta_{\text{opt}} = 0$, $\gamma = 2 \times 10^{-3}$; curve B - $\Delta_{\text{opt}} = 0.5\gamma = 5 \times 10^{-4}$; curve C - $\Delta_{\text{opt}} = \gamma = 10^{-3}$; curve D - $\Delta_{\text{opt}} = 2.5\gamma = 2.5 \times 10^{-4}$. The laser power is $I = 100 \text{ W/cm}^2$. Note that the time scales are shown in units of γ^{-1} .

quantum treatment.

Consider the equation of motion for an anharmonic oscillator subjected to two lasers at different frequencies [see Eq. (2.94)]

$$\ddot{x} + 2\gamma\dot{x} + \omega_{\text{eff}}^2 x = [f_1(t) + f_2(t)]/m, \quad (2.145)$$

where the driving radiation fields are given by

$$f_1(t) = eE_1 \cos(\omega_1 t),$$

$$f_2(t) = eE_2 \cos(\omega_2 t).$$

The steady-state solution of Eq. (2.145) is modulated by the two laser frequencies:

$$x_{\text{s.s.}}(t) = \sum_{i=1,2} [A_i \sin(\omega_i t) + B_i \cos(\omega_i t)],$$

which yields the steady-state power absorption averaged over the period of the field [cf. Eq. (2.98)]

$$\overline{p(t)} = \overline{p_I(t)} + \sum_{i=1,2} \left(\frac{e^2 E_i^2}{4m} \right) \left[\frac{\gamma}{(\Delta_i - K_i^* A_i^2)^2 + \gamma^2} \right], \quad (2.146)$$

where $\Delta_i = \omega_A - \omega_i$ are the detunings of the radiations, and the interference term $\overline{p_I(t)}$ is given by

$$\overline{p_I(t)} = \left(\frac{e}{2m} \right)^2 \left(E_1 E_2 \right) \sum_{i=1,2} \frac{\gamma \cos[(\omega_1 - \omega_2)t] - (\Delta_i - K_i^* A_i^2) \sin[(\omega_1 - \omega_2)t]}{(\Delta_i - K_i^* A_i^2)^2 + \gamma^2}$$

The interference term proportional to $E_1 E_2$ is likely to be negligible, since the magnitudes of the time-averaged quantities $\overline{\cos[(\omega_1 - \omega_2)t]}$ and $\overline{\sin[(\omega_1 - \omega_2)t]}$ are much smaller than those of the direct terms which involve $\overline{\cos(2\omega_i t)}$ and $\overline{\sin(2\omega_i t)}$ for $\omega_1 \neq \omega_2$. Therefore the absorption power $\overline{p(t)}$ is mainly due to the second terms in Eq. (2.146). Two important features of this two-laser excitation are: (i) due to the anharmonicity $K_i^* A_i^2$ there is an optimal detuning for which one gets maximum excitation for a fixed laser intensity; (ii) excitation via a single laser whose intensity equals $(V_1 + V_2)$ is less efficient than that obtained using two lasers at different frequencies. The latter can be understood as follows: In the initial stage of the excitations, the adspecies is excited mainly by the action of the first laser with $\omega_1 < \omega_A$. After the adspecies is highly excited, the second laser with $\omega_2 < \omega_1$ satisfies the near-resonance condition for the excitation of the anharmonic oscillator whose frequency is lower for higher energy. We note that this cooperative effect in utilizing several lasers for the excitation of anharmonic adspecies is due to nonlinear features of the system. The above classical results are consistent with those of a quantum model.⁴⁵

Classical versus quantum models. We can compare the above classical results with those of the quantum models using the following quasiquantum arguments:³⁹

$$e = \mu'(0) ,$$

$$\frac{1}{2} m \omega_0^2 A^2 = \langle n \rangle \hbar \omega_0 ,$$

where e is a classical charge, $\mu'(0)$ is the matrix element of the derivative of the dipole moment A is the amplitude and $\langle n \rangle$ is the quantum average excitation. This correspondence allows us to relate the results of the classical treatment to those of the quantum treatments as follows:

Quantities	Classical	Quantum
Steady-state excitation	Eq. (2.99)	Eq. (2.18), (2.25)
Transient energy	Eq. (2.139a)	Eq. (2.17), (2.76)
Many-body effects	Eq. (2.134)	Eq. (2.10), (2.33)
Equations of motion	Eq. (2.129)	Eq. (2.5), (2.84)
Rotating frame	Eq. (2.120)	Eq. (2.16), (2.32)

(c) "Almost first-principles" treatment. In the model calculations discussed earlier, the vibrational dynamics of IR LSSP were treated in terms of a variety of system parameters, including the laser-adspecies interaction strength V , the energy and phase-relaxation rates, γ_1 and γ_2 , respectively, the anharmonicity of the absorptive potential, ϵ^* , and the frequency mismatch between the laser and the active mode, Δ . From a first-principles point of view, the problem cannot, in general, be reduced to that of an adatom moving in a Morse-type one-dimensional potential. In fact, as will become clear later, the potential can at best be written as

$$V^{(0)}(\vec{r}) \equiv V^{(0)}(\vec{X}, z) = \sum_{\vec{G}} V_{\vec{G}}^{(0)}(z) e^{i\vec{G} \cdot \vec{X}} \quad (2.147)$$

where \vec{G} represents a two-dimensional reciprocal lattice vector, \vec{r} is the position vector of the adatom, $\vec{r} = (x, y, z) = (\vec{X}, z)$ and $V_{\vec{G}}^{(0)}(z)$ is the Fourier component of the potential $V^{(0)}(\vec{r})$ with respect to the x and y coordinates representing the surface plane. The Fourier component $V_{\vec{G}}^{(0)}(z)$ may look like an anharmonic Morse-type potential, but components with $\vec{G} \neq 0$ will in general be nonnegligible and contain important physical information.⁴⁶ This makes it impractical to define actual frequency mismatch and anharmonicity parameters for the system. Furthermore, since the solutions of a potential with two-dimensional periodicity along the xy -plane are broad bands separated by energy gaps which vary as a function of the two-dimensional wave vector,⁴⁷ it is also difficult to conceive of a single active mode with a fixed energy difference. The problems of phonon-stimulated desorption and inelastic scattering of atoms from solid surfaces have recently received considerable attention. The literature has been reviewed,^{48,49} and we shall only make brief comments for the sake of perspective. Treatments of these problems have ranged from classical and semiclassical to quantum mechanical. The latter have been mainly confined to linear-chain models with a Morse-type potential between the outermost lattice atom and the adatom. The few three-dimensional

treatments of these problems⁵⁰⁻⁵² have given rise to some controversy. For example, Bendow and Ying⁵⁰ use a three-dimensional treatment to obtain a value of the pre-exponential factor $\tau_0 \approx 10^{-5}$ s for C/Xe-Ne in Frenkel's formula for the desorption time

$$\tau = \tau_0 e^{E_a/k_B T_s} \quad (2.148)$$

where E_a is an effective well-depth of the adsorptive potential, k_B is Boltzmann's constant and T_s the surface temperature. However, Goodman and Romero⁵¹ obtain a value of $\tau_0 \approx 10^{-12}$ s using both one- and three-dimensional model treatments. This work and that of Kreuzer et al.⁵² further suggest that there is little difference between the results of one- and three-dimensional treatments of the desorption problem. The flash-desorption experiments of Cohen and King⁵³, on the other hand, seem to confirm the kind of trends obtained by Bendow and Ying, and emphasize the need for a deeper analysis of the theory.

In a series of papers, Adelman, Doll and coworkers⁵⁴⁻⁵⁷ have developed the generalized Langevin equation (GLE) approach to both scattering and desorption. This primarily classical approach combines the standard techniques of gas-phase scattering theory and that of generalized Brownian motion developed by Mori,⁵⁸ Kubo⁴⁴ and Zwanzig.⁵⁹ Projection operators are used to separate out the degrees of freedom associated with a 'primary' zone (the 'gas' atom and one or more surface atoms) and those associated with a 'secondary' zone (the rest of the atoms of the solid). The resulting equations of motion include the effects of the motion of the lattice atoms and the projectile as independent random forces with the coupling constants most effectively treated as phenomenological constants. While the Markoff or Brownian limit may not be justified for scattering off pure solids, the theory is appropriate for the treatment of slow processes such as desorption, migration or adsorption of heavy particles, or processes involving a strongly localized interaction between the 'gas' atom and the solid. In related work involving Monte Carlo sampling of classical stochastic trajectories for the incorporation of lattice many-body effects, Tully et al.^{60,61} suggest a technique which may be better suited for treatments of some types of dissociation, desorption and reactions than the Adelman model.

An alternative approach to the problems is represented by the close-coupling treatment of Wolken et al.⁶², who utilize an empirical potential (the London-Eyring-Polanyi-Sato, LEPS, potential) to compute classical trajectories, as well as a quantum mechanical three-dimensional treatment of molecule-solid energy transfer⁶³ in which internal modes of the molecule and one-phonon states of the solid are included. Both treatments give results in qualitative agreement with experiment. For hydrogen recombination on W(001), for example, the angular

distributions of desorbed species are found to be substantially noncosine in form and peaked toward the surface normal, in qualitative agreement with experiment. In another study of the dissociative adsorption of a diatom on a solid surface using the generalized Langevin method with a LEPS potential, Diebold and Wolken⁶⁴ find that energy accommodation and dissociative adsorption depend on the Debye temperature T_D of the solid, with an increase in T_D drastically lowering both energy transfer and the amount of dissociative adsorption.

The inelastic effects in the studies discussed so far have been due to phonon modes of the solid (and, to some extent, internal modes of the incident particle). However, band structure effects,^{46,47,65} which can also give rise to deviations from purely elastic scattering, were not included. By band structure effects we mean the trapping of particles whose wave vectors match those corresponding to bound states of the two-dimensionally periodic potential at the solid surface. This leads to the so-called selective adsorption. Identified in the past with minima in the intensity of specular reflections of atomic beams, selective-adsorption transitions have also been experimentally shown to give rise to maxima,⁶⁶ an observation recently confirmed theoretically by Weare and coworkers.⁶⁷ Very accurate quantum mechanical calculations have established these effects for a variety of systems with He/LiF being a prototype.⁶⁸

In a comparative study of some of the current techniques for treating atomic scattering from surfaces, Masel *et al.*⁶⁹ discuss the CCGM, quasiclassical, Kirchoff and semiclassical approximations. CCGM is an extensively used procedure based on a weak-coupling formalism with a unitarization step whose justification lies mainly in the computational convenience it affords; the Kirchoff approximation is an adaptation of the Eikonal approximation well-known in the field of optics; the semiclassical approximation consists of a description of states of the system in terms of sets of classical trajectories; and the quasiclassical method differs from the semiclassical in that phase interference is ignored and only angle-averaged intensities are computed. The conclusions of Masel *et al.* can be summarized as follows: CCGM is appropriate only for the case of weak coupling; the quasiclassical approximation gives qualitatively correct rainbow scattering but is incapable of reproducing the detailed structures due to quantum interference effects; the Kirchoff and semiclassical approximations provide the best quantitative agreement for scattering off sinusoidal hard walls except at low incident energies, a problem that can be overcome by employing a renormalization procedure.

The many-body aspects of phonon-stimulated migration, desorption and scattering of atoms or molecules at solid surfaces have been treated within a quantum-statistical framework by Metiu and coworkers.⁷⁰⁻⁷⁴ Zwanzig's projection operator

technique⁵⁹ is used to separate out particular degrees of freedom (phonons, migration, desorption) from the overall density matrix, and solutions of Liouville's equation involving correlation functions of the appropriate operators lead to probabilities of finding the particle in given states and at given sites as a function of time. Physical observables such as the mean square displacement can then be computed.⁷² An important facet of this work is the treatment of the case of strong interaction between the adspecies and the surface atoms.⁷¹ The induced distortion of the surface and the resulting change in the interaction potential between the adspecies and the surface are accounted for by renormalizing the Hamiltonian via a canonical transformation. The transformed degrees of freedom correspond to the motion of a pseudomolecule, consisting of the adspecies and the distorted atoms, with a renormalized mass. The other interactions can be treated perturbatively. For the migration problem,⁷¹ contributions to the mean square displacement $\langle R^2 \rangle_t$ can be due to coherent or incoherent hopping or incoherent excitation. It is found that for low temperatures, $\langle R^2 \rangle_t \propto t^2$, i.e., free-particle-like. For high temperatures, on the other hand, $\langle R^2 \rangle_t \propto t$, namely diffusional for short times. In an extension of the above calculation,⁷² horizontal, vertical and oblique transitions were included, namely transitions involving change of state but not site, change of site but not energy, and change of both site and energy, respectively. It is concluded that if tunnelling is minimal and migration is possible only when the particle is excited to a level above the potential barrier along the xy-plane via phonon excitation, the diffusion coefficient has an Arrhenius temperature dependence. If tunnelling is important, non-Arrhenius-type behavior may result.

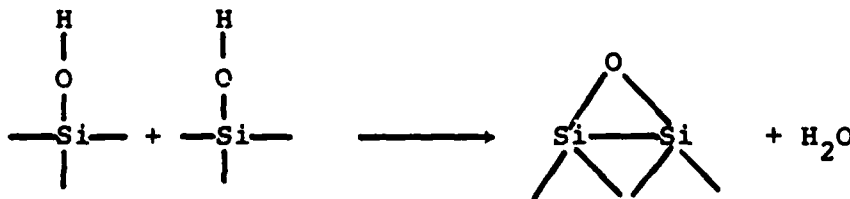
A one-dimensional model has been used to numerically obtain the rate of thermal desorption of an atom from a solid surface.^{73,74} With the atom-solid interaction simulated by a Morse potential between the adatom and the nearest surface atom, energy transfer takes place via a perturbation which is the difference between the instantaneous potential and its thermal average over the lattice atom positions. The transition rates computed with this perturbation and Fermi's golden rule are used in a master equation to obtain the probability of finding the atom in a given state as a function of time. This ignores memory effects which are important only if the relaxation time of the correlation function of the perturbation is of the same order as or larger than the time scale over which the probability changes appreciably. The results show again that the desorption rate does not fit the Arrhenius form except in a small temperature range. Since the potential is not expanded in normal coordinates, all multiphonon transitions are included. Detailed analysis of individual contributions shows that if the vibrational frequency of the chemisorptive bond is larger than the Debye frequency,

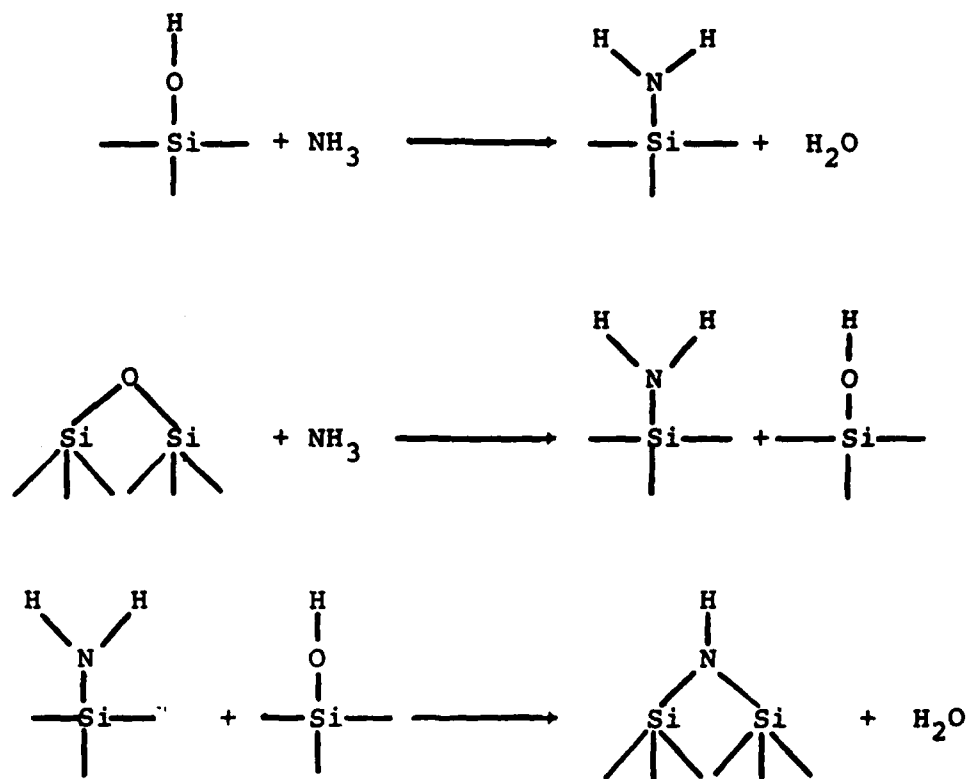
multiphonon processes to all orders must be included.⁷⁴

Kreuzer et al.⁷⁵⁻⁷⁷ have also presented a quantum-statistical theory of adsorption, flash desorption and isothermal desorption. Among the major conclusions of their work are: (i) a confirmation that Frenkel's formula for the desorption time, Eq. (2.148), is valid only for a small temperature range; (ii) the constant E_a can be up to 25% larger than the actual binding energy of the adparticle in the surface potential; (iii) one-dimensional and three-dimensional theories give similar results for the desorption times and the latter can be quite large ($\sim 10^{-5}$ s) as shown by experiment.

To summarize the results of the above survey, we note that, in general, multiphonon processes are important for a correct description of the energetics of surface processes. Physisorption and chemisorption must be treated quite differently, because a straightforward application of perturbation theory is not valid for the latter due to the strong chemical bonds between the adspecies and the surface. Band-structure effects resulting from the two-dimensional periodicity of the surface contain important physical information, but the similarity of results for desorption times from one- and three-dimensional models^{52,53} stresses the need for more first-principles analyses of this aspect of the problem. Most of these studies are effective in providing qualitative pictures of the dynamical processes taking place at the surface, but the dearth of information such as migration or relaxation rates limits their ability to quantitatively describe surface phenomena. Some of the necessary parameters can be obtained theoretically, but they are subject to uncertainties arising from the need to use empirical potentials, low dimensionality and assumptions such as simple additivity of transition rates due to different perturbations.

Let us pass on now to the problem of vibrational degrees of freedom involved in surface processes in the presence of laser radiation. Experimentally the problem has not been studied extensively. One of the earlier experiments involved dehydroxylation and reactions between amino groups and hydroxyl groups on a silica surface:¹¹





As a result of irradiation by a 10 W/cm^2 CO_2 laser, these reactions occurred at rates much higher than those for the corresponding thermal reactions; furthermore, these increased rates were only observed for laser frequencies close to the absorption peaks in the IR spectrum of the adsorbed molecules. While these are clear examples of selective LSSP, the exact mechanism responsible for the selectivity is not obvious. One possibility is the selective laser pumping of a particular vibrational mode of the adsorbed molecules, followed by enhanced migration, dissociation and desorption.¹¹ Alternatively, a mechanism involving electron transfer between adsorption sites has been suggested.¹⁷ Rough estimates of the lifetime of the vibrationally-excited states of the Si-N bond ($\tau \approx 10^{-11}$ s) tend to argue in favor of the electron-hopping mechanism, but there is no conclusive evidence for the validity of the latter. There are other instances of this type of LSSP^{12-14,16,20,78} as well as of the type where radiation is absorbed by the molecules in the gas phase, with subsequent reaction taking place at the solid surface.^{8-10,18,79,80} Again, it is difficult to describe the exact mechanism for the selective reactions, especially insofar as the rate-determining step is concerned.

There has been a steady growth in the theoretical literature on LSSP over the last five years, as reviewed and referred to in this article. However, not much

of this work is of a "first-principles" nature. In what follows we present an "almost first-principles" treatment of laser-stimulated excitation of vibrational degrees of freedom of an adspecies-solid system, as recently developed by Beri et al.⁸¹ This theory is free of phenomenological parameters (except those used to define an effective pair potential between the adatom and lattice atoms) and is therefore capable of providing a quantitative description of LSSP. The formalism attempts to describe the absorption of low-power infrared laser radiation by an adatom vibrating in an effective potential due to the atoms of the solid. This potential has the two-dimensional periodicity of the surface, which gives rise to stationary states with a band structure. At the present stage of the calculation, electronic degrees of freedom of the solid, which provide an important energy relaxation channel in metals, are not being considered. Preliminary theoretical study of such effects have been made by us (see Sec. 2.B) and Metiu et al.^{27,82}

The temporal evolution of the system can be described as follows. At time $t=-\infty$, the adatom gets adsorbed on the surface of the solid in a potential which neglects all lattice vibrations. The stationary states of such a potential correspond to a set of bands which reflect the translational symmetry along the xy-plane. Between $t=-\infty$ and $t=0$ the lattice vibrations are "turned on", modifying the original occupation state of the bands to a new average steady-state configuration at temperature T_B . At $t=0$, a low-power CW IR laser, described by a vector potential \vec{A} and frequency ω_L close to the energy gaps in important occupied regions of k-space, is turned on. It is further assumed that the laser frequency is far removed from important IR absorption bands of the solid. Energy from the electromagnetic field will then be absorbed primarily by the adatom-surface bond (the "adbond"). Since the latter is coupled to the solid, there will be an interchange of energy between the adbond and phonons. This energy interchange is the process of primary interest.

The potential function for an atom or molecule adsorbed on a solid can probably be computed from first-principles. This would involve the solution of a multi-center many-electron problem, necessitating the calculation of a very large number of complicated Coulomb and nonlocal exchange integrals for many positions of the adatom. Such a task is formidable and, to our knowledge, has not been attempted for any real system. Fortunately, knowledge of the detailed potential function is not necessary for a reasonable description of the dynamics of vibrational LSSP. Infrared spectra of diatomic molecules can be fitted quite well by assuming that the atoms interact via simple anharmonic potentials, such as the Morse or Lennard-Jones potential, involving two or three parameters.⁸³ We assume the potential between the atoms of the adparticle and each atom in the lattice to be such a pair potential. The effective potential obtained by summing these up should provide a

good semiquantitative description of the overall interaction — smooth periodic behavior along the xy-plane, a nearly infinite wall at $z=0$, minima for small values of z ($\sim 2\text{\AA}$), and a tail approaching the zero of energy asymptotically. In the case of periodic systems it is convenient to transform the problem into Fourier space, where the smoothness of the potential allows a good representation with only the lowest few components.

There are two distinct vantage points for viewing the energy interchange mentioned earlier. In the thermodynamic point of view, the two subsystems, namely the adbond and the phonon bath, are each assigned average temperatures T_A and T_B , respectively ($T_A > T_B$), so that energy flow is unidirectional and time evolution of the states of the subsystems is not studied. In the microscopic, more deterministic approach, time evolution of the states of the subsystems is followed in detail. Energy transfer in this case can be bidirectional, since upward transitions can take place in the adbond as a result of destruction of high-energy phonons and creation of lower energy ones in the solid. The rest of this section is devoted to a formulation based on the second approach.

The Hamiltonian for an adatom of mass m under the potential $v^{(0)}(\vec{r})$ due to the solid at equilibrium can be written as

$$\mathcal{H}_a^{(0)} = -\frac{\hbar^2}{2m} \nabla_{\vec{r}}^2 + v^{(0)}(\vec{r}) \quad (2.149)$$

where $v^{(0)}(\vec{r})$ is a sum of pair potentials $v(\vec{r}-\vec{R}_\ell^{(0)})$ between the adatom at position \vec{r} and lattice particles at equilibrium positions $\vec{R}_\ell^{(0)}$:

$$v^{(0)}(\vec{r}) = \sum_{\ell} v(\vec{r}-\vec{R}_\ell^{(0)}) \quad (2.150)$$

$v(\vec{r}-\vec{R}_\ell^{(0)})$ can be chosen to be a Morse, Lennard-Jones or other convenient form of pair potential. While isotropic (angle-independent) forms are most convenient, those with angular dependence provide a better representation of band-structure effects.^{46,84} The actual instantaneous potential is obtained by replacing the $\vec{R}_\ell^{(0)}$ by the instantaneous positions \vec{R}_ℓ ,

$$v(\vec{r}) = \sum_{\ell} v(\vec{r}-\vec{R}_\ell) \quad (2.151)$$

and the difference

$$\Delta \mathcal{H} = v(\vec{r}) - v^{(0)}(\vec{r})$$

is the perturbation responsible for energy interchange between the adbond and the lattice vibrations.

The complete Hamiltonian for the adatom-solid system contains, in addition to

$\mathcal{H}_a^{(0)}$ and $\Delta\mathcal{H}$, the Hamiltonian for the harmonic lattice $\mathcal{H}_v^{(0)}$; the interaction of the laser field with the adbond provides another perturbation \mathcal{H}_r . Thus the total Hamiltonian is

$$\mathcal{H} = \mathcal{H}_a^{(0)} + \mathcal{H}_v^{(0)} + \Delta\mathcal{H} + \mathcal{H}_r \quad (2.152)$$

$$\equiv \mathcal{H}^{(0)} + \Delta\mathcal{H} + \mathcal{H}_r, \quad (2.153)$$

where we have defined $\mathcal{H}^{(0)}$ to be the sum of $\mathcal{H}_a^{(0)}$ and $\mathcal{H}_v^{(0)}$. The solutions for the harmonic lattice⁸⁵ and those for the adbond^{46,47,65,84,86} in the potential $v^{(0)}(\vec{r})$ can be obtained by well-known techniques which will be briefly reviewed for completeness. Overall solutions of $\mathcal{H}^{(0)}$ are then just products of solutions of $\mathcal{H}_a^{(0)}$ and $\mathcal{H}_v^{(0)}$.

The transformation of the real coordinates $R_\ell^{(0)}$ of the lattice particles to normal (phonon) coordinates $q_b(\vec{k})$, where b represents a branch in the phonon band structure and \vec{k} is a wave vector in the first Brillouin zone (FBZ) of the reciprocal lattice, gives rise to a Hamiltonian for the harmonic lattice of the form

$$\mathcal{H}_v^{(0)} = (1/2) \sum_{\vec{k}b} \left[\dot{q}_b^2(\vec{k}) + \omega_b^2(\vec{k}) q_b^2(\vec{k}) \right] \quad (2.154)$$

where $\omega_b(\vec{k})$ is the frequency. The transformation is based on a Born-Oppenheimer approximation and the inclusion of only harmonic terms in the interatomic potential Φ_{Ξ} , Ξ being a particular electronic state of the crystal. The crystal is thereby reduced to a set of $3\beta N$ noninteracting one-dimensional harmonic oscillators, where β is the number of atoms in a unit cell and N is the number of unit cells in the crystal.

The Schrödinger equation for the crystal is

$$\frac{1}{2} \sum_{\vec{k}b} \left[-\hbar^2 \frac{\partial^2}{\partial q_b^2(\vec{k})} + \omega_b^2(\vec{k}) q_b^2(\vec{k}) \right] \Psi_v^{(0)} = \mathcal{E}_v^{(0)} \Psi_v^{(0)}, \quad (2.155)$$

where $\Psi_v^{(0)}$ is the total wave function for the crystal in a state $|\{v_b(\vec{k})\}\rangle$ described by the set of phonon occupation numbers $\{v_b(\vec{k})\}$. Since the phonons represent noninteracting harmonic oscillators, $\Psi_v^{(0)}$ can be written as a product of single-oscillator wave functions $\psi_{v_b(\vec{k})}^{(0)}$:

$$\Psi_v^{(0)} = \prod_{\vec{k}b} \psi_{v_b(\vec{k})}^{(0)} [q_b(\vec{k})]. \quad (2.156)$$

The Schrödinger equation, Eq. (2.155), then reduces to $3\beta N$ single-oscillator

equations

$$\Psi_{v_b(\vec{k})}^{(0)} \psi_{v_b(\vec{k})}^{(0)} [q_b(\vec{k})] = \mathcal{E}_{v_b(\vec{k})}^{(0)} \psi_{v_b(\vec{k})}^{(0)} [q_b(\vec{k})] \quad (2.157)$$

where $\Psi_{v_b(\vec{k})}^{(0)}$ is the expression within the braces in Eq. (2.155). The solutions of Eq. (2.157) are well known,

$$\psi_{v_\sigma}^{(0)}(q_\sigma) = \sqrt{2 \frac{v_\sigma \omega_\sigma}{\pi \hbar}} \frac{1}{v_\sigma!} e^{-\omega_\sigma q_\sigma^2 / 2\hbar} H_{v_\sigma} \left[\sqrt{\frac{\omega_\sigma q_\sigma}{\hbar}} \right], \quad (2.158)$$

where H_{v_σ} is the v_σ th-order Hermite polynomial, and we have used the abbreviated forms v_σ , q_σ and ω_σ for $v_b(\vec{k})$, $q_b(\vec{k})$ and $\omega_b(\vec{k})$, respectively. The total lattice vibrational energy of the solid in a state $\{|v_\sigma\rangle\}$ described by the set of phonon occupation numbers $\{v_\sigma\}$ is then given by

$$\mathcal{E}_v^{(0)} = \sum_{\vec{k}b} \mathcal{E}_{v_b(\vec{k})}^{(0)} \quad (2.159)$$

$$= \sum_{\vec{k}b} \left[v_b(\vec{k}) + \frac{1}{2} \right] \hbar \omega_b(\vec{k}). \quad (2.160)$$

It is useful to define phonon creation and annihilation operators a_σ^\dagger and a_σ , respectively,

$$a_\sigma^\dagger = \frac{1}{\sqrt{2\hbar}} \left(\sqrt{\omega_\sigma} q_\sigma - \frac{i}{\sqrt{\omega_\sigma}} \dot{q}_\sigma \right), \quad (2.161)$$

$$a_\sigma = \frac{1}{\sqrt{2\hbar}} \left(\sqrt{\omega_\sigma} q_\sigma + \frac{i}{\sqrt{\omega_\sigma}} \dot{q}_\sigma \right), \quad (2.162)$$

in terms of which

$$\Psi_v^{(0)} = \sum_{\sigma} \hbar \omega_\sigma \left[a_\sigma^\dagger a_\sigma + \frac{1}{2} \right]. \quad (2.163)$$

Use of the relations

$$a_\sigma^\dagger |v_1, v_2, \dots, v_\sigma, v_{\sigma+1}, \dots\rangle = \sqrt{v_\sigma + 1} |v_1, v_2, \dots, (v_\sigma + 1), v_{\sigma+1}, \dots\rangle \quad (2.164)$$

and

$$a_\sigma |v_1, v_2, \dots, v_\sigma, v_{\sigma+1}, \dots\rangle = \sqrt{v_\sigma} |v_1, v_2, \dots, (v_\sigma - 1), v_{\sigma+1}, \dots\rangle \quad (2.165)$$

greatly simplifies the calculation of matrix elements of operators which are functions of phonon coordinates or momenta, q_σ or \dot{q}_σ , between multiphonon states $\{|v_\sigma\rangle\}$. Of particular importance is the lattice displacement operator

$$\vec{u}_\ell \equiv \vec{R}_\ell - \vec{R}_\ell^{(0)} = \left(\frac{\hbar}{2NM} \right)^{\frac{1}{2}} \sum_{\vec{k}b} \frac{\vec{e}_b(\vec{k})}{[\omega_b(\vec{k})]^{\frac{1}{2}}} e^{i\vec{k} \cdot \vec{R}_\ell} \begin{pmatrix} a_{\vec{k}b} + a_{-\vec{k}b}^+ \\ -\vec{k}b \end{pmatrix}, \quad (2.166)$$

M being the mass of the lattice atoms (assuming one atom per unit cell), and $\vec{e}_b(\vec{k})$ a phonon polarization vector.

Let us now examine the nature of the solutions for the adbond, represented by the Schrödinger equation

$$\Psi_a^{(0)} \psi_a^{(0)} = \mathcal{E}_a^{(0)} \psi_a^{(0)}, \quad (2.167)$$

with $\psi_a^{(0)}$ given by Eq. (2.149). The potential $v^{(0)}(\vec{r})$ is periodic along the plane of the surface, i.e.,

$$v^{(0)}(\vec{r} + \vec{x}_\ell^{(0)}) = v^{(0)}(\vec{r}) \quad (2.168)$$

for all two-dimensional (2D) lattice vectors $\vec{x}_\ell^{(0)}$ given by

$$\vec{x}_\ell^{(0)} = \left(x_{1\ell}^{(0)}, x_{2\ell}^{(0)} \right) = n_1 \vec{a}_1 + n_2 \vec{a}_2, \quad (2.169)$$

n_1, n_2 being integers and \vec{a}_1, \vec{a}_2 primitive surface lattice vectors. The periodicity allows a partial Fourier expansion of $v^{(0)}(\vec{r})$ in the 2D real space represented by the plane of the surface with A_u the area of a 2D unit cell on the surface,

$$v^{(0)}(\vec{r}) \equiv v^{(0)}(\vec{x}, z) = \sum_{\vec{G}} v_{\vec{G}}^{(0)}(z) e^{i\vec{G} \cdot \vec{x}}, \quad (2.170)$$

$$v_{\vec{G}}^{(0)}(z) = A_u^{-1} \int d\vec{x} v^{(0)}(\vec{x}, z) e^{-i\vec{G} \cdot \vec{x}}, \quad (2.171)$$

the summation running over all 2D reciprocal lattice vectors (RLV) \vec{G} given by

$$\vec{G} = m_1 \vec{b}_1 + m_2 \vec{b}_2, \quad (2.172)$$

$$\vec{b}_1 = \frac{2\pi(\vec{a}_2 \times \hat{z})}{\vec{a}_1 \cdot (\vec{a}_2 \times \hat{z})}, \quad (2.173)$$

$$\vec{b}_2 = \frac{2\pi(\hat{z} \times \vec{a}_1)}{\vec{a}_1 \cdot (\vec{a}_2 \times \hat{z})}. \quad (2.174)$$

Here \hat{z} is an arbitrary vector in the z-direction and m_1 and m_2 are integers. Thus, for any plane parallel to the surface plane, the 2D RLV are completely specified by two integers m_1 and m_2 , and we can write

$$v_{\vec{G}}^{(0)}(z) \equiv v_{m_1 m_2}^{(0)}(z) \quad (2.175)$$

The Fourier series in Eq. (2.170) converges quite rapidly, and often the function $v_{m_1 m_2}^{(0)}(z)$ becomes negligible for $m_1, m_2 \geq 2$ as compared to its values for $m_1, m_2 < 2$. There is evidence for this in recent calculations using summed pair potentials^{46,47,68} and in the qualitative success of models^{69,87} using pure sinusoidal functions for $v^{(0)}(\vec{r})$.

The stationary states for a single particle in a periodic potential are characterized by a quasicontinuum of quantum numbers, namely 2D wave vectors

$$\vec{\eta} = \frac{v_1}{N_1} \vec{b}_1 + \frac{v_2}{N_2} \vec{b}_2 \quad ; \quad (2.176)$$

v_1 and v_2 are integers, and N_1 and N_2 signify the large number of unit cells along the a_1 - and a_2 -directions, respectively, beyond which the crystal surface is repeated. The single-particle states $\psi_a^{(0)}$ must then satisfy the Born-von Karman boundary conditions on a surface,

$$\psi_a^{(0)}(\vec{r} + N_1 \vec{a}_1) = \psi_a^{(0)}(\vec{r} + N_2 \vec{a}_2) = \psi_a^{(0)}(\vec{r}) \quad , \quad (2.177)$$

leading to Bloch functions

$$\psi_{aj\vec{\eta}}^{(0)}(\vec{r}) = \sum_{\vec{G}} \phi_{aj\vec{\eta}+\vec{G}}^{(0)}(z) e^{i\vec{G}\cdot\vec{r}} e^{i\vec{\eta}\cdot\vec{r}} \quad , \quad (2.178)$$

α and j being quantum numbers representing a band index and quantization of motion in the z -direction, respectively. The summation over all 2D RLV \vec{G} in Eq. (2.178) allows us to restrict $\vec{\eta} = \vec{\eta}_1 + \vec{\eta}_2$ to the 2D FBZ, namely the area defined by

$$-\frac{b_1}{2} \leq \eta_1 \leq \frac{b_1}{2} \quad ; \quad -\frac{b_2}{2} \leq \eta_2 \leq \frac{b_2}{2} \quad . \quad (2.179)$$

Using the expansions of $v^{(0)}(\vec{r})$ and $\psi_{aj\vec{\eta}}^{(0)}(\vec{r})$ in the Schrödinger equation, Eq. (2.167), we get

$$\sum_{\vec{G}} \left[-\frac{\hbar^2}{2m} \nabla_{\vec{r}}^2 + \sum_{\vec{G}'} v_{\vec{G}'}^{(0)}(z) e^{i\vec{G}'\cdot\vec{r}} - \epsilon_{aj\vec{\eta}}^{(0)} \right] \phi_{aj\vec{\eta}+\vec{G}}^{(0)}(z) \exp(i\vec{G}\cdot\vec{r}) \exp(i\vec{\eta}\cdot\vec{r}) = 0. \quad (2.180)$$

Because of symmetry associated with translation of the reciprocal lattice by RLV's, this reduces to

$$\sum_{\vec{G}} \left[\left[-\frac{\hbar^2}{2m} \nabla_z^2 + \frac{\hbar^2}{2m} (\vec{\eta} + \vec{G})^2 - \epsilon_{aj\vec{\eta}}^{(0)} \right] \phi_{aj\vec{\eta}+\vec{G}}^{(0)}(z) + \sum_{\vec{G}', \vec{G}-\vec{G}'} v_{\vec{G}'}^{(0)}(z) \phi_{aj\vec{\eta}+\vec{G}'}^{(0)}(z) \right] \exp[i(\vec{\eta}+\vec{G})\cdot\vec{r}] = 0, \quad (2.181)$$

which in turn leads to a set of coupled differential equations for the $\phi_{\alpha j \vec{\eta} + \vec{G}}^{(0)}(z)$ wave functions,

$$\left[-\frac{\hbar^2}{2m} \frac{d^2}{dz^2} + \frac{\hbar^2}{2m} (\vec{\eta} + \vec{G})^2 - \epsilon_{\alpha j \vec{\eta}}^{(0)} \right] \phi_{\alpha j \vec{\eta} + \vec{G}}^{(0)}(z) + \sum_{\vec{G}'} V_{\vec{G} - \vec{G}'}(z) \phi_{\alpha j \vec{\eta} + \vec{G}'}^{(0)}(z) = 0. \quad (2.182)$$

The functions $\psi_{\alpha j \vec{\eta}}^{(0)}(\vec{r})$ are constructed from solutions of Eq. (2.182).

Let us now consider the terms $\Delta \mathcal{H}$ and \mathcal{H}_r . The simplest situation is one where $\Delta \mathcal{H}$ and \mathcal{H}_r are small independent perturbations which can be assumed to act sequentially but not simultaneously. However, that is seldom the case, and it is necessary to define the limitations of such an approach and available alternatives.

The phenomenological studies described earlier provide some insight into these problems. They suggest that the applicability of a perturbative approach can be based on quantities such as the relative time scales of the adbond vibration and the phonons, the associated energy gap and the effective coupling between the two. Thus, for high temperatures, large optical pumping rates, very strong bonding between the adatom and the surface, or a very small energy difference between the adbond vibrational frequency and the Debye frequency of the solid, a perturbative approach is inadequate. In the case of strong interaction, for example, the separation of adbond degrees of freedom and vibrational degrees of freedom of the solid is inappropriate, and it becomes necessary to define a new basis set which is a combination of the two.⁷¹ A similar situation prevails when the "fundamental" of the adbond vibration is very close to the Debye frequency of the solid. This is analogous to the case where an adatom has valence electrons in a level whose energy is the same as that of one of the valence electronic states of the solid; the resulting strong interaction broadens the electronic level of the adatom and splits it into effective bonding and antibonding levels, completely changing its original form.⁸⁸ The Magnus approximation⁸⁹ is another alternative that has been suggested when dealing with situations involving near-degeneracy or strong interactions. For the case of very intense laser fields, multiphoton processes become important, and processes such as surface damage and melting need to be considered. Such effects are beyond the scope of this review, and we restrict ourselves to low or moderate laser powers.

There are two well-known approaches for dealing with multiphonon effects. The first involves a Taylor expansion of the perturbation potential about the equilibrium configuration of lattice atoms, namely

$$\begin{aligned} \Delta \mathcal{H} &= v(\vec{r}) - v^{(0)}(\vec{r}) \\ &= \sum_{\ell} \vec{u}_{\ell} \cdot \left[\vec{\nabla}_{\ell} v(\vec{r}) \right]_0 + \sum_{\ell \ell'} (\vec{u}_{\ell} \vec{u}_{\ell'}) : \left[\vec{\nabla}_{\ell} \vec{\nabla}_{\ell'} v(\vec{r}) \right]_0 + \sum_{\ell \ell' \ell''} (\vec{u}_{\ell} \vec{u}_{\ell'} \vec{u}_{\ell''}) : \left[\vec{\nabla}_{\ell} \vec{\nabla}_{\ell'} \vec{\nabla}_{\ell''} v(\vec{r}) \right]_0 + \dots \end{aligned} \quad (2.183)$$

The first term leads to one-phonon transitions, the second term to two-phonon transitions and so on, with higher-order terms getting successively more complicated. While the one-phonon term describes the situation where the Debye frequency ω_D is larger than the "active-mode" frequency ω_A of the adbond quite well,⁷⁴ one really needs multiphonon terms to all orders for the case where $\omega_D < \omega_A$. The latter is impractical within the framework of the Taylor expansion of Eq. (2.183). An alternative method, in which $\Delta\mathcal{H}$ is not expanded in terms of lattice displacements, employs instead a Fourier expansion of $V(\vec{r})$ and $V^{(0)}(\vec{r})$ which converges very quickly because of the smoothness of the potential. It can be shown that, with

$$v_{\vec{q}} = V_u^{-1} \int d\vec{r} v(\vec{r}) e^{-i\vec{q}\cdot\vec{r}}, \quad (2.184)$$

V_u being the volume of a unit cell over which the integration is done and \vec{q} a wave vector in the FBZ, one can write

$$v^{(0)}(\vec{r}) = \sum_{\ell} \sum_{\vec{q}} v_{\vec{q}} e^{i\vec{q}\cdot(\vec{r}-\vec{R}_{\ell}^{(0)})} \quad (2.185)$$

and

$$v(\vec{r}) = \sum_{\ell} \sum_{\vec{q}} v_{\vec{q}} e^{i\vec{q}\cdot(\vec{r}-\vec{R}_{\ell})}, \quad (2.186)$$

so that

$$\Delta\mathcal{H} = \sum_{\vec{q}} \left[v_{\vec{q}} e^{i\vec{q}\cdot\vec{r}} \sum_{\ell} \left[e^{-i\vec{q}\cdot\vec{R}_{\ell}} - e^{-i\vec{q}\cdot\vec{R}_{\ell}^{(0)}} \right] \right]. \quad (2.187)$$

Phonon operators to all orders are now included in the lattice sum of exponentials involving \vec{R}_{ℓ} , and this form is retained throughout most of the calculation of the transition rates. A Taylor expansion is still possible in the last stages of the computation if one wishes to analyze the results in terms of contributions due to one, two, three or more phonon processes.

The last term in the Hamiltonian \mathcal{H}_r represents the interaction energy of the laser field with the effective dipole moment of the adbond. If \vec{p} is the momentum of the adatom, e_0 a residual effective charge residing on it, $\vec{A}(\vec{r}, t)$ the vector potential at the position of the adatom at time t , $\vec{\epsilon}$ a unit polarization vector, \vec{k} the wave vector and ω_L the frequency of the laser field, we can write

$$\vec{A}(\vec{r}, t) = A_0 \vec{\epsilon} \exp[i(\vec{k}\cdot\vec{r} - \omega_L t)] + c. c. \quad (2.188)$$

$$\mathcal{H}_r = \frac{e_0}{2m} (\vec{p}\cdot\vec{A} + \vec{A}\cdot\vec{p}). \quad (2.189)$$

If the incoming flux of photons is large enough for absorption to dominate

emission, the complex conjugate part (c.c.) of Eq. (2.188) can be neglected.

Having set up the total Hamiltonian, the temporal evolution of the system can now be described in terms of occupation probabilities and transition rates for the stationary states of $\Psi^{(0)}$. When the laser field is turned on ($t=0$), the system is in a state described by the Hamiltonian $\Psi^{(0)} + \Delta\Psi$; for all subsequent times, the Hamiltonian is $\mathcal{H} = \Psi^{(0)} + \Delta\Psi + \mathcal{H}_r$. Writing the composite zero-order state $|\alpha_j \vec{n}\rangle | \{v_0\} \rangle$ as $|\lambda\rangle$, and the corresponding energy as $\epsilon_\lambda^{(0)}$, the zero-order Schrödinger equation becomes

$$\Psi^{(0)} |\lambda\rangle = \epsilon_\lambda^{(0)} |\lambda\rangle \quad (2.190)$$

In the presence of $\Delta\Psi$, we write the state of the system as a linear combination of the states $|\lambda\rangle$:

$$\Psi = \sum_{\lambda} c_{\lambda}(t) |\lambda\rangle e^{-i\epsilon_{\lambda}^{(0)} t/\hbar} \quad (2.191)$$

Using this expansion in the equation

$$(\Psi^{(0)} + \Delta\Psi)\Psi = i\hbar \frac{\partial \Psi}{\partial t} \quad (2.192)$$

we obtain

$$\frac{d}{dt} c_{\lambda}(t) = (i\hbar)^{-1} \sum_{\lambda'} c_{\lambda'}(t) \langle \lambda | \Delta\Psi | \lambda' \rangle e^{i(\epsilon_{\lambda}^{(0)} - \epsilon_{\lambda'}^{(0)}) t/\hbar} \quad (2.193)$$

Assuming the system to be initially in the state $|\bar{\lambda}\rangle$, we obtain the amplitude for finding the system in the state $|\lambda\rangle$ as an infinite time-ordered series⁹⁰

$$c_{\lambda}(t) = \sum_{s=0}^{\infty} \left\langle \lambda \left| \frac{I_s(t)}{s!} \right| \bar{\lambda} \right\rangle \quad (2.194)$$

$$I_s(t) = (i\hbar)^{-s} \hat{\mathcal{T}} \int_0^t dt_1 \int_0^{t_1} dt_2 \dots \int_0^{t_{s-1}} dt_s \Delta\Psi(t_1) \Delta\Psi(t_2) \dots \Delta\Psi(t_s) \quad (2.195)$$

$\hat{\mathcal{T}}$ being the Dyson chronological operator which orders products of time-dependent operators from left to right, with successively decreasing times. For example,

$$\hat{\mathcal{T}} \hat{\mathcal{O}}(t_1) \hat{\mathcal{P}}(t_2) = \begin{cases} \hat{\mathcal{O}}(t_1) \hat{\mathcal{P}}(t_2), & t_1 > t_2 ; \\ \hat{\mathcal{P}}(t_2) \hat{\mathcal{O}}(t_1), & t_2 > t_1 . \end{cases} \quad (2.196)$$

Also $I_0(t) = 1$, and $\Delta\Psi(t)$ is the perturbation operator in the interaction representation,

$$\Delta\Psi(t) = e^{i\Psi^{(0)} t/\hbar} \Delta\Psi e^{-i\Psi^{(0)} t/\hbar} \quad (2.197)$$

We retain only the $s = 1$ term in Eq. (2.194) to obtain the probability of finding the system in the state $|\lambda\rangle$ for $t \rightarrow \infty$, namely,

$$P_{\lambda}^{(0)} \equiv |c_{\lambda}(t)|^2 = |\langle \lambda | I_1(t) | \bar{\lambda} \rangle|^2 = \hbar^{-2} \left| \int_0^t dt' \langle \lambda | \Delta W | \bar{\lambda} \rangle e^{i(\mathcal{E}_{\lambda}^{(0)} - \mathcal{E}_{\bar{\lambda}}^{(0)})t'/\hbar} \right|^2 \quad (2.198)$$

$$= (2\pi t/\hbar) |\langle \lambda | \Delta W | \bar{\lambda} \rangle|^2 \delta(\mathcal{E}_{\lambda}^{(0)} - \mathcal{E}_{\bar{\lambda}}^{(0)}) \quad (2.199)$$

This expression is based on assumptions inherent in a Fermi Golden rule-type treatment, namely negligible back-transition from the excited states $|\lambda\rangle$ to lower-lying states and a finite small duration τ of the weak perturbation, but one that is larger than the lifetimes of the states $|\lambda\rangle$. For the case of ΔW which does not have a small τ associated with it, the back-transitions need to be considered, so that one uses a formula for the actual probability P_{λ} of finding the system in a state $|\lambda\rangle$ of the type

$$\frac{dP_{\lambda}^{(0)}}{dt} = \sum_{\lambda'} \left[W^{(0)}(\lambda' \rightarrow \lambda) P_{\lambda'}^{(0)} - W^{(0)}(\lambda \leftarrow \lambda') P_{\lambda}^{(0)} \right] \quad (2.200)$$

$W^{(0)}(\lambda' \rightarrow \lambda)$ are transition rates that may be obtained, for example, from Eq. (2.199), where the probability is linear in time, leading to $W^{(0)}$'s which are constants.

With a configuration described by the set of values $\{P_{\lambda}^{(0)}\}$, we now consider the effects of the perturbation

$$\psi' = \Delta W + \psi_r \quad (2.201)$$

If ψ_r represents CW laser radiation, then ΔW and ψ_r must be considered as acting simultaneously. For the sake of simplicity we assume that the probability $P_{\lambda}^{(0)}$ can be factored into one referring to the phonons and another referring to the adbond,

$$P_{\lambda}^{(0)} = P_{\alpha j \vec{n}}^{(0)} P_{\{v_{\sigma}\}}^{(0)} \quad (2.202)$$

An expression for the total transition rate $W_{(\lambda' \rightarrow \lambda)}$ can then be obtained in analogy with Eq. (2.199):

$$W_{(\lambda' \rightarrow \lambda)} = \left(\frac{2\pi}{\hbar} \right) \left| P_{\alpha j \vec{n}}^{(0)} P_{\{v_{\sigma}\}}^{(0)} - P_{\alpha' j' \vec{n}'}^{(0)} P_{\{v_{\sigma}'\}}^{(0)} \right| \left| \langle \lambda | \Delta W | \lambda' \rangle \right|^2 \delta(\mathcal{E}_{\lambda}^{(0)} - \mathcal{E}_{\lambda'}^{(0)}) \quad (2.203)$$

Here $P_{\alpha j \vec{n}}^{(0)}$ is the probability of finding the adbond state $|\alpha j \vec{n}\rangle$ after the laser field ψ_r is turned on and can in turn be obtained by a procedure similar to that used in deriving $P_{\lambda}^{(0)}$.

For the sake of simplicity, we make the following notational substitutions:

$$|\alpha j \vec{n}\rangle \rightarrow |e\rangle \quad (\text{'excited' adbond state})$$

$$\begin{aligned}
|\alpha'j'\vec{n}'\rangle &\rightarrow |g\rangle && \text{('ground' adbond state)} \\
|\{v_0\}\rangle &\rightarrow |i\rangle && \text{('initial' phonon state)} \\
|\{v_0'\}\rangle &\rightarrow |f\rangle && \text{('final' phonon state)}
\end{aligned}$$

Dropping all superscript zeros, Eq. (2.203) then becomes

$$W(fg \leftarrow ie) = \left(\frac{2\pi}{\hbar}\right) \left(P_i P_e - P_f P_g\right) \left| \langle ie | \Delta \mathcal{H} | fg \rangle \right|^2 \delta(\mathcal{E}_i + \mathcal{E}_e - \mathcal{E}_f - \mathcal{E}_g) \quad (2.204)$$

Since the quantities of interest are the rates of transition between adbond states, a summation over all initial and final phonon states $|i\rangle$ and $|f\rangle$ can be performed to give a rate denoted by $W(g \leftarrow e)$. The probabilities P_i and P_f can be written as $Z_\beta e^{-\beta \mathcal{E}_i}$ and $Z_\beta e^{-\beta \mathcal{E}_f}$, respectively, where $\beta \equiv (k_B T_S)^{-1}$ and $Z_\beta \equiv \left(\sum_i e^{-\beta \mathcal{E}_i}\right)^{-1}$. The term involving the probabilities can then be written as

$$\left(P_i P_e - P_f P_g\right) = Z_\beta \left(e^{-\beta \mathcal{E}_i} P_e - e^{-\beta \mathcal{E}_f} P_g\right) \quad (2.205)$$

$$= Z_\beta e^{-\beta \mathcal{E}_i} \left(P_e - P_g e^{-\beta \Delta \mathcal{E}_{eg}}\right), \quad (2.206)$$

where

$$\Delta \mathcal{E}_{eg} = \mathcal{E}_e - \mathcal{E}_g = \hbar \omega_{eg}. \quad (2.207)$$

In writing Eq. (2.206) we have used the fact that, because of the delta function, we must have

$$\mathcal{E}_f - \mathcal{E}_i = \mathcal{E}_e - \mathcal{E}_g. \quad (2.208)$$

Finally, we make the substitution

$$P_{eg} \equiv \left(P_e - P_g e^{-\beta \Delta \mathcal{E}_{eg}}\right) \quad (2.209)$$

to obtain

$$W(g \leftarrow e) = \frac{2\pi Z_\beta}{\hbar} \sum_i \sum_f e^{-\beta \mathcal{E}_i} P_{eg} \left| \langle ie | \Delta \mathcal{H} | fg \rangle \right|^2 \delta(\Delta \mathcal{E}_{eg} - [\mathcal{E}_f - \mathcal{E}_i]). \quad (2.210)$$

Using the Fourier expansion of $\Delta \mathcal{H}$, Eq. (2.187), in Eq. (2.210), we have

$$\begin{aligned}
W(g \leftarrow e) = \frac{2\pi Z_\beta}{\hbar} \sum_i \sum_f P_{eg} \sum_{\vec{q}} \sum_{\vec{q}'} \left\{ \langle e | v_{\vec{q}} e^{i\vec{q} \cdot \vec{r}} | g \rangle \langle g | v_{\vec{q}'}^* e^{-i\vec{q}' \cdot \vec{r}} | e \rangle \right. \\
\left. \sum_{\vec{\ell}} \sum_{\vec{\ell}'} \left\langle i \left| e^{i\vec{q} \cdot \vec{R}_{\vec{\ell}}} - e^{-i\vec{q} \cdot \vec{R}_{\vec{\ell}}^{(0)}} \right| f \right\rangle \left\langle f \left| e^{i\vec{q}' \cdot \vec{R}_{\vec{\ell}'}} - e^{-i\vec{q}' \cdot \vec{R}_{\vec{\ell}'}^{(0)}} \right| i \right\rangle \right\} \delta(\Delta \mathcal{E}_{eg} - [\mathcal{E}_f - \mathcal{E}_i]) \quad (2.211)
\end{aligned}$$

Explicit time dependence can now be introduced by utilizing the delta-function representation

$$\delta(\Delta E_{eg} - [\epsilon_f - \epsilon_i]) = (2\pi\hbar)^{-1} \int_{-\infty}^{\infty} dt e^{i(\Delta E_{eg} - [\epsilon_f - \epsilon_i])t/\hbar} \quad (2.212)$$

Incorporating the phonon energy difference portion of the integrand into the first phonon matrix element, one obtains

$$\langle i | e^{i\epsilon_i t/\hbar} \hat{\Theta} e^{-i\epsilon_f t/\hbar} | f \rangle = \langle i | e^{iW_v^{(0)} t/\hbar} \hat{\Theta} e^{-iW_v^{(0)} t/\hbar} | f \rangle \quad (2.213)$$

Exploiting completeness of the phonon states,

$$\sum_f | f \rangle \langle f | = 1 \quad , \quad (2.214)$$

and the definitions

$$\vec{R}_\ell \equiv \vec{R}_\ell^{(0)} + \vec{u}_\ell \quad , \quad (2.215)$$

$$f_{\vec{q},eg} \equiv \langle e | e^{i\vec{q} \cdot \vec{r}} | g \rangle \quad , \quad (2.216)$$

the transition rate can be written as

$$W(g \rightarrow e) = \hbar^{-2} \sum_{\vec{q}} \sum_{\vec{q}'} v_{\vec{q}} v_{\vec{q}'}^* f_{\vec{q},eg} f_{\vec{q}',eg}^* P_{eg} \sum_{\ell} \sum_{\ell'} \exp \left[-i \left(\vec{q} \cdot \vec{R}_\ell^{(0)} - \vec{q}' \cdot \vec{R}_{\ell'}^{(0)} \right) \right] \\ \times \int_{-\infty}^{\infty} dt \exp(i\omega_{eg}t) \left[Z_{\beta} \sum_i e^{-\beta\epsilon_i} \langle i | \exp \left[-i\vec{q} \cdot \vec{u}_\ell(t) - 1 \right] \exp \left[i\vec{q}' \cdot \vec{u}_{\ell'}(0) - 1 \right] | i \rangle \right] \quad (2.217)$$

Of the four terms in the phonon operator, only the product of exponentials contributes to the diagonal matrix element. The constant terms lead to a delta function with argument ω_{eg} when the Fourier transform is taken, and do not correspond to a transition. The individual exponentials involve operators which, on the whole, create or annihilate at least one phonon, as seen from the form of \vec{u}_ℓ , Eq. (2.166), and therefore have no diagonal matrix elements. The weighted mean of the surviving phonon operators, from the last term within square brackets, represents an ensemble average

$$Z_{\beta} \sum_i e^{-\beta\epsilon_i} \langle i | \exp \left[-i\vec{q} \cdot \vec{u}_\ell(t) \right] \exp \left[i\vec{q}' \cdot \vec{u}_{\ell'}(0) \right] | i \rangle \equiv \left\langle \left\langle \exp \left[-i\vec{q} \cdot \vec{u}_\ell(t) \right] \exp \left[i\vec{q}' \cdot \vec{u}_{\ell'}(0) \right] \right\rangle \right\rangle \quad (2.218)$$

whose evaluation has been discussed extensively in the literature.⁹¹ From the linearity of the operators \vec{u}_ℓ with respect to the creation and annihilation

a_{kb}^\dagger and a_{kb} , it follows that $[\hat{A}, \hat{B}]$ is a c-number, where \hat{A} and \hat{B} are the exponents in the ensemble average, i.e.,

$$\hat{A} \equiv -\vec{q} \cdot \vec{u}_\ell(t) \quad , \quad (2.219)$$

$$\hat{B} \equiv \vec{q}' \cdot \vec{u}_{\ell'}(t) \quad . \quad (2.220)$$

Thus,

$$\exp(\hat{A}) \exp(\hat{B}) = \exp(\hat{A} + \hat{B}) \exp[(1/2)[\hat{A}, \hat{B}]] \quad (2.221)$$

and

$$\langle\langle \quad \rangle\rangle = \langle\langle \exp[-i\vec{q} \cdot \vec{u}_\ell(t) + i\vec{q}' \cdot \vec{u}_{\ell'}(0)] \rangle\rangle \quad (2.222)$$

For operators $\hat{\Theta}$ linear in harmonic oscillator creation/annihilation operators, we have⁹²

$$\langle\langle \exp(i\hat{\Theta}) \rangle\rangle = \exp[-(1/2)\langle\langle \hat{\Theta}^2 \rangle\rangle_T] \quad (2.223)$$

T being the temperature. Use of the above leads to the results^{50,70,93}

$$\langle\langle \quad \rangle\rangle = \exp[-W_{\ell\ell'}(\vec{q}, \vec{q}') + \vec{q} \cdot \vec{C}_{\ell\ell'}^\dagger(t) \cdot \vec{q}'] \quad , \quad (2.224)$$

where

$$W_{\ell\ell'}(\vec{q}, \vec{q}') \equiv (1/2) \langle\langle (\vec{q} \cdot \vec{u}_\ell)^2 + (\vec{q}' \cdot \vec{u}_{\ell'})^2 \rangle\rangle \quad (2.225)$$

is a Debye-Waller-like factor, and

$$\vec{C}_{\ell\ell'}^\dagger(t) = \langle\langle \vec{u}_\ell(t) \vec{u}_{\ell'}(0) \rangle\rangle \quad (2.226)$$

is a correlation function involving the atomic displacements at sites ℓ, ℓ' at times t and 0 . The transition rate, Eq. (2.217), then becomes

$$W(\vec{q} \rightarrow \vec{q}') = \pi^{-2} \sum_{\vec{q}} \sum_{\vec{q}'} v_{\vec{q}} v_{\vec{q}'}^* f_{\vec{q}, eg} f_{\vec{q}', eg}^* P_{eg} \sum_{\ell} \sum_{\ell'} \exp[-i(\vec{q} \cdot \vec{R}_\ell^{(0)} - \vec{q}' \cdot \vec{R}_{\ell'}^{(0)})] \times \int_{-\infty}^{\infty} dt \exp[i\omega_{eg}t - W_{\ell\ell'}(\vec{q}, \vec{q}') + \vec{q} \cdot \vec{C}_{\ell\ell'}^\dagger(t) \cdot \vec{q}'] \quad . \quad (2.227)$$

The clear factorization of the rate expression into two components, one depending on the properties of the adbond and the other on those of the solid, is an attractive feature of this formalism. The basis of this separation lies in the treatment of momentum transfer and energy transfer as independent variables⁹⁴ via the Fourier expansion of ΔW .

The correlation function can be written in terms of specific collective properties of the phonons by using Eq. (2.166):

$$\begin{aligned} \langle\langle \vec{u}_\ell(t) \vec{u}_\ell(0) \rangle\rangle &= (\hbar/2NM) \sum_{\vec{k}b} \frac{\vec{e}_b(\vec{k}) \vec{e}_b^*(\vec{k})}{\omega_b(\vec{k})} \exp\left[i\vec{k} \cdot (\vec{R}_\ell - \vec{R}_{\ell'})\right] \left\{ \left[\bar{n}_{\vec{k}b} + 1 \right] \exp\left[-i\omega_b(\vec{k})t\right] \right. \\ &\quad \left. + \bar{n}_{\vec{k}b} \exp\left[i\omega_b(\vec{k})t\right] \right\}, \end{aligned} \quad (2.228)$$

where $\bar{n}_{\vec{k}b}$ is the Bose function

$$\bar{n}_{\vec{k}b} = \left(e^{\beta\hbar\omega_b(\vec{k})} - 1 \right)^{-1}. \quad (2.229)$$

One can utilize the quasicontinuous nature of the phonon band structure to replace the summation over wave vectors in Eq. (2.228) with an integration over \vec{k} -space,

$$\lim_{V \rightarrow \infty} \sum_{\vec{k}} F(\vec{k}) = \frac{NV}{8\pi^3} \int d\vec{k} F(\vec{k}), \quad (2.230)$$

where V is the volume of the crystal, to obtain

$$\begin{aligned} \vec{C}_{\ell\ell'}(t) &= \frac{\hbar V}{16\pi^3 M b} \int d\vec{k} \frac{\vec{e}_b(\vec{k}) \vec{e}_b^*(\vec{k})}{\omega_b(\vec{k})} \exp\left[i\vec{k} \cdot (\vec{R}_\ell - \vec{R}_{\ell'})\right] \left\{ \exp\left[-i\omega_b(\vec{k})t\right] \right. \\ &\quad \left. + 2\bar{n}_{\vec{k}b} \cos\left[\omega_b(\vec{k})t\right] \right\}. \end{aligned} \quad (2.231)$$

From Eq. (2.227), $W(\mathbf{g}+\mathbf{e})$ is seen to involve the time Fourier transform of $\exp\left[\vec{C}_{\ell\ell'}(t)\right]$. If a cumulants-type expansion is reasonable, the first-order term will dominate. For this case, a convenient expression can be obtained for the Fourier transform, namely,⁸⁵

$$\begin{aligned} \int_{-\infty}^{\infty} dt \left(\exp\left[i\omega_{eg}t\right] \right) \vec{C}_{\ell\ell'}(t) &= \left(\frac{\hbar V}{4\pi^2 M} \right) \left\{ \bar{n}(\omega_{eg}) + 1 \right\} \text{sgn}(\omega_{eg}) \sum_b \int d\vec{k} \left\{ \vec{e}_b(\vec{k}) \vec{e}_b^*(\vec{k}) \right. \\ &\quad \left. \times \exp\left[i\vec{k} \cdot (\vec{R}_\ell - \vec{R}_{\ell'})\right] \delta\left[\omega_{eg}^2 - \omega_b^2(\vec{k})\right] \right\}. \end{aligned} \quad (2.232)$$

Higher-order terms involve Fourier transforms of $\left[\vec{C}_{\ell\ell'}(t)\right]^n$ with $n > 1$. Clearly, the one-phonon term ($n=1$) dominates when $\left|\vec{C}_{\ell\ell'}(t)\right|/a^2 \ll 1$, where a is a typical lattice parameter. Evaluation of individual higher-order terms can be simplified by expressing $W(\mathbf{g}+\mathbf{e})$ as a Taylor expansion in $\vec{C}_{\ell\ell'}(t)$. One proceeds by writing

$$W(\mathbf{g}+\mathbf{e}) = \frac{1}{2\pi} \left(\frac{v_0}{\hbar} \right)^2 \int_{-\infty}^{\infty} dt \exp\left[i\omega_{eg}t\right] \sum_{\ell\ell'} F_{\ell\ell'} \left[\vec{C}_{\ell\ell'}(t) \right] \quad (2.233)$$

and

$$F_{\ell\ell'} \left[\vec{C}_{\ell\ell'}(t) \right] = F_{\ell\ell'}(0) + \sum_{\xi\xi'} \left\{ C_{\ell\ell',\xi\xi'} \left[\frac{\partial F_{\ell\ell'}}{\partial C_{\ell\ell',\xi\xi'}} \right]_0 + \frac{1}{2} C_{\ell\ell',\xi\xi'}^2 \left[\frac{\partial^2 F_{\ell\ell'}}{\partial C_{\ell\ell',\xi\xi'}^2} \right]_0 + \dots + \frac{1}{n!} C_{\ell\ell',\xi\xi'}^n \left[\frac{\partial^n F_{\ell\ell'}}{\partial C_{\ell\ell',\xi\xi'}^n} \right]_0 + \dots \right\}, \quad (2.234)$$

(ξ, ξ') being Cartesian indices (x, y, z) . The transition rate becomes⁸⁵

$$W(\mathbf{g} \rightarrow \mathbf{e}) = \left(\frac{v_0}{\hbar} \right)^2 \sum_{n=1}^{\infty} (n!)^{-1} \rho_{n,\ell\ell',\xi\xi'}(\omega_{eg}) \left[\frac{\partial^n F_{\ell\ell'}}{\partial C_{\ell\ell',\xi\xi'}^n} \right]_0, \quad (2.235)$$

where ρ_n is the Fourier transform of $C_{\ell\ell'}^n$,

$$\rho_{n,\ell\ell',\xi\xi'}(\omega_{eg}) = (2\pi)^{-1} \int_{-\infty}^{\infty} dt e^{i\omega_{eg}t} C_{\ell\ell',\xi\xi'}^n(t). \quad (2.236)$$

Use of the relationship

$$\int_{-\infty}^{\infty} d\omega_1 F_{\omega_1}(f_1) F_{\omega-\omega_1}(f_2) = F_{\omega}(f_1-f_2), \quad (2.237)$$

where $F_{\omega}(f)$ is the Fourier transform of $f(t)$ at ω ,

$$F_{\omega}(f) \equiv (2\pi)^{-1} \int_{-\infty}^{\infty} dt f(t) e^{i\omega t}, \quad (2.238)$$

gives a useful recursion relation between the ρ 's:

$$\rho_{n+1,\ell\ell',\xi\xi'}(\omega_{eg}) = \int_{-\infty}^{\infty} d\omega \rho_{n,\ell\ell',\xi\xi'}(\omega) \rho_{1,\ell\ell',\xi\xi'}(\omega_{eg}-\omega). \quad (2.239)$$

In developing Eq. (2.227) for the transition rate, the two-dimensional periodicity along the xy -plane has not been explicitly exploited. Important physical effects and simplifications of the formalism are associated with this periodicity, some of which we now examine.

The potential. The nature of the potentials $v^{(0)}(\vec{r})$ and $v(\vec{r})$ in Eqs. (2.150), (2.151), (2.185) and (2.186) is very different along the z -direction as compared to that along the xy -plane. Both must approach a constant for large z and be

essentially oscillatory on the xy-plane near the surface. It may also be necessary to allow for different contributions to the potentials due to ions at or near the surface and those deep in the bulk. Formally, the latter is accomplished by affixing an extra index to the pair potentials in Eqs. (2.150) and (2.151), namely,

$$v^{(0)}(\vec{r}) = \sum_{\ell} v_{z\ell} \left(\vec{r} - \vec{R}_{\ell}^{(0)} \right) \quad (2.240)$$

$$v(\vec{r}) = \sum_{\ell} v_{z\ell} \left(\vec{r} - \vec{R}_{\ell} \right) \quad (2.241)$$

Inclusion of these effects is probably most practical for purposes of a phenomenological description of LSSP. Writing Eqs. (2.185) and (2.186) in the forms

$$v^{(0)}(\vec{r}) = \sum_{q_z} \sum_{\vec{Q}} \left\{ \sum_{z_{\ell}^{(0)}} \left[\sum_{\vec{x}_{\ell}^{(0)}} e^{-i\vec{Q} \cdot \vec{x}_{\ell}^{(0)}} \right] e^{-iq_z z_{\ell}^{(0)}} v_{\vec{q}} \right\} e^{i\vec{q} \cdot \vec{r}} \quad (2.242)$$

and

$$v(\vec{r}) = \sum_{q_z} \sum_{\vec{Q}} \left\{ \sum_{z_{\ell}} \left[\sum_{\vec{x}_{\ell}} e^{-i\vec{Q} \cdot \vec{x}_{\ell}} \right] e^{-iq_z z_{\ell}} \right\} v_{\vec{q}} e^{i\vec{q} \cdot \vec{r}} \quad (2.243)$$

the summation over $\vec{x}_{\ell}^{(0)}$ in Eq. (2.242) reduces to $\delta(\vec{Q} - \vec{G})$, with $\vec{q} \equiv (\vec{Q}, q_z)$ and \vec{G} a primitive 2D reciprocal lattice vector in the plane of the surface. Such a reduction does not take place in Eq. (2.243) because the \vec{x}_{ℓ} are not fixed vectors. Because of the smallness of the atomic displacements from equilibrium, it is reasonable to use a sharply peaked (Gaussian or Lorentzian) function $\mathcal{D}_{\vec{G}}(\vec{Q})$, with the peak at $\vec{Q} = \vec{G}$, to replace the summation over \vec{x}_{ℓ} in Eq. (2.243). Eqs. (2.242) and (2.243) may therefore be written as

$$v^{(0)}(\vec{r}) = \sum_{q_z} \sum_{\vec{Q}} \left[\sum_{z_{\ell}^{(0)}} \left\{ \delta(\vec{Q} - \vec{G}) e^{-iq_z z_{\ell}^{(0)}} \right\} v_{\vec{q}} \right] e^{i\vec{q} \cdot \vec{r}} \quad (2.244)$$

and

$$v(\vec{r}) = \sum_{q_z} \sum_{\vec{Q}} \left[\sum_{z_{\ell}} \left\{ \mathcal{D}_{\vec{G}}(\vec{Q}) e^{-iq_z z_{\ell}} \right\} v_{\vec{q}} \right] e^{i\vec{q} \cdot \vec{r}} \quad (2.245)$$

The term $\mathcal{D}_{\vec{G}}(\vec{Q})$ represents the "inelasticity" of the transition process viewed as a scattering event, namely the departure from purely diffractive scattering described by $\delta(\vec{Q} - \vec{G})$ in Eq. (2.244). The averaging procedure implied in the use of $\mathcal{D}_{\vec{G}}(\vec{Q})$ is not always appropriate. In particular, if the characteristic time scale of the

overall relaxation process is comparable to or smaller than a typical period of vibration of the atoms in the solid, no such averaging is possible. Examination of Eqs. (2.211) - (2.217) with the aim of applying the forms (2.244) and (2.245) of the potential reveals a substantial simplification by allowing a reduction of the summations over \vec{R}_ℓ and \vec{R}_ℓ , to those over only z_ℓ and z_ℓ . This is an important step in establishing the connection between three-dimensional and one-dimensional treatments of LSSP.

Polarization eigenvectors. The terms $N^{-1/2} \vec{e}_b(\vec{k}) e^{i\vec{k} \cdot \vec{R}_\ell}$ in Eq. (2.166) represent components of the eigenvectors of the dynamical matrix in the harmonic approximation.⁸⁵ The z-component of \vec{k} must clearly be complex in order for the displacement function to damp out for $z \gg 0$. The displacement operator may then be written as

$$\vec{u}_\ell = \left(\frac{\hbar}{2NM} \right)^{1/2} \sum_b \sum_{\vec{k}} \left\{ \sum_{k_z} \frac{\vec{e}_b(k_z, \vec{k}) e^{ik_z z_\ell}}{\omega_b(k_z, \vec{k})} \right\} e^{i\vec{k} \cdot \vec{X}_\ell} \begin{bmatrix} a_{kb} + a_{-kb}^\dagger \\ -kb \end{bmatrix}. \quad (2.246)$$

Assuming a knowledge of the form of $\omega_b(\vec{k})$, the expression in curly brackets depends only on b , \vec{k} and z_ℓ , all dependence on k_z having been absorbed in the summation. This represents another point at which a phenomenological approach could be applied effectively, since a model for $\omega_b(\vec{k})$ could be introduced along with assumptions regarding the range of values for k_z .

Models for dispersion. In addition to $\vec{e}_b(\vec{k})$, a knowledge of $\omega_b(\vec{k})$ is necessary for actual evaluation of $W(q \rightarrow e)$. Detailed information on the form of $\omega_b(\vec{k})$ is available from experimental and theoretical studies of a number of systems, but for the present semiquantitative study, a model such as the Einstein or Debye model may suffice. In the former, phonon dispersion is entirely suppressed by assuming the form

$$\omega_b(\vec{k}) = \omega_0, \text{ a constant,} \quad (2.247)$$

which neglects all correlations between displacements of different lattice atoms, and by ascribing a single vibrational frequency to all points \vec{k} on all branches b . This model precludes energy transfer over a range of energies but does provide the simplest picture of phonon band structure. The Debye model, on the other hand, assumes a linear dispersion

$$\omega_b(\vec{k}) = v_s k \quad (2.248)$$

independently of branch index, and thereby allows for energy transfer over a (quasi-) continuous range. The use of Eq. (2.248) in conjunction with assumptions of isotropy and simple cubic structure reduces the expression for $\vec{C}_{\ell\ell}(\vec{k}, t)$ and the

Fourier transforms of $\left[\hat{C}_{ll}(t) \right]^n$ to computationally convenient forms.

(ii) Desorption and migration. The theory of laser-stimulated excitation can be applied to the dynamics of desorption and migration by specifying appropriate variables such as the mean square displacement $\langle R^2 \rangle$ or a threshold energy beyond which the adspecies shall be considered desorbed (or 'free'). There have been only a few attempts to apply theoretical methods to these problems due to the inherent difficulty associated with the many-body nature of the heterogeneous system. We shall review some of the quantum statistical techniques applied to these problems. In an early attempt, Slutsky and George⁹⁵ modeled the adbond as a truncated harmonic oscillator at the end of a linear chain, and considered the adatom desorbed when it reached the uppermost level. Couplings to acoustic phonon modes of the surface lattice and to the external coherent radiation field were represented in a second quantized form of the Hamiltonian. With a^\dagger, a the creation/annihilation operators for the adbond, the thermal average of the mean number of quanta at time t ,

$$\langle n(t) \rangle = \langle \langle a^\dagger(t) a(t) \rangle \rangle, \quad (2.249)$$

was obtained in a simple form. Since the anharmonicity of an actual potential will cause saturation for higher occupation states, the model of a harmonic oscillator overestimates the efficiency of the laser stimulation.

Some of these limitations were dealt with in the work of Lin and George,³⁰ where multiphoton effects, multiphonon effects and anharmonicity were considered within a quantum-stochastic treatment. A variety of line-broadening mechanisms were invoked to account for low-level excitation where anharmonicity and laser-adbond frequency mismatch have to be compensated for. In an associated calculation³¹ not directly applied to desorption, feedback between the phonon modes and the adbond was studied, and selective energy absorption was seen to peak at the same time for a range of values of the energy relaxation rate γ_1 . For some values of γ_1 , selective excitation was seen to initially drop and later pick up, suggesting a feedback mechanism in operation.

Other calculations of laser-stimulated desorption^{24,25,96} have employed either a Morse potential^{25,96} or a square-well potential.²⁴ Up to this stage, numerical calculations of LSSP which provide agreement with experiment to within one, two or even three orders of magnitude are considered acceptable! Details of the potentials therefore do not have a profound influence on the relative accuracy of the results. In the model of Jedrzejek *et al.*,²⁵ the adatom is considered desorbed if it occupies one of the continuum states of the Morse potential between the adatom and the outermost atom of a linear chain. The occupation probability

P_n for a state $|n\rangle$ is obtained by solving a master equation

$$\frac{\partial P_n}{\partial t} = \sum_m \left[W(n \leftarrow m) P_m(t) - W(m \leftarrow n) P_n(t) \right], \quad (2.250)$$

where $W(n \leftarrow m)$ is the total transition rate taken to be a simple sum of the rates due to phonons and the laser field as independent driving forces,

$$W(n \leftarrow m) = W^{\text{phonon}}(n \leftarrow m) + W^{\text{laser}}(n \leftarrow m). \quad (2.251)$$

Evaluation of the former has been discussed previously.⁷⁴ A golden rule form is used for $W^{\text{laser}}(n \leftarrow m)$ and as in most other calculations, a linewidth Γ_{nm} is ascribed to the transition. Estimates of the first mean passage time⁹⁷ to the continuum states as a function of laser power lead to the conclusion that, for CO/Cu, laser intensities of the order of 10^{10} W/cm² are needed. Similarly, in a purely classical calculation of laser-induced desorption of O from Si and H from Pb, threshold intensities greater than 10^8 W/cm² were obtained.⁹⁸ These results are fundamentally different from those of Lin *et al.*³⁰ An important physical mechanism which must be considered in laser-induced desorption is laser heating of the phonon modes and a feedback of energy to the adbond. This is manifested through the addition of an interference term in Eq. (2.251), and a first step in this direction to include the synergistic photon-phonon effect has been taken.^{35,99,100}

In dealing with the problem of laser-stimulated migration of excited adspecies, we begin with the dynamical Hamiltonian⁴²

$$H(t) = H_0(Q_1, Q_2, \dots, Q_j) + \sum_{k, k'} V_{kk'}(Q_1, Q_2, \dots, Q_j) c_k^\dagger c_{k'} + H_{AF}(t), \quad (2.252)$$

where H_0 is the unperturbed Hamiltonian of the system (with normal coordinates Q_j), $V_{kk'}(Q_j)$ is the lattice-site-dependent interaction potential of the system, and c_k^\dagger and $c_{k'}$ are the site-operators of the Bloch states $|k\rangle$ and $\langle k'|$, respectively, which can be expressed in terms of Wannier functions in the site-representation as

$$c_k^\dagger \equiv |k\rangle = \frac{1}{\sqrt{N}} \sum_n e^{i\vec{k} \cdot \vec{R}_n} |n\rangle, \quad (2.253)$$

$$c_{k'} \equiv \langle k'| = \frac{1}{\sqrt{N}} \sum_m e^{-i\vec{k}' \cdot \vec{R}_m} \langle m|. \quad (2.254)$$

Taylor expansion of the interaction potential, namely

$$V_{kk'}(Q_1, Q_2, \dots, Q_j) = V_0 + \sum_{j=1}^j \left(\frac{\partial V}{\partial Q_j} \right)_0 Q_j + \dots + \sum_{i,j'} \sum_p \frac{1}{p!(p+1)!} \left(\frac{\partial^{p+1} V}{\partial Q_i (\partial Q_{j'})^p} \right)_0 Q_i Q_{j'}^p + \dots, \quad (2.255)$$

gives us the general forms for the intramolecular couplings, p being the order of the multiphonon processes. Using the second-quantization expression of Eq. (2.255) and the Wannier site representation in Eqs. (2.253) and (2.254), we obtain, from Eq. (2.252), the microscopic model Hamiltonian as follows:

$$H(t) = H_A^0 + H_B^0 + H_C^0 + H_C' + H_1 + H_2 + H_3 + H_4 + H_{AF}(t), \quad (2.256a)$$

$$H_A^0 = \sum_n \hbar \omega_A a_n^\dagger a_n, \quad H_B^0 = \sum_j \hbar \omega_j b_j^\dagger b_j, \quad H_C^0 = E_0 \sum_n c_n^\dagger c_n, \quad (2.256b)$$

$$H_C' = \sum_{n,j} X_{nj} c_n^\dagger c_n (b_j^\dagger + b_j) + \sum_n Y_n c_n^\dagger c_n (a_n^\dagger + a_n) + \sum_{nj} Z_{nj} c_n^\dagger c_n (a_n^\dagger + a_n) (b_j^\dagger + b_j), \quad (2.256c)$$

$$H_1 = \sum_{n \neq m} J_{nm} c_n^\dagger c_m, \quad (2.256d)$$

$$H_2 = \sum_{n \neq m} K_{mn} c_n^\dagger c_m (a_n^\dagger + a_n), \quad (2.256e)$$

$$H_3 = \sum_j \sum_{n \neq m} G_{nm}^j c_n^\dagger c_m (b_j^\dagger + b_j), \quad (2.256f)$$

$$H_4 = \sum_j \sum_{n \neq m} W_{mn}^j c_n^\dagger c_m (a_n^\dagger + a_n) (b_j^\dagger + b_j) + [\text{higher-order terms}], \quad (2.256g)$$

$$H_{AF}(t) = \sum_{n \neq m} V(t) K_{nm} c_n^\dagger c_m (a_n^\dagger + a_n). \quad (2.256h)$$

The coupling parameters X_{nj} , Y_n , Z_{nj} , J_{nm} , K_{nm} , G_{nm}^j and W_{nm}^j are related to the derivatives of the interaction potential $V(Q_j)$ by

$$G_{nm}^j = F_{mn} X_{nj} = F_{nm} \left(\frac{\partial V}{\partial Q_j} \right)_0 \alpha_j, \quad (2.257a)$$

$$K_{nm} = F_{nm} Y_n = F_{nm} \left(\frac{\partial V}{\partial Q_A} \right)_0 \alpha_A, \quad (2.257b)$$

$$W_{nm}^j = F_{nm} Z_{nj} = F_{nm} \left(\frac{\partial^2 V}{\partial Q_A \partial Q_j} \right)_0 \alpha_A \alpha_j, \quad (2.257c)$$

$$J_{nm} = F_{nm} V_0, \quad F_{nm} = \frac{1}{N} e^{i\mathbf{K} \cdot (\mathbf{R}_n - \mathbf{R}_m)}, \quad (2.257d)$$

$$\alpha_A = \left[\hbar / \left(2m_A \omega_A \right) \right]^{\frac{1}{2}}, \quad \alpha_j = \left[\hbar / \left(2m_j \omega_j \right) \right]^{\frac{1}{2}}. \quad (2.257e)$$

The last term, H_{AF} - Eq. (2.256h), describes the active-mode/laser-field interaction in which

$$V(t) = \left[\hbar / \left(2m_A \omega_A \right) \right]^{\frac{1}{2}} (\mu_0' E) \cos(\omega t). \quad (2.257f)$$

Important features of $H(t)$ are: (i) the ground state site energy of the adspecies E_0 is perturbed by H_C' , which includes changes in site n due to direct interactions with the lattice and due to active-mode excitation, as well as an indirect interaction with the phonons via the active mode; (ii) the terms H_C^0 and H_1 represent parallel motion of the adspecies, $|J_{nm}|^2$ in H_1 being related to the intersite transition probability from site n to site m due to coherent motion; (iii) the terms H_2 and H_3 represent the perpendicular vibrational-motion-induced intersite transitions due to the active mode A and the bath modes B of the adspecies/surface system, respectively; (iv) H_4 is the A and B mode coupling-induced intersite transition; (v) finally, the excitation of the active mode, governed by $H_{AF}(t)$, provides the dominant driving force for intersite migration of the adspecies.

For the case of chemisorption on a lattice site, the equilibrium position of the adspecies is shifted due to the distortion of the lattice. In this case the adspecies-phonon interaction is very strong and perturbation theory cannot be used. It is possible, however, to use a canonical transformation to go to lattice-dressed operators A_n^+ , A_n , B_j^+ , B_j and $C_n^+ C_n$ which take into account the shifted equilibrium position of the adspecies and the lattice distortion.⁷¹ By employing the canonical transformation

$$Q = e^{-S} q e^S, \quad (2.258)$$

where Q stands for the dressed operator of q (q may be a_n^+ , a_n , b_j^+ , b_j , c_n or c_n^+), the generator of the transformation is given by

$$S = \sum_{n,j} c_n^+ c_n \left[\alpha_n (a_n^+ - a_n) + \beta_{nj} (b_j^+ - b_j) \right], \quad (2.259)$$

where α_n and β_{nj} are chosen as functions of the coupling constants, X_n^j and Y_n , so that the total energy of the system is minimized, i.e., $\partial H / \partial \alpha_n = \partial H / \partial \beta_{nj} = 0$.

The transformed total Hamiltonian of Eq. (2.256) in general is very complicated and will not be presented here. Instead, we investigate a simple case in which only the single-phonon coupling is included. The following model Hamiltonian written in terms of dressed operators is considered:

$$H(t) = \tilde{H}_0 + \tilde{H}_{AB} + \tilde{H}_C' + \tilde{H}_{AF}(t), \quad (2.260a)$$

$$\tilde{H}_0 = \tilde{E}_0 \sum_n C_n^\dagger C_n = \kappa \omega_{\text{eff}} A^\dagger A + \sum_j \kappa \omega_j B_j^\dagger B_j, \quad (2.260b)$$

$$\tilde{H}_{AB} = \sum_{n \neq m, j} \kappa \tilde{W}_{nm}^j C_n^\dagger C_n \left(A^\dagger B_j + AB_j^\dagger \right), \quad (2.260c)$$

$$\tilde{H}'_C = \sum_{n, j} \kappa \tilde{Z}_{nj} C_n^\dagger C_n \left(A^\dagger B_j + AB_j^\dagger \right), \quad (2.260d)$$

$$\tilde{H}_{AF}(t) = \sum_{n \neq m} \tilde{V}_{nm}(t) C_n^\dagger C_n \left(A^\dagger + A \right), \quad (2.260e)$$

$$\omega_{\text{eff}} = \omega_A - 2\epsilon^* A^\dagger A, \quad (2.260f)$$

where \tilde{E}_0 is the distortion energy, \tilde{W}_{nm}^j and \tilde{Z}_{nj} are the transformed coupling constants of W_{nm}^j and Z_{nj} , respectively, and $\tilde{V}(t)$ is the transformed laser-adspecies coupling constant of $V(t)K_{nm}$. Employing the many-body technique described in the previous sections, we obtain the equation of motion for the ensemble average $\langle\langle\langle \dots \rangle\rangle\rangle$ (over the A and B modes and the lattice site coordinates) of the active (A) mode and the lattice site transition probability:

$$\frac{d\langle A \rangle}{dt} = -i \langle \omega_{\text{eff}}(t) \rangle \langle A \rangle - iV(t) - \left[(\gamma_1 + \gamma_2 + \gamma_M) / 2 \right] \langle A \rangle, \quad (2.261a)$$

$$\frac{d\langle\langle n_A \rangle\rangle}{dt} = -i \langle\langle V(t)A^\dagger - V(t)A \rangle\rangle - (\gamma_1 + \gamma_M) \left(\langle\langle n_A \rangle\rangle - \bar{n}_0 \right), \quad (2.261b)$$

$$\frac{d\langle\langle p_n \rangle\rangle}{dt} = -2\gamma_M \left[\left(\langle\langle n_A \rangle\rangle + 1 \right) \bar{n}_B + \left(\bar{n}_B + 1 \right) \langle\langle n_A \rangle\rangle \right] \left[2\langle\langle p_n \rangle\rangle - \langle\langle p_{n+1} \rangle\rangle - \langle\langle p_{n-1} \rangle\rangle \right]. \quad (2.261c)$$

Here γ_2 is a dephasing factor and γ_1 is the phonon-coupling-induced damping factor given by^{100,101}

$$\gamma_1 = \sum_j |\tilde{Z}^j|^2 \gamma_B / \left[\Delta_j^2 + (\gamma_B/2)^2 \right], \quad (2.262a)$$

$$\Delta_j = \langle \omega_{\text{eff}} \rangle - \omega_j, \quad (2.262b)$$

where γ_B is the decay factor of the phonon (B) modes due to anharmonic coupling. In Eq. (2.262a) and in what follows we assume only nearest-neighbor contributions, namely, $Z_{nm}^j = Z_{n, n\pm 1}^j = Z^j$, etc. The migration-induced damping factor γ_M is given by¹⁰¹

$$\gamma_M = \sum_j |\tilde{W}^j|^2 \left[\frac{(\gamma_B/2) \cos(\lambda_j) - \Delta_j \sin(d\lambda_j)}{\Delta_j^2 + (\gamma_B/2)^2} \right], \quad (2.263)$$

where λ_j and d are the wavelength of the B-mode vibration and the lattice spacing

of the substrate. We note that both γ_1 and γ_M are given by a Lorentzian form which is due to the finite lifetime of the phonon modes, γ_B^{-1} , and thus give us a nonzero relaxation rate even for $\omega_{\text{eff}} > \omega_j$.⁹⁹ A simplified model which assumes an infinite phonon lifetime, i.e., $\gamma_B = 0$, results in delta functions for both γ_1 and γ_M , i.e., $\gamma_{1,M} \propto \int_j F(\omega_j) \delta(\omega_j - \omega_{\text{eff}})$, which are zero for single-phonon processes when $\omega_{\text{eff}} > \omega_j$.⁹⁵

From the coupled equations [Eq. (2.261)], we can calculate the lattice site occupation probability $\langle\langle P_n(t) \rangle\rangle$, which in turn gives us the mean-square displacement of the adspecies

$$\langle R^2(t) \rangle \equiv d^2 \sum_n n^2 \langle\langle P_n(t) \rangle\rangle, \quad (2.264)$$

and the diffusion (migration) coefficient

$$D = \lim_{t \rightarrow \infty} \left(\frac{\langle R^2(t) \rangle}{2t} \right). \quad (2.265)$$

The site probability function $\langle\langle P_n(t) \rangle\rangle$ is in general not analytically available due to the time-dependent excitation $\langle\langle n_A(t) \rangle\rangle$ which is nonlinearly coupled [Eq. (2.260e)]. For tractable results, we investigate the large damping case, $\gamma_{1,2} \gg \gamma_M$, such that the adspecies reaches its steady-state excitation $X \equiv \langle\langle n_A(t) \rangle\rangle_{\text{s.s.}}$ which is governed by a cubic equation [Eq. (2.25)]. Using this steady-state excitation, we may solve Eq. (2.261c) to obtain the quasi-steady-state site probability

$$\langle\langle P_n(t) \rangle\rangle = I_n(4Wt) e^{-4Wt} \quad (2.266)$$

where I_n is a modified Bessel function and

$$W = \left(2\bar{n}_B X + X + \bar{n}_B \right) \gamma_M. \quad (2.267)$$

Thus, from Eq. (2.264) and using the recursion relation for the modified Bessel functions, we obtain the mean-square displacement, which in turn yields the migration coefficient

$$D = 4Wd^2. \quad (2.268)$$

This is related to the laser intensity by a power law, I^p , $1 \leq p \leq 3$, since $W \propto I^p$, $p=1$ for low excitations for the harmonic case, $\epsilon^* = 0$, and $p=1/3$ for high excitations. We note that the above laser-enhanced migration constant, $D \propto W$, is governed by an Arrhenius form for the high-temperature limit, $kT \gg \hbar\omega_j$,

$$D = D_0 \exp \left(-E_A/kT \right), \quad (2.269)$$

where

$$E_A \propto \left[|\tilde{w}_j|^2 + |\tilde{z}_j|^2 \right] \hbar\omega_A \quad (2.270)$$

is the "activation energy" for migration. We finally note that the above Arrhenius form for the migration coefficient resulting from single-phonon processes is not necessarily true for multiphonon processes.^{100,101}

B. Electronic degrees of freedom

(i) Excitation to surface states and charge transfer. In a crystalline solid, the energy levels associated with the electrons form a number of quasicontinuous valence and conduction bands. For a metal the upper valence band and lower conduction band overlap; in a semiconductor, these two bands are separated by an energy gap. The electron charge density associated with these energy bands is more or less uniformly distributed throughout the crystal. With the addition of a surface, however, a number of additional bands and local states are formed.¹⁰² These surface bands correspond to a charge density localized in the surface region. By using a laser to excite electrons to or from these surface bands, the surface charge density could be increased or decreased.¹⁰³ The subsequent Coulombic interaction with an adspecies could enhance various surface processes.¹⁰⁴

Experimental studies¹⁰⁵ of synchrotron radiation on metal surfaces have already demonstrated that photon-stimulated desorption can occur through surface electronic excitation. This desorption process involves the excitation of a core electron of the adspecies, which is localized in the surface region, to the bulk energy bands of the solid. The resultant Coulombic repulsion is the cause of the desorption.¹⁰⁶

Studies¹⁰⁷ have also been conducted on the effects of laser radiation on the bulk electronic states. Using experimental band structures and time-dependent perturbation theory, the photon absorption rate for electronic states has been calculated for a variety of semiconductors. This rate can be quite appreciable for resonant laser frequencies.

In the following two sections, we will extend these time-dependent perturbation studies of the photon absorption processes to include surface states. Using a simple one-dimensional (1D) model, we will first examine the bulk electronic structure of a semiconductor. From this starting point, we will then show the origin of the surface states and calculate the photon absorption rate for excitation to these states. The effect on adspecies interaction will then be addressed. Finally, in the second section we will extend the theory developed in the first section for semiconductors to the case of a metal. This discussion will center around the effect of lattice vibrations on the photon absorption process.

(a) Semiconductors. For 1D wide-band semiconductors of infinite extent, the valence electron wave function can be written in terms of plane waves:¹⁰⁸

$$\psi_k(z) = \sum_G A_G e^{i(k-G)\left(z-\frac{a}{2}\right)}, \quad (2.271)$$

where k is the electron wave number, G is a reciprocal lattice wave vector, a is the lattice constant, and z is the direction parallel to the chain. Atoms are positioned at integer values of z/a . The plane waves with $G \neq 0$ represent the lattice scattering of the electron.

If the semiconductor chain is now truncated at $z = a/2$, the surface can reflect the plane waves; subsequently, the wave function within the semiconductor can now be written

$$\psi_k(z) = \sum_G \left[A_G e^{i(k-G)\left(z-\frac{a}{2}\right)} + B_G e^{-i(k-G)\left(z-\frac{a}{2}\right)} \right], \quad (2.272)$$

or in trigonometric representation

$$\psi_k(z) = \sum_G A'_G \sin \left[(k-G)\left(z-\frac{a}{2}\right) + \theta_{k-G} \right], \quad (2.273)$$

with the phase factor θ_{k-G} being obtained by matching with the wave function external to the semiconductor:

$$\psi_k(z) = \sum_G C_G e^{-q_{k-G}\left(z-\frac{a}{2}\right)}. \quad (2.274)$$

Eqs. (2.273) and (2.274) can be written in compact form as

$$\psi_k(z) = \sum_G \alpha_G \phi_{k-G}(z), \quad (2.275)$$

where $\phi_{k-G}(z)$ are the solutions to the particle in a square well potential:

$$\phi_{k-G}(z) = \left(\frac{2}{L}\right)^{\frac{1}{2}} \sin \left[(k-G)\left(z-\frac{a}{2}\right) + \theta_{k-G} \right] \quad (2.276)$$

for $z < a/2$ and

$$\phi_{k-G}(z) = \left(\frac{2}{L}\right)^{\frac{1}{2}} \sin \theta_{k-G} e^{-q_{k-G}\left(z-\frac{a}{2}\right)} \quad (2.277)$$

for $z > a/2$, with

$$q_{k-G} = \sqrt{2W - (k-G)^2} \quad (2.278)$$

$$\tan \theta_{k-G} = \frac{G-k}{q_{k-G}}, \quad (2.279)$$

where L is the length of the crystal and W is the sum of the work function and the

Fermi energy. If we assume

$$|\theta_{k-G}| = 0 \rightarrow \frac{\pi}{2} \quad (2.280)$$

our basis state will be odd in k ; on the other hand, if

$$|\theta_{k-G}| = \frac{\pi}{2} \rightarrow \pi \quad (2.281)$$

our basis state will be even in k .

In principle, the sum in Eq. (2.275) is over an infinite number of terms; however, the coefficients become very small as G increases. Consequently, within the nearly-free-electron (NFE) approximation,¹⁰⁸ we need only consider the lowest-order terms in G . Eq. (2.275) will now become

$$\psi_k(z) = \alpha_k \phi_k(z) + \alpha_{k-g} \phi_{k-g}(z) \quad (2.282)$$

where $g = 2\pi/a$. To obtain the parameters in Eq. (2.282), we must solve the Schrödinger equation:

$$\left[\frac{1}{2} \frac{d^2}{dz^2} + V(z) \right] \psi_k(z) = E_k \psi_k(z) \quad (2.283)$$

with

$$V(z) = \sum_{\ell=0}^N v(z+\ell a) \quad , \quad (2.284)$$

where N is the number of ions in the chain and $v(z+\ell a)$ is the screened potential for the ion at lattice site ℓa . Inserting Eq. (2.282) into (2.283) yields the secular equations:

$$\alpha_k \left[\frac{k^2}{2} - E_k \right] + \alpha_{k-g} V_g = 0 \quad (2.285a)$$

$$\alpha_k V_g^* + \alpha_{k-g} \left[\frac{(k-g)^2}{2} - E_k \right] = 0 \quad (2.285b)$$

where

$$V_g = \langle k-g | V(z) | k \rangle \quad . \quad (2.286)$$

We will assume that the matrix element, V_g , is independent of all k but the Fermi wavenumber k_F (on-Fermi-surface approximation).¹⁰⁹

To have a non-zero solution for the parameters in Eq. (2.285), the energy must be

$$E_k = \frac{1}{4} \left\{ \left[k^2 + (k-g)^2 \right] \pm \sqrt{\left[k^2 - (k-g)^2 \right]^2 + 4 E_g^2} \right\} \quad , \quad (2.287)$$

where the energy gap is given by

$$E_g = 2|V_g| . \quad (2.288)$$

After normalization the wave function is now

$$\psi_k(z) = \frac{1}{\sqrt{1 + \left[\frac{E_k - k^2/2}{V_g} \right]^2}} \left\{ \phi_k(z) + \frac{E_k - k^2/2}{V_g} \phi_{k-g}(z) \right\} . \quad (2.289)$$

Eqs. (2.287) and (2.289) constitute the solutions for the energies and wave functions for the bulk electrons in a 1D semiconductor. In our model we assume that $V_g > 0$. If the wave function, Eq. (2.289), is not to vanish at the top or bottom of the energy range, the basis states should be odd in k for the lower branch and even for the upper branch of the energy. The range of the phase factors, Eqs. (2.280) and (2.281), will be chosen accordingly.

The energy dispersion relation for this system is depicted in Fig. 13. The valence band (V) and the conduction band (C) are, respectively, the minus and plus branch solutions to Eq. (2.287). If the system is unexcited, the electronic states are completely occupied up to the top of the valence band and all other states are emptied.

In addition to this discussion of the bulk states, we are also interested in the surface electronic states.¹⁰³ To find these surface states the energy expression, Eq. (2.287), is analyzed for other solutions.¹⁰² It can be seen that real energies can be obtained if the electron wave number is

$$k = \frac{g}{2} + i\kappa . \quad (2.290)$$

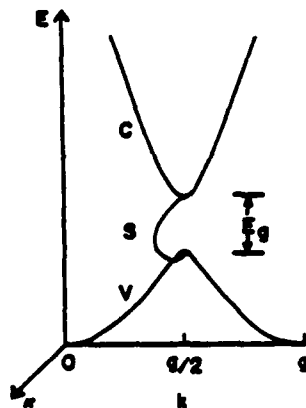


Fig. 13. Dispersion relationship in complex crystal momentum space ($k+i\kappa$) for a finite linear chain. The valence, surface and conduction bands are labeled V, S and C, respectively.

Inserting this into Eq. (2.287) we obtain

$$E_{\kappa} = \frac{1}{2} \left[\left(\frac{g}{2} \right)^2 - \kappa^2 \pm \sqrt{E_g^2 - \kappa^2 g^2} \right] , \quad (2.291)$$

where the range in values are for

$$|\kappa| = 0 \longrightarrow \frac{E_g}{g} . \quad (2.292)$$

To obtain the wave function for the surface states on the inside of the semiconductor, we insert Eq. (2.290) into our bulk wave function expansion, Eq. (2.273):

$$\psi_{\kappa}(z) = \sum_G A_G \sin \left[\left(\frac{g}{2} - G + i\kappa \right) \left(z - \frac{a}{2} \right) + \alpha + i\beta \right] , \quad (2.293)$$

where we have assumed that since k is complex it is reasonable by Eq. (2.279) that the phase factor is also complex:

$$\theta_{\kappa, G} = \alpha + i\beta . \quad (2.294)$$

If we now put Eq. (2.293) into exponential form and separate the real and imaginary components, we get

$$\psi_{\kappa}(z) = \sum_G A_G \left[e^{i \left[\left(\frac{g}{2} - G \right) \left(z - \frac{a}{2} \right) + \alpha \right]} - e^{-\left[\kappa \left(z - \frac{a}{2} \right) + \beta \right]} - e^{-i \left[\left(\frac{g}{2} - G \right) \left(z - \frac{a}{2} \right) + \alpha \right]} e^{\kappa \left(z - \frac{a}{2} \right) + \beta} \right] , \quad (2.295)$$

where a factor of $2i$ was absorbed into the coefficients.

Since there is no preferred surface, we expect

$$\left| \psi_{\kappa} \left(z = \frac{a}{2} \right) \right|^2 = \left| \psi_{\kappa} \left(z = \frac{a}{2} - L \right) \right|^2 . \quad (2.296)$$

For this to be valid, the wave function, Eq. (2.295), placed in this expression will yield terms like

$$\cosh(2\beta) - \cos(2\alpha) = \cosh[2(\beta - \kappa L)] - \cos[(G - g)L + 2\alpha] . \quad (2.297)$$

But g and G are reciprocal lattice vectors; therefore,

$$(G - g) L = n2\pi , \quad (2.298)$$

where n is an integer. Consequently, Eq. (2.297) becomes

$$\cosh(2\beta) = \cosh(2\beta - 2\kappa L) . \quad (2.299)$$

This condition only holds if

$$\beta = \frac{\kappa L}{2} \quad (2.300)$$

Following Lundqvist's¹⁰² lead, we will also assume

$$\kappa < 0 \quad (2.301)$$

Using Eqs. (2.300) and (2.301) in Eq. (2.297), we note that near the surface at $z = a/2$ the first term in our wave function is large and the second term is very small. Near the other surface at $z = a/2 - L$, the reverse is true. Thus the first term of Eq. (2.295) yields information on the surface electronic charge near $z = a/2$ and the second term, near $z = L - a/2$. Since we are only interested in the surface at $z = a/2$ and we assume L is very large, our surface wave function becomes

$$\psi_{\kappa}(z) = \sum_G A_G e^{i \left[\left(\frac{g}{2} - G \right) \left(z - \frac{a}{2} \right) + \alpha \right]} e^{-\kappa \left(z - \frac{a}{2} \right)} \quad (2.302)$$

where the exponentials depending on L have been absorbed into the coefficients.

It should be noted that, unlike the bulk wave function expansion, Eq. (2.273), the terms in this expression are not solutions to the particle in the square well since they would produce imaginary energies. Furthermore, the wave functions given by Eq. (2.302) are not acceptable bulk wave functions since they cannot be put into the Bloch form:¹⁰²

$$\psi_{\kappa}(z) = e^{i\kappa z} u_{\kappa}(z) \quad (2.303)$$

where $u_{\kappa}(z)$ has the periodicity of the lattice. The previously obtained bulk solutions, Eq. (2.282) with Eq. (2.277), can be cast into a form similar to this by adding the complex conjugate to the right side of Eq. (2.303).

To complete our solution we need to obtain the coefficients of Eq. (2.302). First, as for the bulk series, we truncate the surface series to two terms via the NFE approximation.¹⁰⁸ Then we insert our wave function into the Schrödinger equation to obtain our surface secular equation. This gives us an internal wave function similar in form to Eq. (2.289):

$$\psi_{\kappa}(z) = C_s \left\{ e^{i \left[\left(\frac{g}{2} \right) \left(z - \frac{a}{2} \right) + \alpha \right]} + \frac{E_{\kappa} - \frac{1}{2} \left(\frac{g}{2} + i\kappa \right)^2}{V_g} e^{-i \left[\left(\frac{g}{2} \right) \left(z - \frac{a}{2} \right) + \alpha \right]} \right\} e^{-\kappa \left(z - \frac{a}{2} \right)} \quad (2.304)$$

where C_s is the normalization constant. Using Eqs. (2.288) and (2.291), the coefficient of the second term can be written

$$\frac{E_{\kappa} - \frac{1}{2} \left(\frac{g}{2} + ik \right)^2}{V_g} = -e^{-i2\delta} \quad (2.305)$$

Inserting this into Eq. (2.304) and factoring, the wave function becomes

$$\psi_{\kappa}(z) = C_s \sin \left[\left(\frac{g}{2} \right) \left(z - \frac{a}{2} \right) + \theta_{\kappa} \right] e^{-\kappa \left(z - \frac{a}{2} \right)}, \quad (2.306)$$

where

$$\theta_{\kappa} = \alpha + \delta \quad (2.307)$$

and we have absorbed all factored constants into C_s .

To obtain the solution external to the semiconductor, we assume that the surface electrons feel a constant potential for $z > \frac{a}{2}$. Consequently,

$$\psi_{\kappa}(z) = C_s \sin \theta_{\kappa} e^{-q_{\kappa} \left(z - \frac{a}{2} \right)}, \quad (2.308)$$

where

$$q_{\kappa} = \sqrt{2(W - E_{\kappa})} \quad (2.309)$$

and

$$\tan \theta_{\kappa} = \frac{\left(\frac{g}{2} \right)}{\kappa - q_{\kappa}} \quad (2.310)$$

To be consistent with our bulk wave functions which are odd in k for the valence band and even for the conduction band, the surface phase factor has the range

$$|\theta_{\kappa}| = 0 \rightarrow \frac{\pi}{2} \quad (2.311)$$

for the lower surface

$$|\theta_{\kappa}| = \frac{\pi}{2} \rightarrow \pi \quad (2.312)$$

for the upper surface energy branch.

The normalization constant may be obtained by assuming the charge density is symmetric about the center of the semiconductor chain:

$$\int_{-\frac{L+a}{2}}^{\infty} dz |\psi_{\kappa}(z)|^2 = \frac{1}{2} \quad (2.313)$$

Using the surface wave function in this expression, we obtain

$$C_s = \left[\frac{e^{KL} - 1}{2\kappa} + \frac{\sin^2 \theta_\kappa}{g_\kappa} + \left(1 - (-1)^N e^{KL} \right) \frac{2\kappa \cos(2\theta_\kappa) - g \sin(2\theta_\kappa)}{(2\kappa)^2 + g^2} \right]^{-\frac{1}{2}} \quad (2.314)$$

For our purposes, L is considered very large (infinite) and κ is non-zero and negative, Eq. (2.301). Therefore

$$C_s = \left[\frac{\sin^2 \theta_\kappa}{g_\kappa} - \frac{1}{2\kappa} + \frac{2\kappa \cos(2\theta_\kappa) - g \sin(2\theta_\kappa)}{(2\kappa)^2 + g^2} \right]^{-\frac{1}{2}} \quad (2.315)$$

The surface states are completely determined by Eqs. (2.306), (2.309) and (2.315). The dispersion relation for the surface band(s) is illustrated in Fig. 13. Note that the surface band extends into the complex plane. Also, there is no surface state at the branch point which occurs near the center of the band:

$$E = \frac{1}{2} \left[\left(\frac{g}{2} \right)^2 - \left(\frac{E_g}{g} \right)^2 \right] \quad (2.316)$$

If we now shine a laser on our 1D semiconductor, we can induce electronic transitions from the bulk valence band to the surface states. To determine the transition rate, an integral of the following form must be evaluated:

$$H_{kk}(t) \equiv \langle k | \vec{A} \cdot \vec{p} | k \rangle \quad (2.317)$$

where \vec{A} is the vector potential of the laser radiation and \vec{p} is the momentum operator of the electron. Under the dipole approximation and assuming the laser is polarized parallel to the chain, $H_{kk}(t)$ becomes

$$H_{kk}(t) = -i \left(\frac{2\pi I}{137} \right)^{\frac{1}{2}} \left(\frac{e^{-i\omega t}}{\omega} \right) \langle k | \frac{d}{dz} | k \rangle \quad (2.318)$$

where I is the laser intensity and ω is the angular frequency.

The bulk wave function, Eq. (2.289), and the surface wave function, Eq. (2.306), can be written in the form

$$\psi_k(z) = e^{ikz} u_k(z) - e^{-ikz} u_k^*(z) \quad (2.319)$$

and

$$\psi_k(z) = e^{-\kappa \left(z - \frac{a}{2} \right)} e^{i \left(\frac{g}{2} \right) z} u_k(z) \quad (2.320)$$

where

$$u_k(z) = \frac{-i e^{-ik\frac{a}{2}}}{\sqrt{(2L) \left[1 + \left[\frac{E_k - k^2/2}{v_g} \right]^2 \right]}} \left(e^{i\theta_k} + \frac{E_k - k^2/2}{v_g} e^{i\theta_{k-g}} \right) \quad (2.321)$$

and

$$u_k(z) = C_s \sin \left[\left(\frac{g}{2} \right) \left(z - \frac{a}{2} \right) + \theta_k \right] e^{-i \left(\frac{g}{2} \right) z} \quad (2.322)$$

Both $u_k(z)$ and $u_{-k}(z)$ have the periodicity of the lattice. Using Eqs. (2.319) and (2.320), the integral in Eq. (2.318) now becomes

$$M \equiv \left\langle k \left| \frac{d}{dz} \right| k \right\rangle = \int_{\frac{a}{2}-L}^{\frac{a}{2}} dz e^{-\kappa \left(z - \frac{a}{2} \right)} e^{-i \left(\frac{g}{2} \right) z} u_k^*(z) \frac{d}{dz} \left[e^{ikz} u_k(z) \right] - \int_{\frac{a}{2}-L}^{\frac{a}{2}} dz e^{-\kappa \left(z - \frac{a}{2} \right)} \times e^{-i \left(\frac{g}{2} \right) z} u_k^*(z) \frac{d}{dz} \left[e^{-ikz} u_k^*(z) \right] \quad (2.323)$$

where we have assumed that for large L the contribution of the exponential tails, Eq. (2.289) with Eq. (2.277) and Eq. (2.308), to the integral will be negligible. The integration in Eq. (2.323) can be rewritten

$$\int_{\frac{a}{2}-L}^{\frac{a}{2}} dz \dots = \sum_{\ell=0}^{N-1} \int_{-\frac{a}{2}-\ell a}^{\frac{a}{2}-\ell a} dz \dots \quad (2.324)$$

If we change the variable of integration to $z + \ell a$ and exploit the periodicity of $u_k(z)$ and $u_{-k}(z)$, we obtain

$$M = \sum_{\ell=0}^{N-1} e^{i \left(\frac{g}{2} - k \right) \ell a} e^{-\kappa \ell a} B - \sum_{\ell=0}^{N-1} e^{i \left(k - \frac{g}{2} \right) \ell a} e^{-\kappa \ell a} B^* \quad (2.325)$$

where

$$B = \int_{-\frac{a}{2}}^{\frac{a}{2}} dz e^{-\kappa \left(z - \frac{a}{2} \right)} e^{-i \left(\frac{g}{2} \right) z} u_k^*(z) \frac{d}{dz} \left[e^{ikz} u_k(z) \right] \quad (2.326)$$

The transition probability is related to the square of Eq. (2.325):

$$M^2 = \sum_{m=0}^{N-1} \sum_{\ell=0}^{N-1} e^{i\left(\frac{g}{2}-k\right)(\ell-m)a} e^{\kappa(\ell+m)a} BB^* - \sum_{m=0}^{N-1} \sum_{\ell=0}^{N-1} e^{i\left(k-\frac{g}{2}\right)(\ell+m)a} e^{\kappa(\ell+m)a} B^{*2} + \text{c.c.} \quad (2.327)$$

where c.c. indicates the complex conjugate. If we change the range of summation, the sums in front of the first integral become

$$S_1 \equiv e^{\kappa(N-1)a} \sum_{m=\frac{1-N}{2}}^{\frac{N-1}{2}} \sum_{\ell=\frac{1-N}{2}}^{\frac{N-1}{2}} e^{i\left(\frac{g}{2}-k\right)(\ell-m)a} e^{\kappa(\ell+m)a} \quad (2.328)$$

Changing the summation variables to $s = \ell+m$ and $d = \ell-m$, we get

$$S_1 = e^{\kappa(N-1)a} \sum_{d=1-N}^{N-1} e^{i\left(\frac{g}{2}-k\right)da} \sum_{s=1-N+|d|}^{N-1-|d|} e^{\kappa sa} \quad (2.329)$$

where the prime signifies a count with an increment of 2. If N is very large, the sum over s will be only significantly affected by large values of d . Therefore for large N , we can approximate this function by

$$S_1 \approx e^{\kappa(N-1)a} \sum_{d=1-N}^{N-1} e^{i\left(\frac{g}{2}-k\right)da} \sum_{s=1-N}^{N-1} e^{\kappa sa} = e^{\kappa(N-1)a} \left[\frac{e^{\kappa Na} - e^{\kappa(1-N)a}}{e^{2\kappa a} - 1} \right] \sum_{d=1-N}^{N-1} e^{i\left(\frac{g}{2}-k\right)da} \quad (2.330)$$

Taking the limit as N goes to infinity, the function takes the form

$$S_1 = \frac{2\pi}{a} \frac{\delta\left(k-\frac{g}{2}\right)}{1-e^{2\kappa a}} \quad (2.331)$$

where $\delta\left(k-\frac{g}{2}\right)$ is the Dirac delta function.

The sums in front of the second integral of Eq. (2.327) are

$$S_2 = \sum_{m=0}^{N-1} \sum_{\ell=0}^{N-1} e^{i\left(k-\frac{g}{2}\right)(\ell+m)a} e^{\kappa(\ell+m)a} \quad (2.332)$$

The maximum value for this expression occurs at $k=\frac{g}{2}$ and falls off rapidly as you move from this point. Since for $k=\frac{g}{2}$ terms containing the sum of Eq. (2.332) are the only contribution to Eq. (2.327), the total must be much smaller than the value for $k=\frac{g}{2}$. Furthermore, it should be noted that when $k=\frac{g}{2}$ or $\kappa=0$, the first sum and the second are equal. Therefore, we will assume

$$S_2 \approx S_1 \quad (2.333)$$

Combining Eqs. (2.323), (2.325), (2.327), (2.331) and (2.333), we obtain

$$M^2 \approx \frac{2\pi}{a} \delta\left(k - \frac{g}{2}\right) \frac{\left| \left\langle \kappa \left| \frac{d}{dz} \right| k \right\rangle_0 \right|^2}{1 - e^{-2\kappa a}} \quad (2.334)$$

where the subscript zero indicates integration over the first unit cell. From Eq. (2.334), we see that the transition from a bulk to a surface state is only permitted if the real part of the crystal momentum, k , remains unchanged. This selection rule is not too surprising since it is an exact restriction on laser-induced transitions between bulk bands.¹¹⁰ Furthermore, for our model, it confines us to the top of the valence band where the density of states is a maximum (infinite) and the laser frequency needed for a transition is a minimum.

To first order, the transition rate from the valence band to the surface band is

$$T = \frac{2\pi}{t} \sum_{\kappa} \sum_k \left| \int_0^t dt' H_{\kappa k}(t') e^{i\omega_{\kappa k}(t')} \right|^2 \quad (2.335)$$

where

$$\omega_{\kappa k} = E_{\kappa} - E_k \quad (2.336)$$

Converting the sums to integrals, we get

$$T = \frac{2\pi}{t} \left(\frac{L}{\pi} \right) \left(\frac{2g}{E_g} \right) \int_0^g dk \int_0^{-E_g/g} d\kappa \left| \int_0^t dt' H_{\kappa k}(t') e^{i\omega_{\kappa k}(t')} \right|^2 \quad (2.337)$$

Using Eq. (2.318), we can perform the integration over t' and take the limit as t goes to infinity

$$T = \frac{8\pi}{137} \frac{IgL}{E_g \omega^2} \int_0^g dk \int_0^{-E_g/g} d\kappa \left| \left\langle \kappa \left| \frac{d}{dz} \right| k \right\rangle \right|^2 \delta(\omega_{\kappa k} - \omega) \quad (2.338)$$

Using the selection rule, Eq. (2.334), along with Eq. (2.323), this can be simplified to

$$T = \frac{8\pi}{137} \frac{I g^2 L}{E_g \omega^2} \int_0^{-E_g/g} d\kappa \frac{\left| \left\langle \kappa \left| \frac{d}{dz} \right| \frac{g}{2} \right\rangle_0 \right|^2}{1 - e^{-2\kappa a}} \delta(\omega_{\kappa k} - \omega) \quad (2.339)$$

After evaluating the integral over κ , the expression reduces to

$$T = \frac{8\pi}{137} \frac{I g^2 L}{E_g \omega^2} \frac{\left| \left\langle \kappa \left| \frac{d}{dz} \frac{g}{2} \right\rangle_0 \right|^2}{1 - e^{2\kappa a}} \left| \frac{d\kappa}{dE} \right|, \quad (2.340)$$

where κ in Eq. (2.340) refers to the state obeying the resonance condition:

$$\omega = \frac{1}{2} \left[E_g - \kappa^2 \pm \left(E_g^2 - \kappa^2 g^2 \right)^{\frac{1}{2}} \right]. \quad (2.341)$$

We now define the absorption cross section, σ :

$$\sigma \equiv \omega T / I \quad (2.342)$$

Using the wave functions, Eqs. (2.289) and (2.306), in Eq. (2.340) and taking the limit as L goes to infinity, the cross section becomes

$$\sigma = \frac{2\pi}{137} \frac{g^4}{E_g \omega \kappa^2} \frac{1 - e^{\kappa a}}{1 + e^{\kappa a}} C_s^2 \left| \frac{d\kappa}{dE} \right| \left[\frac{\kappa_g \cos \left(\theta_{\kappa + \frac{\theta}{2}} \right) + 2\kappa^2 \sin \theta_{\kappa} \cos \frac{\theta}{2} + g^2 \sin \left(\theta_{\kappa - \frac{\theta}{2}} \right)}{\theta^2 + g^2} \right]^2. \quad (2.343)$$

With Eq. (2.291) we can also readily evaluate the derivative:

$$\left| \frac{d\kappa}{dE} \right| = \left| \frac{\frac{1}{2} \frac{\left(E_g^2 - g^2 \kappa^2 \right)^{\frac{1}{2}}}{\kappa}}{2 \left(E_g^2 - g^2 \kappa^2 \right)^{\frac{1}{2}} \pm g^2} \right|. \quad (2.344)$$

Eqs. (2.343) and (2.344) constitute the cross section for electronic transitions from the valence band to the surface band. Although this cross section is quite complicated, we can readily deduce its behavior by analyzing the expressions at various limits.

If the exciting laser radiation is at a frequency near $\frac{1}{2}E_g$ [Eq. (2.316)], where $\kappa = -E_g/g$, Eq. (2.344) will vanish, and thus

$$\sigma_{\omega \approx E_g/2} = 0. \quad (2.345)$$

This is exactly what one would expect since this mid-gap energy is a branch point at which no surface states exist.

If the laser is near a frequency of 0 or E_g , the cross section becomes

$$\sigma_{\omega \rightarrow 0} = \frac{\pi}{137} \frac{a g^6}{\left[\left(\frac{g}{2} \right)^2 - \frac{g^2}{2} \right]^2} \frac{E_g}{\left(\frac{1}{2} g^2 - E_g \right)^2} \left| \frac{1}{\kappa} \right| \quad (2.346)$$

$$\sigma_{\omega \rightarrow E_g} = \frac{4\pi}{137} \frac{ag^4}{E_g \left(E_g + \frac{1}{2}g^2 \right)} \left| \frac{1}{\kappa} \right| \quad (2.347)$$

At both extremes, $\kappa \rightarrow 0$ and Eqs. (2.346) and (2.347) diverge. This occurs because at the surface band edges the charge associated with the surface states becomes more and more delocalized throughout the lattice until at $\kappa=0$, the charge is completely delocalized. At this point the surface states become bulk states, and instead of cross sections, one should consider absorption coefficients.

Fig. 14 depicts the behavior of the cross section over the entire frequency range. The values for the lattice constant, $a=2.35 \text{ \AA}$, and the energy gap, $E_g = 1.17 \text{ eV}$, were taken to be those of silicon.¹¹

To illustrate what laser power is required for a certain surface absorption rate, we will consider exciting a surface state at $0.4 E_g$. This corresponds to a laser frequency of about 10^{15} Hz which falls in the IR. From Fig. 14, the cross section is about 3 \AA^2 . If we assume our laser intensity is 1 W/cm^2 , the transition rate is about 4×10^{-5} photons absorbed per second. Since an electron is excited for each photon absorbed and the effective charge depth, $|1/2\kappa|$ [see Eq. (2.306)], is about 8 atomic layers, the transition rate is about 5×10^{-6} electrons per surface atom per second. To obtain the transition rate per unit surface area, we divide by the surface area of the end atom, whereby we obtain 10^{10} photons absorbed per cm^2 per sec. This figure is quite large considering the low power of the laser. Consequently, using such a laser can lead to appreciable charge excitation in the surface region.

Since our ultimate goal is to use the laser to charge the surface, we wish to excite states with the smallest charge depth and consequently the largest κ .

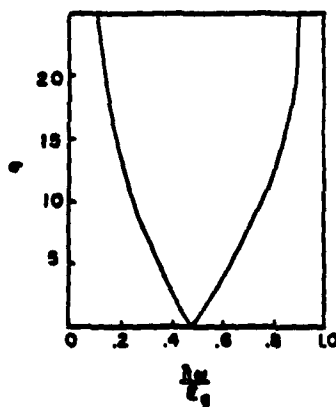


Fig. 14. Absorption cross section for surface states, σ , in \AA^2 versus the frequency of the exciting laser radiation.

For silicon at maximum value of κ the surface charge depth is about 3 lattice constants. Since the charge depth increases as we move away from this mid-gap region, we are mostly interested in laser frequencies near $0.5 E_g$. As seen in Fig 14, the cross section is quite substantial near the mid-gap region, and subsequently, we could readily increase the surface charge by using a laser of moderate intensity. Even at $\omega = 0.4 E_g$ we have seen that the charge depth is only about 8 lattice parameters, and we could excite this state with a very low power laser. Consequently, we would expect a laser tuned to a frequency around $0.5 E_g$ to be an effective controller of surface charge.

To examine the effect of this excitation on the surface charge, we can readily obtain the electron density profile of our excited system.¹⁰⁴ To obtain this density, we must sum the individual densities of all occupied states:

$$n(z) = \sum_k \left| \psi_k(z) \right|^2, \quad (2.348)$$

where the wave functions were previously given in Eqs. (2.289) and (2.306).

Changing to an integral we obtain

$$n(z) = \frac{8L}{(2\pi)^3} \int d\vec{k} \left| \psi_k(z) \right|^2, \quad (2.349)$$

where we have assumed that the wave function had plane wave components parallel to the surface. If we now convert to cylindrical coordinates, we can readily write the electron charge density for the ground state:

$$n_0(z) = \frac{2L}{\pi^2} \int_0^{k_F} dk \left(E_F - E_k \right) \left| \psi_k(z) \right|^2, \quad (2.350)$$

where the subscript 0 indicates ground state and k_F is the Fermi crystal momentum with energy E_F . In our model for a semiconductor, this corresponds to the state at the top of the valence band where

$$k_F = \frac{g}{2}, \quad (2.351)$$

$$E_F = \frac{1}{2} \left[\left(\frac{g}{2} \right)^2 - E_g \right]. \quad (2.352)$$

Using Eq. (2.289) in Eq. (2.350) with parameters typical of silicon,^{111,112} we have calculated the ground state electron density profile and have shown our results by the solid line in Fig. 15. The oscillation of the charge as one goes into the bulk of the crystal is due to the concentration of the electron charge around the ions at the lattice points ($z = na$; $n = 0, -1, -2, \dots$). The exponential

tail on the vacuum side is typical of electron density profiles for a truncated system.

If the semiconductor is now exposed to a laser with an energy less than the band gap, the ground state electron density profile will be altered due to excited surface states. Using the definition of the charge density, Eq. (2.348), we can readily write down an expression for our new charge density:

$$n(z) = n_0(z) - \left| \psi_k(z) \right|^2 + \left| \psi_\kappa(z) \right|^2, \quad (2.353)$$

where $n_0(z)$ refers to the previously calculated ground state density, Eq. (2.350). We have assumed that our laser excited an electron from valence band state k to surface state κ . From our previous cross section calculation, we have discovered the selection rule that requires the conservation of the real part of the crystal momentum in surface state excitations. Consequently the valence state that will be excited lies at the top of the valence band with $k = \frac{g}{2}$. From Eq. (2.289) we can determine the density of this bulk state:

$$\left| \frac{\psi_g}{2}(z) \right|^2 = \frac{4}{L} \sin^2 \left[\frac{g}{2} \left(z - \frac{a}{2} \right) + \theta \right] \quad (2.354a)$$

for the internal density, and

$$\left| \frac{\psi_g}{2}(z) \right|^2 = \frac{4}{L} \sin^2 \theta \frac{e^{-2q_g \left(z - \frac{a}{2} \right)}}{2q_g} \quad (2.354b)$$

for outside the crystal. From this equation we see that the charge of the bulk

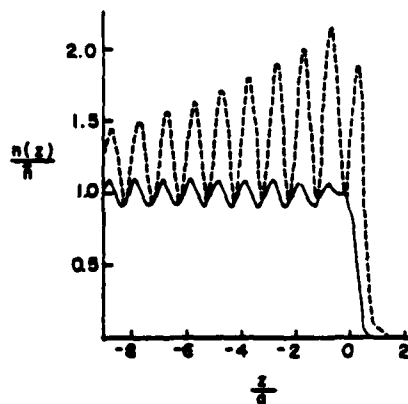
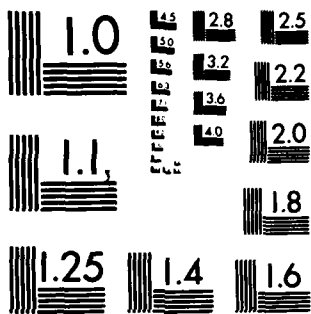


Fig. 15. Electron density distribution at the surface. The solid line represents the ground electronic state, and the dashed line represents the system with the excited surface state $\kappa = -0.5(2V_g/g)$ in the lower branch.



MICROCOPY RESOLUTION TEST CHART
NATIONAL BUREAU OF STANDARDS-1963-A

state that is being excited goes as $1/L$. Therefore, for a very large system we would in effect be taking only an infinitesimal amount of charge from everywhere in the semiconductor to populate the surface state. Consequently, for a large system, the charge of one bulk state is negligible in Eq. (2.353). The total density of the excited state then becomes

$$n(z) = n_0(z) + |\psi_\kappa(z)|^2 \quad (2.355)$$

Using Eq. (2.308) we can obtain the density contribution from surface state κ :

$$|\psi_\kappa(z)|^2 = C_s^2 \sin^2 \left[\left(\frac{g}{2} \right) \left(z - \frac{a}{2} \right) + \theta_\kappa \right] e^{-2\kappa \left(z - \frac{a}{2} \right)} \quad (2.356a)$$

for $z < \frac{a}{2}$ and

$$|\psi_\kappa(z)|^2 = C_s^2 \sin^2 \theta_\kappa e^{-2q_\kappa \left(z - \frac{a}{2} \right)} \quad (2.356b)$$

for $z < \frac{a}{2}$. Inserting Eq. (2.356) into Eq. (2.355) along with the results for the ground state, Eq. (2.350), one obtains the solution for the charge density of the excited state of the semiconductor. We have calculated this density for $\kappa = -0.5 E_g/g$ in the lower branch surface and depicted the results by the dashed line in Fig. 15. As can be seen by this plot, the charge in the excited surface state produces a total electronic charge in the surface region that is twice as great as the bulk average. If one excites surface states closer to the branch point near the gap center [see Eq. (2.316)], the charge concentration in the first few layers of the surface will increase up to about thrice the average density.

If there is a charged adspecies above the surface, this excess charge in the surface region can produce a very large effect on the adspecies-surface interaction. This interaction can be written classically as

$$U(z_I) = - \int d\vec{r} n(z) v(r) \quad (2.357a)$$

with

$$r = \left[x^2 + y^2 + (z - z_I)^2 \right]^{\frac{1}{2}}, \quad (2.357b)$$

where $v(r)$ is the electron-ion potential of the adspecies at z_I . We will assume that $v(r)$ is Coulombic in nature with Thomas-Fermi screening:⁹³

$$v(r) = \frac{z e^{-\lambda r}}{r}, \quad (2.358a)$$

where λ is the screening parameter,

$$\lambda^2 = \frac{6\pi\bar{n}}{E_F} , \quad (2.358b)$$

and Z is the charge on the adspecies. A more appropriate screening function would be similar to those developed for finite metals,¹¹³ but this simple model, Eq. (2.358), should serve to give us the magnitude of the interaction of the surface with the adspecies. Since the Thomas-Fermi screening parameter depends on the average bulk electron density, \bar{n} , we would expect this parameter to be much larger than one calculated based on the average charge density between an adatom and the surface. Consequently, the use of a screening parameter based on the bulk electron density would underestimate the actual interaction.

Bearing this limitation in mind, Eqs. (2.357) and (2.358) are combined and the integration is performed in the x and y directions to give

$$U(z_I) = - \frac{2\pi Z}{\lambda} \int_{-\infty}^{\infty} dz n(z) e^{-\lambda|z-z_I|} . \quad (2.359)$$

Inserting the excited state density, Eq. (2.355), into this expression, we obtain

$$U(z_I) = - \frac{2\pi Z}{\lambda} \int_{-\infty}^{\infty} dz n_0(z) e^{-\lambda|z-z_I|} - S_U(z_I) . \quad (2.360)$$

The first term in this equation represents the interaction of the adspecies with the semiconductor in the ground state and will not be considered here. The second term is the change in the potential induced by the excited surface state and is given by

$$S_U(z_I) = \frac{2\pi Z}{\lambda} \int_{-\infty}^{\infty} dz |\psi_{\kappa}(z)|^2 e^{-\lambda|z-z_I|} . \quad (2.361)$$

Inserting the expression for the density contribution from the surface state, Eq. (2.356), we get

$$S_U(z_I) = \frac{2\pi Z C_s^2}{\lambda} \left\{ \int_{-\infty}^{\infty} dz \sin^2 \left[\frac{q}{2} \left(z - \frac{a}{2} \right) + \theta_{\kappa} \right] e^{-2\kappa \left(z - \frac{a}{2} \right) - \lambda |z-z_I|} \right. \\ \left. + \sin^2 \theta_{\kappa} \int_{\frac{a}{2}}^{\infty} dz e^{-2q_{\kappa} \left(z - \frac{a}{2} \right) - \lambda |z-z_I|} \right\} . \quad (2.362)$$

After much algebra, this equation can be reduced to yield an interaction of the form

$$\frac{{}^s U(z_I)}{z} = e^{-\lambda z_I} A(\kappa) - e^{-2q_\kappa z_I} B(\kappa) \quad (2.363)$$

where

$$A(\kappa) = \frac{C_s^2 \pi e^{\frac{\lambda a}{2}}}{\lambda} \left[\frac{\sin^2 \theta_\kappa}{\left[q_\kappa - \frac{\lambda}{2} \right]} - \frac{1}{2\kappa - \lambda} + \frac{(2\kappa - \lambda) \cos(2\theta_\kappa) - g \sin(2\theta_\kappa)}{(2\kappa - \lambda)^2 + g^2} \right] \quad (2.364)$$

and

$$B(\kappa) = \frac{C_s^2 4\pi \sin^2 \theta_\kappa}{(2q_\kappa)^2 - \lambda^2} e^{q_\kappa a} \quad (2.365)$$

Eq. (2.363) has been evaluated for a number of surface states, and the results are plotted in Fig. 16. As one moves to larger $|\kappa|$ (energies near the gap center), the curves clearly show that both the magnitude and the range of the surface charge interaction increase. Since we have found that the surface charge also increases under these circumstances, this is exactly what is expected. All curves, however, show an appreciable contribution to the potential produced by the surface states with $|\kappa| > 0.01 E_g/g$.

In order to give a better comparison of the surface charge interaction among the various surface states, we have plotted the change in potential at $z_I = a$ for all surface states in Fig. 17. The upper branch states are at a higher energy [positive sign in Eq. (2.291)] than the lower branch states. Therefore, the exponential tail of the charge density and, subsequently, the interaction is slightly greater.

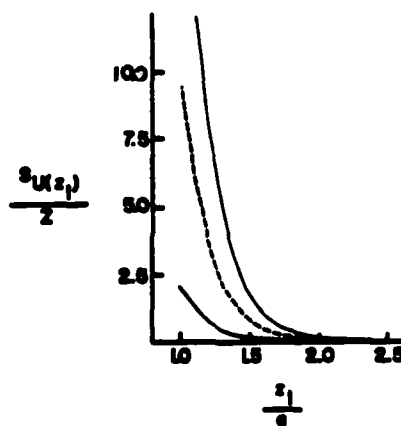


Fig. 16. The magnitude of the surface interaction potential (in millihartrees) at various distances from the surface. The solid line represents the system with excited state $\kappa \approx -(2V_g/g)$; the dashed line, $\kappa = -0.5(2V_g/g)$; and the dotted line, $\kappa = -0.1(2V_g/g)$, all in the lower energy branch.

Thus we see that an appreciable effect on an adspecies-surface interaction can be produced by use of a laser to localize electronic charge in the surface region. If the adspecies is positively charged, the possibility of adsorption is enhanced; on the other hand, if the adspecies is negative, desorption can be induced. In a more complete model of a semiconductor, both occupied and empty surface states could exist in the ground state. A laser could then be used to excite holes as well as electrons to these surface states and thus adsorption or desorption could be enhanced for the same charged adspecies.

Because the concentration of charge is so large in the surface region, one would expect the effective interaction length to be greater than that indicated by Fig. 16. The exponential decay of the surface interaction is probably an artifact of the assumed Thomas-Fermi screening. The dielectric screening problem would have to be addressed more carefully in order to improve these results.

The surface charge is also large enough that it is conceivable that such a large charge displacement could lead to a lattice rearrangement. Such an effect could lower the charge in the surface region. On the other hand, the new surface states would probably be more stable and, subsequently, have a larger lifetime. To study these effects a self-consistent field calculation would have to be performed.

The major limitation of the above model, however, is its one-dimensionality. The three-dimensional interaction potential may be quite complex depending not only on the distance from the surface but also on the position of the adspecies with respect to the plane of the surface. Also, most common semiconductors have indirect band-gaps¹¹¹ (the minimum in the conduction band is not over the maximum in the valence band), and the form of the wave function in such a gap is not

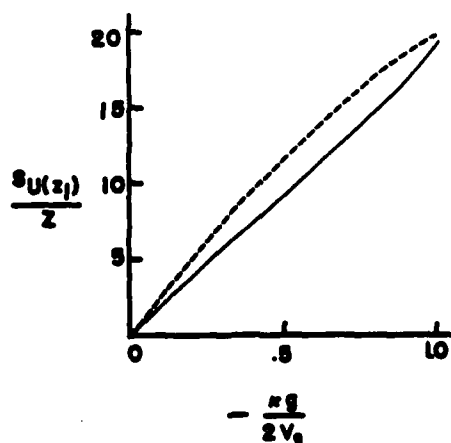


Fig. 17. The magnitude of the surface interaction potential (in millihartrees) at a distance $z_1=a$ for the system with various excited surface states. The solid line represents surface states in the lower energy branch; the dashed line, the upper energy branch.

readily obtainable from a 1D model. Finally, in a real semiconductor, the surface states are not necessarily confined to the gap between the valence and conduction bands.¹¹⁴

Nonetheless, our contention that lasers can be used to control surface charge density in semiconductors and, subsequently, enhance surface processes has been substantiated. Since metals also play an important role in catalysis, the effect of lasers on metal surfaces will also be examined in terms of a simple model.

(b) Metals. As with wide-band semiconductors, the valence electron wave function of a metal of infinite extent can be written as a sum of plane waves, Eq. (2.271). Consequently, if we model a metal as a truncated 1D chain, we will obtain equations for the bulk and surface wave functions and their related energies which are of the same forms as the wave functions, Eqs. (2.289), (2.306) and (2.308), and the energies, Eqs. (2.287) and (2.291), of our model semiconductor. The band structure for the metal can also be illustrated by Fig. 13. However, whereas the V band is the valence band of the semiconductor, for the metal the V band corresponds to an overlapping valence and conduction band that is characteristic of a metal. Consequently, for the metal the lower band is only partly occupied. The C band would correspond to an upper conduction band.

For example, in the case of sodium¹¹¹ the top of the lower band lies at 3.8 eV, but the band is only occupied up to 3.1 eV in the ground state. Also, whereas the energy gap is about 1 eV for most common semiconductors, for sodium the energy gap is 0.45 eV.

If we shine a laser on our metal, we wish to see if we can also populate the surface state and thus increase the surface charge. However, because of the selection rule we previously developed,¹⁰³ we must conserve the real part of the crystal momentum when we excite electrons into the surface states. But there are no occupied bulk states with real momentum at or near $\frac{g}{2}$ which is the real momentum of the surface state. To overcome this problem we suggest not only exciting the electrons with a laser but also with the vibrational energy of the crystal. The laser photons would supply us with the energy we need to get to the surface states, and the phonons would supply the needed crystal momentum.¹¹⁵

For our model system, we write the Schrödinger equation

$$i \frac{\partial \psi(z,t)}{\partial t} = H(t) \psi(z,t) \quad (2.366)$$

$$H(t) = H^0 + H^f(t) + H^p(t) \quad (2.367)$$

where H^0 is the electronic Hamiltonian of our system in the ground state, $H^f(t)$ is the coupling of the electrons to the laser field, and $H^p(t)$ is the coupling of the electrons to the phonons. We expand our wave function in terms of the stationary

states $\phi_k(z)$:

$$\psi(z,t) = \sum_k c_k(t) \phi_k(z) e^{-iE_k t} \quad (2.368)$$

Using this expression in Eq. (2.366) and assuming that $c_k(0) = 0$ for $k > k_F$ and $c_k(0) = 1$ for $k < k_F$, we obtain

$$c_k(t) = -i \int_0^t dt' \left\{ \langle k | H^f(t') | k' \rangle + \langle k | H^p(t') | k' \rangle \right\} e^{i\omega_{kk'} t'} \quad (2.369)$$

where

$$\omega_{kk'} = E_k - E_{k'} \quad (2.370)$$

To get our transition rate to first order, we would sum the square of Eq. (2.369) over all initial states k' from 0 to k_F and over all final states $k = \frac{1}{2}g + ik$ for all surface states k . However, the field coupling term between k and k' would vanish since the wavenumber of the field is too small to assure conservation of crystal momentum. The phonon coupling term will conserve this momentum, but the energy of a phonon (for sodium, maximum phonon energy is about 0.015 eV) is not sufficient to assure conservation of energy. Consequently, the phonon term and the overall transition rate in first-order perturbation theory is zero. Therefore, we will have to carry our calculations to higher order.

Using Eq. (2.369) in Eq. (2.368) and then inserting into the Schrödinger equation, Eq. (2.366), we obtain the second-order solution:

$$c_k(t) = - \sum_{k'} \int_0^t dt' \left\{ H_{kk'}^f e^{-i\omega_f t'} + H_{kk'}^p e^{-i\omega_p t'} \right\} e^{i\omega_{kk'} t'} \\ \times \int_0^{t'} dt'' \left\{ H_{k'k''}^f e^{-i\omega_f t''} + H_{k'k''}^p e^{-i\omega_p t''} \right\} e^{i\omega_{k'k''} t''} \quad (2.371)$$

where

$$H^{f,p}(t) = H^{f,p} e^{-i\omega_{f,p} t} \quad (2.372)$$

ω_f being the frequency of the laser field and ω_p the frequency of the phonon. The matrix elements are defined:

$$H_{kk'}^{f,p} \equiv \langle k | H^{f,p} | k' \rangle \quad (2.373)$$

If we multiply Eq. (2.371) out, we will obtain terms that are second order in the field, $H_{kk'}^f$, $H_{k'k''}^f$, and in the phonons, $H_{kk'}^p$, $H_{k'k''}^p$. Again, if we consider initial states k'' lying below the Fermi energy and final states k as in the surface band,

the second-order field terms will vanish since they do not conserve crystal momentum, and the second-order phonon terms will vanish since they do not conserve energy. Using this fact, we can simplify Eq. (2.371):

$$c_k(t) = - \sum_{k'} H_{kk'}^f H_{k'k''}^p \int_0^t dt' e^{i(\omega_{kk'} - \omega_f)t'} \int_0^{t'} dt'' e^{i(\omega_{k'k''} - \omega_p)t''} - \sum_{k'} H_{kk'}^p H_{k'k''}^f \int_0^t dt' e^{i(\omega_{kk'} - \omega_p)t'} \int_0^{t'} dt'' e^{i(\omega_{k'k''} - \omega_f)t''} \quad (2.374)$$

The first term in this equation represents the electron being excited by a phonon from initial state k'' below the Fermi energy to an intermediate state k' which lies between the Fermi level and the top of the lower band. From here, the electron is excited to the final state k in the surface band by a photon. The second term involves a photon exciting an electron from the initial state k'' below the Fermi level to an intermediate state k' which lies in the upper conduction band. From there we are scattered into the final surface state k by a phonon. Since both the conduction band and the upper conduction fall off rapidly as you move away from the surface state region (see Fig. 13), the excitation of an electron to the upper conduction band involves a large energy mismatch. The subsequent scattering by a phonon into the final state will also involve a large energy mismatch since the intermediate state can be very high in the upper conduction band. Consequently, we would expect the second term in Eq. (2.374) to be very small when compared to the first term, and thus we will disregard it.

Assuming the time, t , becomes very large, we can now find the modulus of Eq. (2.374):

$$\frac{|c_k(t)c_k^*(t)|}{t} = 2\pi\delta(\omega_{kk''} - \omega_f - \omega_p) \left[\sum_{k'} \frac{H_{kk'}^f H_{k'k''}^p}{\omega_{k'k''} - \omega_p} \right]^2 + 2\pi \sum_{k'} \left[\frac{H_{kk'}^f H_{k'k''}^p}{\omega_{k'k''} - \omega_p} \right]^2 \delta(\omega_{kk'} - \omega_f). \quad (2.375)$$

To proceed further we must first evaluate $H_{kk''}^p$.

When the system is at rest, the electronic Hamiltonian can be written as

$$H^0 = \frac{1}{2} \frac{d^2}{dz^2} + \sum_l v(z-z_l) \quad (2.376)$$

where $v(z-z_l)$ is the screened potential between the electron at position z and the ion at equilibrium position z_l . If there is a disturbance in the lattice (a phonon), the ion will change position to $z_l + u_l(t)$. Consequently, our Hamiltonian will become

$$H(t) = \frac{1}{2} \frac{d^2}{dz^2} + \sum_{\ell} v(z-z_{\ell}-u_{\ell}(t)) \quad (2.377)$$

If we assume the lattice is not too greatly perturbed by the phonon, we can expand the potential in terms of a first-order Taylor expansion:

$$H(t) = H^0 - \sum_{\ell} v'(z-z_{\ell}) u_{\ell}(t) \quad (2.378)$$

where $v'(z-z_{\ell})$ is the gradient of the electron-ion potential evaluated at equilibrium. The displacement, $u_{\ell}(t)$, can be written as

$$u_{\ell}(t) = U_{\ell} e^{-i\omega t} \quad (2.379)$$

Using this in Eq. (2.372), we get

$$H^P = - \sum_{\ell} v'(z-z_{\ell}) U_{\ell} \quad (2.380)$$

and the subsequent matrix element will be

$$H_{kk'}^P = - \sum_{\ell} U_{\ell} \int dz \phi_k^*(z) v'(z-z_{\ell}) \phi_{k'}(z) \quad (2.381)$$

where $\phi_k(z)$ is the eigenfunction of H^0 . If we neglect the exponential tail of the wave function by assuming the system is very large, we can approximate the wave function in a metal by [see Eq. (2.289)]

$$\phi_k(z) = L^{-\frac{1}{2}} e^{ikz} \quad (2.382)$$

Using this in Eq. (2.381), we obtain

$$H_{kk'}^P = - \frac{i(k-k') v(k-k')}{N} \sum_{\ell} U_{\ell} e^{-i(k-k')z_{\ell}} \quad (2.383)$$

where $v(k-k')$ is the $(k-k')$ -th component of the Fourier transform of the electron-ion potential. It is also convenient to express the displacement magnitude, U_{ℓ} , in terms of the phonon annihilation, $a(K)$, and creation, $a^{\dagger}(K)$, operators:¹¹⁰

$$U_{\ell} = \left(\frac{1}{NM} \right)^{\frac{1}{2}} \sum_K \left(\frac{2\omega_K^P}{K} \right)^{-\frac{1}{2}} \left[e^{iKz_{\ell}} a(K) + e^{-iKz_{\ell}} a^{\dagger}(K) \right] \quad (2.384)$$

where M is the mass of the lattice atom and K is the wavevector of the phonon. We can now write for the phonon matrix element

$$H_{kk'}^p = -i \left(\frac{1}{NM} \right)^{\frac{1}{2}} \sum_K \left(\frac{\omega_p}{\omega_K} \right)^{-\frac{1}{2}} (k-k') v(k-k') \frac{1}{N} \sum_{\ell} e^{i[K+(k'-k)]z_{\ell}} a(K) + \frac{1}{N} \sum_{\ell} e^{-[K+(k-k')]z_{\ell}} a^{\dagger}(k) \quad (2.385)$$

But the sums over the exponentials are delta functions. Therefore,

$$H_{kk'}^p = -i \left(\frac{1}{NM} \right)^{\frac{1}{2}} \frac{(k-k') v(k-k')}{\left(2\omega_{k-k'}^p \right)} [a(k-k') + a^{\dagger}(k'-k)] \quad (2.386)$$

Inserting this into Eq. (2.375) and then averaging over the eigenstates of the phonon number operator, $|n(K)\rangle$, we will obtain terms of the form

$$\langle n(K) | a(K) a(K') | n(K) \rangle = 0 \quad (2.387a)$$

$$\langle n(K) | a^{\dagger}(K) a^{\dagger}(K') | n(K) \rangle = 0 \quad (2.387b)$$

$$\langle n(K) | a(K) a^{\dagger}(K') + a^{\dagger}(K) a(K') | n(K) \rangle = \delta_{K,K'} [2n(K)+1] \quad (2.387c)$$

where $\delta_{K,K'}$ is the Kronecker delta function and $n(K)$ is the population of phonon state K . We have assumed that $K = k-k'$. Using Eqs. (2.386) and (2.387) in Eq. (2.375), we obtain

$$\begin{aligned} \left\langle n(K) \left| \frac{c_k(t) c_{k'}^*(t)}{t} \right| n(K) \right\rangle &= \left(\frac{2\pi}{NM} \right) \delta(\omega_{kk''} - \omega_f - \omega_p) \sum_{k'} \frac{\left(H_{kk'}^f \right)^2 (k'-k'')^2 v(k'-k'')^2 [2n(k'-k'')+1]}{2\omega_p (\omega_{k'k''} - \omega_p)^2} \\ &+ \left(\frac{2\pi}{NM} \right) \sum_{k'} \frac{\left(H_{kk'}^f \right)^2 (k'-k'')^2 v(k'-k'')^2 [2n(k'-k'')+1]}{2\omega_p (\omega_{k'k''} - \omega_p)^2} \delta(\omega_{kk'} - \omega_f) \quad (2.388) \end{aligned}$$

If we assume the frequency of our exciting radiation is nearly equal (except for the phonon contribution) to the difference between the frequencies of the initial and final states, the second term in Eq. (2.388) will vanish. If we now sum over all initial and final states in Eq. (2.388), we will obtain the total second-order transition rate:

$$T = \left(\frac{2\pi}{NM} \right) \sum_{k'} \sum_{k''} \frac{(k'-k'')^2 v(k'-k'')^2 [2n(k'-k'')+1]}{2\omega_p (\omega_{k'k''} - \omega_p)^2} \sum_k \left(H_{kk'}^f \right)^2 \delta(\omega_{kk''} - \omega_f - \omega_p) \quad (2.389)$$

The field matrix element can be readily evaluated using Eqs. (2.318), (2.334) and (2.372):

$$\left(H_{kk'}^f \right)^2 = \left(\frac{2\pi I}{137} \right) \left(\frac{2\pi}{a} \right) \frac{\delta(k'-\frac{g}{2})}{\omega_f^2} \frac{\left| \left\langle \kappa \left| \frac{d}{dz} \left| \frac{g}{2} \right\rangle_0 \right. \right|^2}{(1 - e^{-2ka})} \quad (2.390)$$

where we have replaced the final-state wave number k , which equals $\frac{g}{2} + i\kappa$, with

the surface state index κ .

As we did in going from Eq. (2.335) to Eq. (2.337), the sums can be converted to integrals. Then, if we use Eq. (2.390), we obtain for the transition rate

$$T = \left(\frac{1}{NM}\right) \left(\frac{L}{\pi}\right) \int dk'' \frac{\left(\frac{g}{2}-k''\right)^2 v \left(\frac{g}{2}-k''\right)^2 \left[2n\left(\frac{g}{2}-k''\right)+1\right]}{2\omega_p \left(\frac{\omega}{2}k'' - \omega_p\right)^2} T^{(1)}\left(\kappa, \frac{g}{2}\right), \quad (2.391)$$

where $T^{(1)}\left(\kappa, \frac{g}{2}\right)$ is the first-order transition rate between state $\frac{g}{2}$ and surface state κ induced by the laser field and is given by Eq. (2.340). In obtaining $T^{(1)}\left(\kappa, \frac{g}{2}\right)$ we made use of the fact that $\omega_p \ll \omega_f$. Converting to an integral over the frequency of the initial state, Eq. (2.391) now becomes

$$T = \left(\frac{a}{2\pi M}\right) \int d\omega_{k''} \left(\frac{dk''}{d\omega_{k''}}\right) \frac{\left(\frac{g}{2}-k''\right)^2 v \left(\frac{g}{2}-k''\right)^2 \left[2n\left(\frac{g}{2}-k''\right)+1\right]}{\omega_p \left(\frac{\omega}{2}k'' - \omega_f\right)^2} T^{(1)}\left(\kappa, \frac{g}{2}\right). \quad (2.392)$$

Since the initial states are not near the band edge, we can write [see Eq. (2.287)]

$$\omega_{k''} = (k'')^2/2 \quad (2.393a)$$

$$\frac{dk''}{d\omega_{k''}} = \frac{k''}{2\omega_{k''}}. \quad (2.393b)$$

If we assume a thermal distribution of phonons and electrons, we need only consider the integral within an interval $k_B T_L$ (T_L is the lattice temperature) around the Fermi energy.¹⁰⁸ At room temperature, this interval is small and thus we can consider the integrand to be constant:

$$T \approx \left(\frac{ak_B T_L}{2\pi M}\right) \left(\frac{k_F}{2E_F}\right) \frac{\left(\frac{g}{2}-k_F\right)^2 v \left(\frac{g}{2}-k_F\right)^2 \left[2n\left(\frac{g}{2}-k_F\right)+1\right]}{\omega_p \left(\frac{\omega}{2}k_F - \omega_p\right)^2} T^{(1)}\left(\kappa, \frac{g}{2}\right). \quad (2.394)$$

Since $T^{(1)}\left(\kappa, \frac{g}{2}\right)$ is the only term that depends on ω we would expect that the cross section based on this transition rate would be qualitatively similar to that depicted in Fig. 14 with the distance from the Fermi energy to the top of the band added to the laser frequency.

For sodium at room temperature we can readily evaluate Eq. (2.394):

$$T = 2.38 \times 10^{-4} T^{(1)}\left(\kappa, \frac{g}{2}\right). \quad (2.395)$$

Since the various physical constants for sodium are not significantly different from those for silicon, we would expect the first-order rates to be roughly comparable. From the last section and Fig. 14, we see that a significant photon absorption in silicon could be induced with a low-power laser (1 to 10 W/cm²). From Eq. (2.394), therefore, we would expect to produce a similar effect in sodium with a moderate power laser (10 to 100 kW/cm²). Consequently, as with a semiconductor, we would expect a laser to act as an efficient controller of surface charge in a metal. Subsequent interactions with adspecies would likewise be effected.

Not only does this formalism apply to metals but also to semiconductors when one is considering the excitation of electronic states that do not have the same real momentum as the surface states. When there is a direct band gap as in our model, this would be insignificant when compared to direct transitions. But, in the case of the semiconductor with indirect energy gaps, the electron-phonon coupling could play an important role in surface state excitation.

For a more realistic picture of a metal we would also have to go to a three dimensional model. Furthermore, not only the phonon effect on the electrons (considered here), but also the electron effect on the phonons would have to be studied. Nonetheless, we have clearly demonstrated that lasers can effect the surface charge on metals as well as semiconductors.

(ii) Predissociation. A process which is central to a wide range of chemical reactions catalyzed by a metal surface is the dissociation of one of the reactants, or partial dissociation due to bond stretching, as it adsorbs onto the surface. Another process which has received attention is laser-induced dissociation of gas-phase molecules. We want to entertain the idea of synergistic catalysis, where the surface and the laser combine to increase the dissociation rate above that caused by the surface alone or the laser alone. The situation we shall consider is laser-induced predissociation, where a visible or UV laser couples the ground electronic state of a diatomic molecule to an excited electronic state in which the molecule can dissociate. Two specific effects of the surface will be included: the surface magnetic field (SMF) and the phonon "continuum." The former can be as strong as 10⁷ G, such as in the case of ferromagnetic materials,¹¹⁶ and gives rise to Zeeman splitting of the electronic states of the diatomic molecule.¹¹⁷ The latter is referred to as a "continuum" since the phonon levels are assumed to be much more closely spaced than the vibrational levels of the adsorbing diatomic molecule.

The combined effects of the laser and the surface can probably be most easily visualized in terms of Fig. 18. This is a schematic drawing of the multiwell configuration among the laser-dressed and SMF-split electronic levels of H₂ adsorbed on a metal surface, where R is the internuclear separation. R_c is the point of an avoided crossing, and R_t is the inner classical turning point on the ground

electronic state embedded in the phonon continuum (represented symbolically by the vertical slashes). The laser-dressing gives rise to the three avoided crossings indicated by the primed quantities $V_{i,j}'$ (due to spin-electric dipole and spin-magnetic quadrupole coupling). The fourth avoided crossing designated by the unprimed quantity V_{12} is due to just the SMF. Each V designates a vibrational quasibound well, where V_1 is the diabatic well $V_1 + \hbar\omega$ and V_{ij} is the adiabatic well generated from diabatic curves i and j . Each p_j designates a local transition probability.

The term "predissociation" is used in the sense that the laser-shifted ground singlet state (shifted up by the photon energy $\hbar\omega$) is coupled to the continuum of the repulsive triplet states. Strictly speaking, one could call this type-I predissociation,¹¹⁸ where the laser induces crossings (or more appropriately, avoided crossings) between the singlet and each of the triplet states. A similar situation exists for the case of NO, with a modification due to the different spin multiplicities of the states as shown in Fig. 19. (the vertical slashes indicating the phonon continuum have been omitted). For a sufficiently high combination of the initial vibrational state and $\hbar\omega$, the dressed $^2\Pi$ state becomes predissociative by radiative coupling to the continuum of the $^2\Sigma^+$ state.

Starting from the picture provided by Figs. 18 and 19, we have derived a semi-classical expression for the total width Γ (and hence predissociative rate).^{119,120} The idea is to use classical trajectories as input for a description of the interference of the quasibound nuclear motion in the multiwell system. The widths, energies and shifts for each of the wells can be obtained by locating the poles of

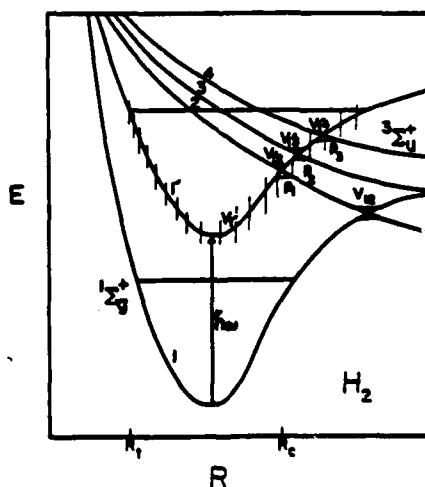


Fig. 18. Schematic drawing of the multiwell configuration among the laser-dressed and SMF-split electronic levels of H_2 adsorbed on a metal surface. See the text for further details.

the S-matrix element for oscillatory motion within the wells.¹²¹ We use the electronic-field representation¹²² (combined photon-dressing and SMF-splitting) for the electronic states and limit our consideration to single-photon absorption. For a combination of N wells, the semiclassical S-matrix takes the form

$$S_N \propto \prod_{j=1}^N \sum_{n_j=0}^{\infty} \exp\left[(2i\alpha_j - i\pi)n_j\right] (w_j)^{n_j}, \quad (2.396)$$

where α_j is the classical action integral for a single pass in the j th well, and $w_j > 0$ is the appropriate multiplicative combination of p_j and $(1-p_j)$ factors in the j th well, which can be calculated by the Landau-Zener formula or the Miller-George semiclassical approach.¹²³ By locating the poles in Eq. (2.396) we obtain the following expression for the width Γ_j for the quasibound levels in the j th well:

$$\Gamma_j = -\log(w_j)/\alpha'_{0j}, \quad (2.397)$$

where α'_{0j} , the energy derivative of the action integral, is approximately equal to the constant $\pi/h\nu_j$ ($\nu_j \equiv$ exact resonance frequency in the j th well). The total width is then given as

$$\Gamma = \frac{1}{m} \sum_{i=1}^N w_i \Gamma_i, \quad (2.398)$$

where m is the multiplicity of the ground electronic state, and

$$\sum_{i=1}^N (w_i/m) = 1. \quad (2.399)$$

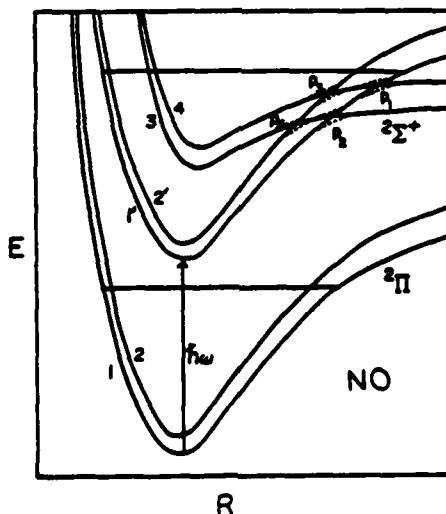


Fig. 19. Schematic drawing of the multiwell configuration among the laser-dressed and SMF-split electronic levels of NO adsorbed on a metal surface.

To incorporate the effects of surface-phonon-adsorbate coupling, we assume the adsorbate to be embedded in a phonon-bath continuum with a finite probability of transition (energy loss) into the continuum from any internuclear distance R of the potential. This in turn decreases the local transition probability p at each avoided crossing, where we are assuming the transition to the phonon continuum to be irreversible. The decreased or modified probability can be expressed as

$$\bar{p}_j \equiv \eta_j p_j \quad , \quad (2.400)$$

where η_j is a survival factor such that $\eta_j=1$ represents a phonon-free situation and $\eta_j=0$ represents a situation where the energy has leaked totally into the phonon bath. A formal expression is available for η_j , involving a phase integral and a phonon-induced level width,¹¹⁹ but is not shown here since we shall simply parametrize η in our calculations. [Another approach described elsewhere¹²⁴ for incorporating phonon coupling is to carry out a "double dressing", where the electronic curves of the adsorbate are simultaneously photon-dressed and phonon-dressed.]

In Fig. 20 we present qualitative results for Γ , the total width in the presence of the laser and the SMF, for the case where all $\eta_j=1$. Along the vertical axis we are actually plotting the unitless quantity $\alpha'_0 \Gamma$, where we assume α'_{0j} to be the same for each well, i.e., $\alpha'_{0j} \approx \alpha'_0 = \text{constant}$. For a comparative study we have considered different cases corresponding to different ratios of the p_j 's. These probabilities may be written as $p_j = \exp(-\theta_j)$, where θ_j is a dynamical factor

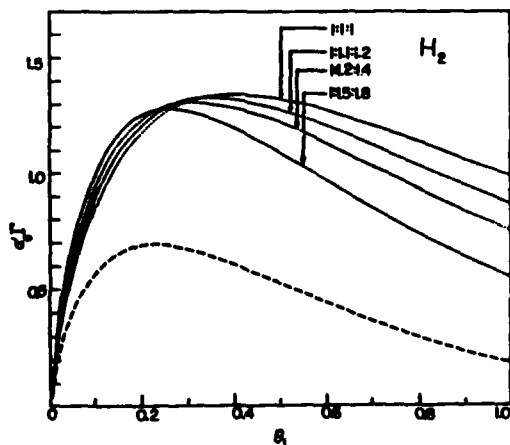


Fig. 20. Relative dissociation rates of adsorbed H_2 in a phonon-free situation, resulting from the combined action of the laser and the SMF (dotted curves). θ_1 is proportional to the laser power density, and the ratios refer to $\theta_1:\theta_2:\theta_3$. The dashed curve is for gas-phase laser-induced predissociation.

dependent on the strength of the radiative coupling, velocity at the avoided crossing and the geometry of the crossing curves, and can be taken to be proportional to the laser power density. The results for H_2 are plotted versus θ_1 , where the lowest (dashed) curve represents gas-phase laser-induced predissociation and the upper (dotted) ones are for the adsorbed molecule subjected to the combined action of the laser and the SMF. Four different ratios of $\theta_1:\theta_2:\theta_3$ are indicated (we have not accounted for the fourth avoided crossing at the far right in Fig. 18). The main conclusion to be drawn from Fig. 20 is that the interference of the quasi-bound nuclear motion in the multiwell configuration due to the SMF serves to enhance the dissociation rate of H_2 for all laser powers. For the simplest case where all p_j are equal, we estimate an enhancement due to the SMF of about 20% for a laser power density of 100 MW/cm^2 . Similar results are obtained for NO , although with a somewhat greater enhancement. For O_2 , where the ground state is a triplet and the upper is a singlet, there is a diminution at low laser powers which becomes an enhancement as the power increases.

In Fig. 21 we present qualitative results for $\alpha_0^1 \Gamma$, the predissociation rate in the presence of the laser, SMF and phonons (dotted curves), and for comparison we also display the gas-phase laser-induced rate (dashed curve) and the phonon-free laser/SMF-induced rate (solid curve). We have taken the survival factors η_j to be the same at all the avoided crossings, given as $\exp(-\beta)$ where $\beta > 0$, where the various values of β are indicated in parentheses after the ratios. We see that the phonon coupling results in a dramatic enhancement at low laser power densities as compared to the phonon-free situation. However, higher laser powers dampen the

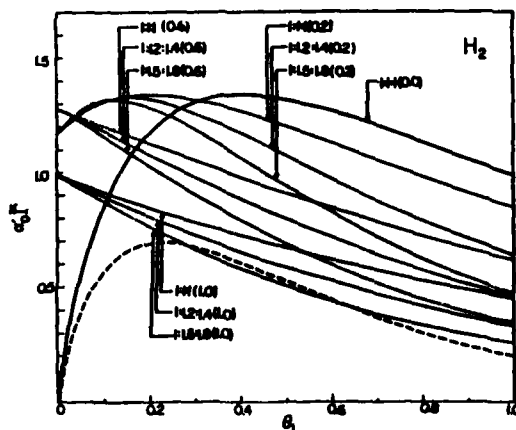


Fig. 21. Relative dissociation rates of H_2 in the presence of the laser, SMF and phonon continuum (dotted curves). The dashed curve is for gas-phase laser-induced predissociation, and the solid curve is for laser/SMF-induced predissociation.

local probabilities more, and the net result is a lowering of the dissociation rate. Although we have not included a feedback from the phonons to the admolecule, i.e., we assume just a damping of the local probabilities due to phonon coupling, most likely such feedback would not reverse the trend observed in Fig. 21.

(iii) Ionization - thermionic and photoelectric. We shall now study another aspect of laser-induced transient effects, namely the emission of electrons from laser-heated surfaces. To calculate the laser-generated current density, J , we employ the generalized Richardson equation^{125,126}

$$J = \sum_{n=0}^{N+1} J_n, \quad (2.401)$$

with

$$J_n = a_n I_0^n A (1-R)^n T_s^2 F(\delta), \quad (2.402)$$

where J_n represents the current density produced by pure thermionic emission for $n=0$ and by n -photon ionization for $n>0$; A and A_n are the Richardson constant and the appropriate coefficient related to the matrix element of the quantum n -photon process, respectively; $F(\delta)$ is the Fowler function with argument $\delta = \eta h\nu - \phi$, where $h\nu$ and ϕ are the photon energy and system work function; and N is the largest integer less than $\phi/h\nu$. T_s is the surface temperature calculated from the heat diffusion equation

$$\frac{\partial T}{\partial t} = D \frac{\partial^2 T}{\partial z^2}, \quad (2.403)$$

with initial and boundary conditions

$$T(z,0) = T_0, \quad (2.404a)$$

$$K \frac{\partial T}{\partial z} \Big|_{z=0} = -(1-R) I(z,t) \Big|_{z=0}, \quad (2.404b)$$

where D and K are the thermal diffusivity and the thermal conductivity and are related by $D=K/\rho c$, ρ and c being the mass density and the specific heat of the solid; T_0 is the initial temperature of the system; R is the reflectivity of the surface; and $I(z,t)$ represents the intensity of the incident laser pulse.

Employing the Green's function technique, we obtain an integral expression for the surface temperature, i.e., solution of the diffusion equation at $z=0$,^{127,128}

$$T_s(r,0,t) = T_0 + \frac{I_0(1-R)}{(\pi K \rho c)^{1/2}} \exp \left[-\left(\frac{r}{d} \right)^2 \right] \int_{-\infty}^t dt' g(t-t') / (t')^{1/2}. \quad (2.405)$$

For an arbitrary laser pulse shape, the above integration must be carried out numerically. For the case of a rectangular pulse with constant intensity

I_0 and duration t_p , the integration can be performed analytically. This yields an expression for the maximum surface temperature $T_s = 2I_0(1-R)t_p^{1/2}/(\pi K\rho c)^{1/2}$, which, however, tends to overestimate actual experimental results. We therefore propose triangular pulses to better approximate an actual pulse, e.g., a Gaussian or an asymmetric long-tail pulse. The effect of the triangular pulse shape on the temperature and its time delay can be analyzed by means of an exact analytic solution of the diffusion equation.

A triangular temporal dependence of the laser pulse takes the form

$$g(t) = I_0 t/a, \quad 0 \leq t \leq a \tag{2.406a}$$

$$= I_0 (a+b-t)/b, \quad a \leq t \leq a+b \tag{2.406b}$$

$$= 0, \quad \text{otherwise} \tag{2.406c}$$

which has a peak intensity at $t=t_1^*=a$ with a pulse energy $(a+b)I_0/2$, and whose shape is governed by the ratio between a and b . From Eq. (2.405), the surface temperature generated by the above triangular pulse can be given exactly, in the form¹²⁶

$$T_s(r,0,t) = T_0 + B(r)I_0 T_1(t), \quad 0 \leq t \leq b \tag{2.407a}$$

$$= T_0 + B(r)I_0 \sum_{i=1}^3 T_i(t), \quad a \leq t \leq a+b \tag{2.407b}$$

$$= T_0 + B(r)I_0 \sum_{i=1}^4 T_i(t), \quad a+b \leq t \tag{2.407c}$$

where

$$B(r) = (1-R)\exp[-(r/d)^2]/(\pi K\rho c)^{1/2} \tag{2.408a}$$

$$T_1(t) = 4t^{3/2}/3a, \tag{2.408b}$$

$$T_2(t) = -2(t-a)^{3/2}(2t+a)/3a, \tag{2.408c}$$

$$T_3(t) = 2(t-a)^{3/2} - 4(t-a)^{5/2}/3b, \tag{2.408d}$$

$$T_4(t) = 4(t-a-b)^{3/2}/3b. \tag{2.408e}$$

By setting $[\partial T_s(r,0,t)/\partial t]_{t=t_2^*} = 0$ we obtain the rise time for the maximum surface temperature, $t_2^* = aL^2/(L^2-1)$, which then gives us the delay time by means of the simple expression

$$\Delta t = t_2^* - t_1^* = a/(L^2-1), \tag{2.409}$$

where $L = (a+b)/b$ and $t_1^* = a$ is the rise time of the peak laser intensity.

To show the effect of the pulse shape on the surface temperature, we plot the analytical results for the rectangular and triangular pulses and the numerical result for a Gaussian pulse (with FWHM=18.8 ns) in Fig. 22. It is seen that when

the laser pulse is Gaussian, the surface temperature is overestimated by a rectangular pulse but is well approximated by a triangular pulse with equal sides ($a=b$). Note that in the surface temperature profiles the laser energies ($\int g(t)dt$) of different pulses are all the same, and the surface temperatures are normalized to the maximum value generated by a rectangular pulse.

For a low work function material, e.g., a cesiated tungsten surface with $\phi \approx 2.0$ eV subjected to pulsed laser radiation with intensity $I_0 \approx 50 \text{ MW/cm}^2$ and photon energy $h\nu = 1.165$ eV, we may use limiting forms of the Fowler function, for surface temperature $T_s < 2000$ K. This results in the following expression for the total current density from pure thermionic emission and from one- and two-photon photoelectric effects:

$$J = J_0 + J_1 + J_2 \quad (2.410a)$$

with

$$J_0 = a_0 A T_s^2 \exp(-\phi/kT_s), \quad (2.410b)$$

$$J_1 = (a_1/a_0) I_0 (1-R) J_0 \exp(-h\nu/T_s), \quad (2.410c)$$

$$J_2 = a_2 A I_0^2 (1-R)^2 \left[(2h\nu - \phi)^2 / 4k^2 + \left(\frac{\pi}{6} e^{-\delta} \right) T_s^2 \right]. \quad (2.410d)$$

The above equations are valid for a material with low work function or low ionization energy, and hence are more applicable to metal adspecies rather than

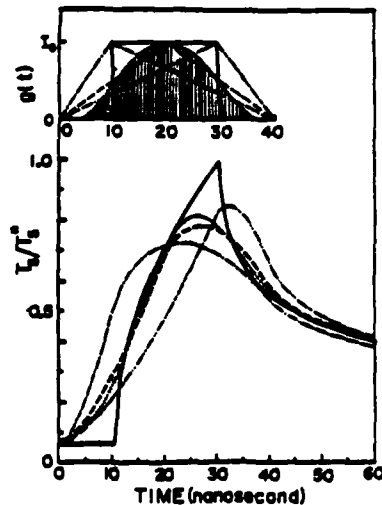


Fig. 22. Normalized surface temperature profiles (T_s/T_s^*) for rectangular (solid line —), Gaussian (dotted line ...), and triangular pulses with $a = b/3$ (dash-dot-dashed ---), $a = b$ (dashed ---) and $a = 3b$ (dash-dot-dotted -...-). $T_s^* \propto I_0 t_p^2$ is the maximum surface temperature generated by a rectangular pulse with duration $t_p = 20$ ns. The intensity profiles $g(t)$ are also shown, where the Gaussian pulse has a FWHM = 18.8 ns and all pulses with different shapes have the same energy $I_0 t_p$.

nonmetal adspecies. Note that, from the expression in Eq. (2.410), the one-photon emission current density J_1 is equivalent to that of the pure thermionic emission J_0 enhanced by a factor $a_1 I_0 \exp(h\nu/KT_s)$,¹²⁹ which is photon energy and intensity dependent. For the two-photon process, the current density J_2 is independent of T_s provided T_s is sufficiently low, where the "cold" electrons generated by two-photon ionization dominate the current density. At sufficiently high surface temperatures, we expect the pure thermionic effect to be the major component of the total current density, and a much higher power law for the intensity dependence, $J(t) = J_0 I^m(t)$, is expected. This power law provides information about the shape of the emitted current. For example, a Gaussian laser intensity, $I(t) = I_0 \exp(-t^2/B^2)$, gives a Gaussian current density, $J(t) = J_0 \exp(-t^2/\beta^2)$, with a narrower width $\beta = B/\sqrt{m}$ if it follows the power law. In general, we expect an intensity-dependent exponent, m , due to the mixture of pure thermionic emission and multiphoton ionization.

Fig. 23 shows the surface temperature (normalized to its peak value) generated by a Gaussian laser pulse (at the hot spot center) and also shows the corresponding current density (only the pure thermionic current is plotted). We note that the surface temperature and the associated current profiles may be well approximated by the results generated by a triangular pulse with $a = b$ in Eq. (2.407), which gives the peak surface temperature $T_s^* \propto I_0 (a+b)^{1/2}$.

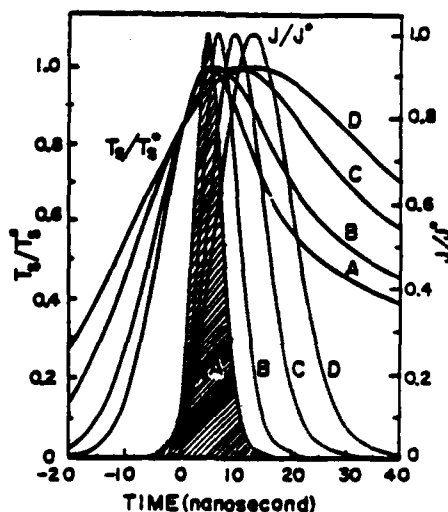


Fig. 23. The normalized surface temperature and current density (J/J^*) as a function of time generated by Gaussian pulses for [intensity(MW/cm^2), FWHM(ns)] = (A) (57.73,15), (B) (50,20), (C) (40.82,30) and (D) (35.35,40). Note that all of these pulses have the same peak surface temperature T_s^* , which is well approximated by $T_s^* = [(1-R)/(\pi K \rho c)^{1/2}] I_0 (2/\sqrt{3})^{3/2} a^{1/2}$, as in the case for an isosceles triangle.¹²⁶

(iv) Resonance fluorescence. The phenomenon of resonance fluorescence for a two-level atom in the gas phase has been known for some time.¹³⁰ However, considerably less work has been done for a two-level atom near or adsorbed on a solid surface. In the absence of a surface or when the adatom is far from the surface, the dynamics of the population inversion and the power spectrum of the system may be described by the usual optical Bloch equations. When a surface is present, particularly a metal, the following factors become important: (i) nonradiative energy relaxation of the excited adatom via electron-phonon coupling; (ii) radiative spontaneous decay and stimulated emission produced by both the applied field and the reflected field; (iii) the oscillatory behavior of the lifetime of the adatom due to the interference between the applied field and the reflected field; (iv) the reflectivity and refraction index of the surface; (v) surface-induced dephasing of the dipole; and (vi) the interaction between the adatom and plasmons; as a first step, one can assume that the effects of the conduction electrons in the metal just provide a reflected field acting back on the adatom.

Combining the standard techniques for the two-level atom in the gas phase^{130,131} with the many-body techniques described in the previous sections, we obtain the surface-dressed Bloch equations (SBE):^{132,133}

$$\frac{d}{dt} \begin{pmatrix} u \\ v \\ w \end{pmatrix} = \begin{pmatrix} -\tilde{\gamma}_2 & -\tilde{\Delta} & 0 \\ \tilde{\Delta} & -\tilde{\gamma}_2 & \Omega \\ 0 & -\Omega & -\tilde{\gamma}_1 \end{pmatrix} \begin{pmatrix} u \\ v \\ w \end{pmatrix} + \tilde{\gamma}_1 \begin{pmatrix} 0 \\ 0 \\ w_{eq} \end{pmatrix} . \quad (2.411)$$

u and v are the components, in units of the transition moment, of the adatomic dipole moment "in phase" and "in quadrature" with the applied field. w is the population inversion, with the equilibrium value w_{eq} , where $w_{eq} = -1$ for the adatom initially in its ground state and $w_{eq} = 1$ for the excited state. $\Omega = |\mu_{12} E_0|/\hbar$ is the Rabi frequency, where μ_{12} is the electric-dipole transition matrix element between the adatomic states $|1\rangle$ and $|2\rangle$, and E_0 is the amplitude of the applied electric field which is assumed to have a slowly-varying envelope. $\tilde{\gamma}_1$ and $\tilde{\gamma}_2$ are the relaxation factors for the inversion and for the dipole, respectively, and $\tilde{\Delta}$ is the effective detuning of the laser field frequency with respect to the adatomic transition frequency. These surface-dressed parameters are related to the surface-free parameters by

$$\tilde{\Delta} = \Delta + \delta\omega_F + \delta\omega_B , \quad (2.412a)$$

$$\tilde{\gamma}_1 = 2(\gamma_B + A/2) , \quad (2.412b)$$

$$\tilde{\gamma}_2 = \gamma_B + A/2 + \gamma_2 + \gamma_R , \quad (2.412c)$$

where $\Delta = \omega_0 - \omega$ is the surface-free detuning, A is the Einstein coefficient for spontaneous emission, $\delta\omega_F$ and $\delta\omega_B$ are the frequency shifts due to the applied field and phonons, respectively, and γ_B and γ_2 are the phonon-induced energy (T_1) and phase (T_2) relaxation rates, respectively.³³ γ_R represents the effects of the quantized reflected field $f(d) \equiv \text{Re } f(d) + i \text{Im } f(d)$,

$$\gamma_R = 2 |u_{12}|^2 \text{Im } f/\hbar, \quad (2.413)$$

whose forms for the perpendicular and parallel orientations of the dipole with respect to the surface are¹³⁴

$$f_{\perp}(d) = -R \left(\frac{2}{\chi^3} \right) \left[\left[\frac{1}{(2\hat{d})^3} - \frac{i}{(2\hat{d})^2} \right] e^{2i\hat{d}} \right], \quad (2.414a)$$

$$f_{\parallel}(d) = R \left(\frac{1}{\chi^3} \right) \left[\left[\frac{1}{(2\hat{d})^3} + \frac{1}{2\hat{d}} - \frac{i}{(2\hat{d})^2} \right] e^{2i\hat{d}} \right]. \quad (2.414b)$$

The reduced distance is $\hat{d} = d/\lambda = 2\pi d/\lambda$, where d is the distance of the adatom from the surface and λ is the wavelength of the field. R is the reflectivity of the surface.

The steady-state population inversion is found analytically to be (for $w_{eq} = -1$)

$$w_{s.s.} = \left[1 + \frac{(\tilde{\gamma}_2/\tilde{\gamma}_1)\Omega^2}{\tilde{\Delta}^2 + \tilde{\gamma}_2^2} \right]^{-1}, \quad (2.415)$$

which is sensitive to the reduced distance and dipole orientation through the surface-dressed parameters $\tilde{\gamma}_1$, $\tilde{\gamma}_2$ and $\tilde{\Delta}$. We see from the above equation that the criterion for the weak-field limit in the SBE, given by

$$\Omega^2 \ll \left(\tilde{\Delta}^2 + \tilde{\gamma}_2^2 \right) \tilde{\gamma}_1/\tilde{\gamma}_2, \quad (2.416)$$

is a weaker condition than in the surface-free optical Bloch equations due to the surface-dressed parameters. Further work is in progress in our laboratory to obtain the power spectrum as a function of \hat{d} .

3. Gas-Surface Interactions

A. Diffraction

We first present a semiclassical formalism for atom-surface scattering in the absence of radiation,¹³⁵ and then indicate how it can be extended to include the effects of a laser field.¹³⁶ We assume an atomic beam to be normally incident

(in the z -direction) on the surface, with high enough energy such that the same equation of motion can describe the normal motion of all atoms leading to different channels which contribute to diffraction. This assumption can be expressed as

$$\vec{G}_{mn}^2 = (m^2 + n^2) \left(\frac{2\pi}{a} \right)^2 \ll k^2, \quad (3.1)$$

where a is the lattice spacing (taken to be the same in the x - and y -directions), m and n denote the order of diffraction, \vec{G}_{mn} is the reciprocal lattice vector for the mn -channel, and k is the wave number for the incident atoms. The surface structure is periodic in the xy -plane, and the atom-surface potential is taken to be

$$V(x, y, z) = V_0(z) + V_1(z) [\cos(2\pi x/a) + \cos(2\pi y/a)], \quad (3.2)$$

where specific forms will be assigned shortly to V_0 and V_1 when we carry out numerical calculations.

Due to Eq. (3.2) we can separate the motion in the z -direction from that in the xy -plane, which we treat classically by the equation of motion

$$\frac{1}{2}\mu \dot{z}^2 + V_0(z) = E, \quad (3.3)$$

where μ is the mass of the atom with incident energy $E = \hbar^2 k^2 / 2\mu$. The incident atom motion then satisfies a two-dimensional Schrödinger equation of the form

$$i\hbar \frac{\partial \psi(x, y, t)}{\partial t} = \left\{ -\frac{\hbar^2}{2\mu} \left(\frac{\partial^2}{\partial x^2} + \frac{\partial^2}{\partial y^2} \right) + V_1[z(t)] [\cos(2\pi x/a) + \cos(2\pi y/a)] \right\} \psi(x, y, t). \quad (3.4)$$

Here V_1 is time-dependent through $z(t)$ which satisfies Eq. (3.3), and this time-dependence constitutes the semiclassical nature of the present approach.

The wave function ψ can be expanded in terms of diffraction states

$$\psi(x, y, t) = \sum_{mn} b_{mn}(t) \exp(i\vec{G}_{mn} \cdot \vec{R} - iE_{mn} t), \quad (3.5)$$

where \vec{R} is the projection of the position vector of the incident atom onto the surface, and $E_{mn} = \hbar^2 \vec{G}_{mn}^2 / 2\mu$. Substituting Eq. (3.5) into (3.4) and assuming $V_1(t)$ to be significant only for a short time interval over which $(E_{(m+1)n} - E_{mn})t/\hbar$ and $(E_{m(n+1)} - E_{mn})t/\hbar$ for the important channels may be considered to be constant, we obtain a set of coupled equations for b_{mn} . The coefficient b_{mn} represents the diffraction amplitude for the mn -channel. Using the boundary condition $b_{mn}(-\infty) = \delta_{mn,00}$ we obtain the diffraction probability in the form

$$|b_{mn}(\infty)|^2 = J_m^2[u(\infty)] J_n^2[u(\infty)], \quad (3.6)$$

where J_m is the normal Bessel function of the m -th order, and

$$u(t) = \hbar^{-1} \int_{-\infty}^t dt' V_1(t'). \quad (3.7)$$

The above theory has been applied to the Ne-W(110) system, where we have used the Lennard-Jones-Devonshire potential for V_0 and V_1 ,

$$V_0(z) = D \exp[-\alpha(z-z_0)] \left\{ \exp[-\alpha(z-z_0)] - 2 \right\} \quad (3.8a)$$

$$V_1(z) = -2\beta D \exp[-2\alpha(z-z_0)] \quad (3.8b)$$

with values of parameters in atomic units taken from the literature as^{137,138} $D = 6.3 \times 10^{-4}$, $\alpha = 0.582$ and $\beta = 0.01$. The agreement of Eq. (3.6) with the results of exact close-coupling calculations¹³⁸ is excellent, as seen by the table below for an incident collision energy $E = 2.3245 \times 10^{-3}$ hartree:

Table 1. Diffraction probabilities for Ne-W(110)

Channel mn	J_m^2 J_n^2	Close Coupling ^a
00	0.4005	0.4016
10	0.1096	0.1099
20	0.0064	0.0061
30	0.00016	0.00014
11	0.0300	0.0299
22	0.0001	0.0001
21	0.0017	0.0017
31	0.00004	0.000036

^aYinnon et al.¹³⁸

To extend this picture to atom-surface scattering in the presence of laser radiation, we view the incident atom as made up of two electronic states, with a separate atom-surface potential correlating to each state:¹³⁶

$$V_i(x,y,z) = V_{0,i}(z) + V_{1,i}(z) [\cos(2\pi x/a) + \cos(2\pi y/a)], \quad (3.9)$$

where the subscript i indicates the state ($i=1$ or 2). [One can also generate multiple potentials by allowing for electronic excitations with the substrate.^{82,104}] We envision a situation where the photon energy $\hbar\omega$ is resonant with the potential difference $V_{0,2} - V_{0,1}$ at some normal distance $z=z_r$. If z_r is sufficiently large that the short-ranged potentials $V_{1,1}$ and $V_{1,2}$ are negligibly small, we can safely assume that the electronic excitation due to the laser and the diffractive transition due to the surface are well separated in time, and hence can be treated separately. Fig. 24 represents schematically the potential curves for the two electronic states 1 and 2, where curve 1 is shifted up by $\hbar\omega$ to cross curve 2 at $z=z_r$. A transition from 1 to 2 then involves the absorption of a photon, such that the laser field loses one photon. We should point out here that the laser need not be resonant with the asymptotic ($z=\infty$) states of the isolated atom.

As the atoms prepared in state 1 move toward the surface, they come to the crossing point z_r before diffraction occurs. A certain fraction of the atoms makes a transition to state 2 and then undergoes diffractive scattering with the surface as if they were prepared in state 2 with incident energy $E + \Delta$ (see Fig. 24). The normalized diffraction intensities for these atoms are then given by Eq. (3.6) with V_1 in Eq. (3.7) replaced by $V_{1,2}$. For a sufficiently high laser intensity (MW/cm^2 or higher), an observable fraction of atoms may give diffraction patterns characteristic of state 2, which could be different from those of state 1.

B. Phonon excitation.

We now consider a gas atom-surface collision process in the presence of laser radiation, where the laser frequency is chosen such that all transitions except a particular surface vibrational one, i.e., a phonon excitation, can be neglected.¹³⁹ The phonon can be excited by both the incident atom and the radiation. The basic assumptions of the model are the following: (1) the gas atom interacts directly only with the surface atom which it strikes; (2) the interaction between the gas atom and the surface atom is given by a truncated harmonic potential characterized by the well depth D and the interaction range b (see Fig. 25); (3) the surface atom is connected to the remainder of the solid by a spring whose force constant is determined by the vibrational frequency of the surface atom, with effects of lattice relaxation on this atom represented by a frictional force; (4) only motion perpendicular to the surface is considered; and (5) surface atom vibrations are coupled to the laser field via a dipole moment of the form $M_0 + M_1 z$, where z is the normal displacement of the surface atom from its equilibrium position. The

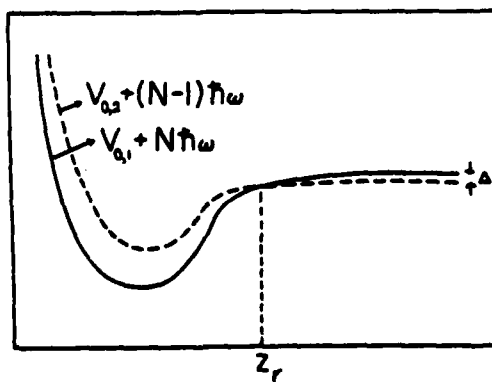


Fig. 24. Schematic representation of the potential energy curves for $V_{0,1}$ and $V_{0,2}$. N is the number of photons in the external field.

motions of the surface and incident atoms are then treated classically (Newton's laws), with the effects of the field represented by a classical time-dependent driving force.

The equations of motion to be solved are given by

$$m_g \ddot{y} = -m_s \omega^2 (y-z) \quad (3.10)$$

$$m_s \ddot{z} + m_s \gamma z + m_s \omega_s^2 z = m_s \omega^2 (y-z) + M_1 E_0 \cos(\omega_L t + \theta) , \quad (3.11)$$

where m_g (m_s) is the mass of the gas (surface) atom; y is the displacement of the gas atom measured from the minimum point of the gas-surface interaction potential where $z=0$; E_0 , ω_L and θ denote the electric field strength, frequency and phase of the laser radiation, respectively; ω_s is the surface vibrational frequency; γ denotes the damping caused by lattice relaxations; and ω is defined by

$$V(y-z) = \frac{D}{b} (y-z)^2 \equiv \frac{1}{2} m_s \omega^2 (y-z)^2 . \quad (3.12)$$

At time $t=0$, the gas atom enters the interaction region with initial velocity v_0 and is subject to the harmonic potential shown in Fig. 25 until it leaves the region at $t=t_1$, which is when the relative displacement $y-z$ equals b for the first time since $t=t_0$. Partial boundary conditions are then given by

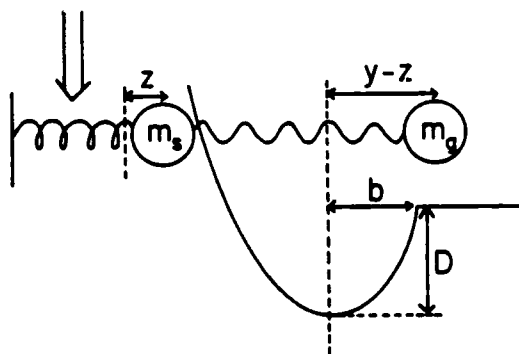


Fig. 25. Schematic diagram of a gas atom incident on a surface in the presence of a laser field. m_g and m_s are the masses of the gas and solid atoms, respectively, which are subject to a truncated harmonic potential with well depth D and interaction range b ; y and z are the displacements of the gas and solid atoms, respectively, from their equilibrium positions. The laser radiation is represented by the thick arrow.

$$y(0) - z(0) = b, \quad \dot{y}(0) = -v_0, \quad (3.13)$$

$$y(t_1) - z(t_1) = b, \quad \dot{y}(0) = v_0. \quad (3.14)$$

Before the scattering occurs, i.e., for $t \leq 0$, the surface atom interacts with the laser radiation only, and $z(0)$ and $\dot{z}(0)$ can be found by solving Eq. (3.11) without the driving term $m_s \omega^2 (y-z)$. The result is

$$z(0) = \frac{M_1 E_0}{m_s q} \cos(\theta - \beta), \quad (3.15)$$

$$\dot{z}(0) = -\frac{\omega_L M_1 E_0}{m_s q} \sin(\theta - \beta), \quad (3.16)$$

where

$$q = \left[\left(\omega_s^2 - \omega_L^2 \right)^2 + \gamma^2 \omega_L^2 \right]^{\frac{1}{2}}, \quad (3.17)$$

$$\tan \beta = \frac{\gamma \omega_L}{\omega_s^2 - \omega_L^2}. \quad (3.18)$$

Our task is to solve Eqs. (3.10) and (3.11) for $0 \leq t \leq t_1$ under the boundary conditions stated in Eqs. (3.13)-(3.18), and we adopt a perturbative approach which is valid provided $z(t)$ is small compared to b throughout the scattering process. The approach involves an iterative substitution of lower-order solutions (beginning with zero-order) to find higher-order solutions, and the first-order result for the total energy transferred to the surface atom averaged over θ is

$$\langle \Delta E \rangle^{(1)} = \frac{1}{2\pi} \int_0^{2\pi} d\theta \int_0^{t_1^{(1)}} dt \dot{z}^{(2)}(t) \left[f_1^{(1)}(t) + M_1 E_0 \cos(\omega_L t + \theta) \right], \quad (3.19)$$

where

$$f_1^{(1)}(t) = m_s \omega^2 \left[y^{(1)}(t) - z^{(1)}(t) \right], \quad (3.20)$$

$t_1^{(1)} > 0$ is a solution to

$$y^{(1)}[t_1^{(1)}] - z^{(1)}[t_1^{(1)}] = b, \quad (3.21)$$

and the superscript indicates the order of a given solution. Eq. (3.19) can be shown to have the form

$$\langle \Delta E \rangle^{(1)} = \Delta E_{\text{gas}}^{(1)} + \langle \Delta E \rangle_{\text{laser}} + I, \quad (3.22)$$

where $\Delta E_{\text{gas}}^{(1)}$ is the first-order energy transfer in the absence of the laser, $\langle \Delta E \rangle_{\text{laser}}$ is the energy transfer in the absence of the gas atom, and I represents an interference effect between the two types of transfer. I has the interesting

result in the limiting case of small b and high v_0 (but still low enough for the perturbative treatment to be valid) that $I > 0$ if $\omega_L > \omega_s$ and $I < 0$ if $\omega_L < \omega_s$.

The above theory can be illustrated with the example of He-W scattering in the presence of a laser field, with the following values of parameters: D , 65 K; b , 0.4 Å; T_g (helium gas temperature), 400 K; ω_s , 2.494×10^{13} Hz; γ , 2.261×10^{13} Hz; and M_1 (dipole derivative), 10^9 debyes/cm. The value of D is chosen according to Ref. 140, b is chosen to fit experimental data of energy accommodation coefficients,¹⁴¹ and ω_s and γ are chosen according to the prescription⁵⁷ for the Brownian parameters with the Debye temperature for W taken to be 330 K. The calculated value of $\Delta E_{\text{gas}}^{(1)}$ is 2.8×10^{-4} eV, and the energy accommodation coefficient α_E is found to be

$$\alpha_E = \frac{\Delta E_{\text{gas}}^{(1)}}{\frac{1}{2} m v_0^2} \approx 0.017 .$$

This is in agreement with the experimental data¹⁴¹ and results from the choice of the parameter b to get such agreement. The interference term I in Table 2 below is 0.1% to 1% of $\Delta E_{\text{gas}}^{(1)}$ and ΔE_{laser} .

Table 2. Results of the He-W calculation. ω_L is the laser frequency, the laser intensity is taken as 10 GW/cm² and $\Delta E_{\text{gas}}^{(1)} = 2.8 \times 10^{-4}$ eV.

ω_L (10^{13} Hz)	$\langle \Delta E \rangle_{\text{laser}}$ (10^{-4} eV)	I (10^{-4} eV)
2.706	2.94	0.0031
2.6	3.01	-0.00063
2.494	3.04	-0.0046
2.388	3.01	-0.0080
2.282	2.93	-0.013

A stronger interference can be expected for higher incident energy or laser intensity, although then the perturbation treatment would fail and numerical methods would have to be adopted to integrate the equations of motion. It is disappointing that the laser intensity is so high (most of the processes discussed in this review article occur with considerably lower intensities), and this raises concerns about surface damage. While the process discussed previously for diffraction may also require high intensities, there are laser-induced phenomena in gas-surface collisions where the intensity need not be high, such as ion neutralization to be discussed later, where the laser excites electrons to surface states of the substrate during the collision.

C. Collisional ionization and neutralization

We shall discuss first a model for collisional ionization of an adspecies by an impinging atom, and then shall turn to a treatment of ion neutralization where an impinging positive ion picks up an electron from a surface. There has been both experimental¹⁴² and theoretical¹⁴³ interest in Penning ionization, where metastable He* atoms impinge on a CO-covered Pd surface resulting in electron emission from CO. We have considered theoretically the problem of gas-phase Penning ionization of He* atoms in the presence of a laser field,¹⁴⁴ where photon absorption and stimulated emission results in interesting structure in the energy spectra of the emitted electrons. An attractive feature of this process is that there is a continuous range of laser frequencies for which this structure can be observed, since the laser is coupling bound and continuum electronic states. Furthermore, since this coupling can occur over a wide range of internuclear distances, lower laser intensities should be required than for electronic bound-bound coupling (such as in Fig. 24 where the radiative interaction is localized at $z=z_r$).

Motivated by the work of Refs. 142-144, we have developed a formalism to treat the problem of Penning ionization of an adsorbed atom on a metallic solid surface in the presence of laser radiation.¹⁴⁵ The ionizing agents are taken to be excited atoms and laser radiation with frequency low compared to the inverse of characteristic collision times. The laser frequency is also taken to be much less than characteristic band structure resonances of the pure metallic surface so that photoemission need not be considered as a competing process. We also require it to be far from resonance with vibrations or phonons of the adatom-surface system to exclude laser-induced desorption or migration.

The physical constraints of short collision time and low laser frequency permit the use of the quasistatic approximation, where the energy of the system is considered to be adiabatically conserved within the duration of a characteristic collision time. The short collision time also warrants the use of the impulse approximation in the treatment of the projectile atom-adatom collision dynamics. Within this approximation, the collision between the projectile atom (B) and the adatom-surface (AS) system is assumed to be mediated by a single electron possessing a characteristic momentum and energy distribution determined by virtue of its being part of the AS + field system, and otherwise considered to be free. The time-dependent differential ionization cross section can then be written as

$$d^6\sigma(t) = \frac{2\pi}{\hbar} S(\vec{p}_1, \epsilon_1; t) \left| T_{E_f p_f p; E_i p_i p_1} \right|^2 \frac{1}{v_0} \frac{d^3 p_d^3 p_f}{(2\pi\hbar)^3} \quad (3.23)$$

The various quantities are explained as follows: S , the time-dependent spectral function, describes the momentum (\vec{p}_1) and energy (ϵ_1) distribution of an electron

in the AS + field system. T is an electron-atom scattering matrix element, describing the collision between a projectile atom B in the initial internal state $|i\rangle$ with kinetic energy $p_i^2/2m_B$ and a free electron with momentum \vec{p}_1 , to produce B in the de-excited internal state $|f\rangle$ with final kinetic energy $p_f^2/2m_B$ and a free electron with momentum \vec{p} . $E_i - E_f$ is the transfer of internal excitation of B , and v_0 is its incident velocity.

The treatment of the problem can thus be separated into two parts: the determination of an electron spectral function (S) for the AS + field system and the calculation of an electron-atom T -matrix element. The latter problem has been well studied by atomic physicists, and we have focused our attention on the former problem dealing with the AS + field system. The Green's function formalism for many-body problems provides a natural framework for the computation of S . We shall not go into the details here, but simply indicate that within the quasistatic approximation it can be shown that

$$S(\vec{p}_1, \epsilon_1; t) = \frac{1}{\pi} \lim_{\eta \rightarrow 0} \text{Im} \tilde{G}_A(\vec{p}_1, \epsilon_1 - i\eta; t) \quad (3.24)$$

where \tilde{G}_A is the advanced single-particle Green's function for the AS + field system. To obtain \tilde{G}_A we first calculate the space-time Green's function and take its Fourier transform to obtain the energy-momentum Green's function $G(\vec{p}, \vec{p}, \epsilon; t)$, which is related in a straightforward fashion to \tilde{G}_A .

Let us now consider the process of ion neutralization, where a positive ion impinges on a surface and picks up an electron to leave as a neutral atom.^{146,147} It was shown in Sec. 2.B.1 that the excitation of electrons from a bulk valence band to surface states in a semiconductor results in an increased electronic charge in the surface region. This suggests that the neutralization probability can be significantly enhanced if the semiconductor surface is electronically excited, since the impinging ions have easier access to the excited surface electrons than to the bulk electrons. Little attention so far has been given to dynamical gas-surface processes where the surface is electronically excited, with some exceptions such as studies of Auger neutralization¹⁴⁸ and certain energy-transfer phenomena.⁸² Here we want to look at resonance neutralization of ions at electronically-excited semiconductor surfaces.¹⁴⁹

The electronic wave function of the entire system can be written as

$$\psi(\vec{r}_1, \vec{r}_2, \dots, \vec{r}_n, t) = C_I(t) \phi_I + \sum_{j=1}^m C_F^j(t) \chi_F(\vec{r}_j) \phi_F(\vec{r}_1, \vec{r}_2, \dots, \vec{r}_{j-1}, \vec{r}_{j+1}, \dots, \vec{r}_n) \quad (3.25)$$

where ϕ_I describes the electronic state of the surface before collision, \vec{r}_i is the position vector of the i -th electron, χ_F denotes the atomic wave function of the j -th electron which is picked up by the incoming ion, \vec{r}_j' is the position vector

of the j th electron measured from the nucleus of the departing atom ($\vec{r}_j = \vec{r}_j - \vec{R}$), and ϕ_F denotes the wave function of the remaining $(n-1)$ electrons on the surface. We have ignored electrons that are bound to the incident ion in writing ϕ_I , so that our approach is most readily applicable to incoming protons, and have neglected contributions from states other than the initial and final states, ϕ_I and $\chi_F \phi_F$. We shall assume the position vector \vec{R} of the incoming ion to be a known function of time.

Substituting Eq. (3.25) into the Schrödinger equation, we arrive at a set of coupled differential equations for the coefficients C_I and C_F^j . Going to a continuum limit such that each electron is now labelled by its energy E instead of j , we find the neutralization rate Γ to be given by

$$\Gamma(t) = \frac{\pi}{\hbar} \rho(E_0) H_{FF}^{E_0}(t) H_{FI}^{E_0}(t) \quad (3.26)$$

$\rho(E)$ is the energy distribution of electrons, and its variation with respect to E is assumed to be slow. $E_0 = E_0(t)$ is the energy which satisfies the relation

$$H_{II}(t) - H_{FF}^{E_0}(t) = 0 \quad (3.27)$$

The various time-dependent matrix elements are given as

$$H_{II}^E = \langle \phi_I | H | \phi_I \rangle, \quad H_{FF}^E = \langle \chi_F(E) \phi_F | H | \chi_F(E) \phi_F \rangle \quad (3.28)$$

$$H_{IF}^E = \langle \phi_I | H | \chi_F(E) \phi_F \rangle, \quad H_{FI}^E = \langle \chi_F(E) \phi_F | H | \phi_I \rangle, \quad (3.29)$$

where H is the sum of the kinetic and potential energy operators of all n electrons. According to Eq. (3.27), at time t the transfer of a surface electron of energy E_0 to the ion is an energy-conserving process, where H_{II} and $H_{FF}^{E_0}$ represent the diabatic potentials correlating to the initial and final states, respectively, of the projectile. The resonance energy E_0 varies from $-W$ at t_1 to $(-W+E_g)$ at t_2 , where W is the work function and the transfer of a surface electron to the incident ion occurs at a time between t_1 and t_2 .

We have introduced several approximations to evaluate $\Gamma(t)$,¹⁴⁹ such as the neglect of interaction between electrons on the surface, a one-dimensional treatment of the lattice and a symmetrized form for H_{IF}^E and H_{FI}^E .¹⁴⁷ This results in a form for $\Gamma(t)$ as

$$\Gamma(t) = \Gamma_0 N_{E_0}^2 f_{E_0}^2 [z(t)] \quad (3.30)$$

where Γ_0 depends on a variety of quantities such as $\rho(E_0)$ and W , N_{E_0} is a normalization constant for an electron with energy E_0 , and f_{E_0} is a function of the time-dependent ion (atom)-surface separation (i.e., distance normal to the surface).

From an inspection of N_{E_0} it can be shown that the neutralization rate is larger by a factor of $|2\kappa_E L|$ for a surface electron than for a bulk electron, where κ_E is the imaginary part of the crystal momentum and L is the length of the solid. The physical reason for this is that a surface electron has a greater probability to be found in the region of the surface (thus a greater normalization constant) and therefore can be more easily picked up by the incident ion.

A suggested candidate for testing this idea is the $\text{He}^+\text{-Si}(111)$ system. For neutralization into $\text{He}^*(2^3\text{S})$ the asymptotic defect Δ ranges from ~ 0.07 eV to ~ 1.17 eV, where the lower number corresponds to the asymptotic difference between H_{II} and H_{FF}^{-W} (the energy is measured relative to the ionization level of the solid), and the upper number corresponds to the asymptotic difference between H_{II} and $H_{\text{FF}}^{-W+E_g}$ ($E_g \approx 1.1$ eV). As the ion approaches the solid, H_{II} comes into resonance with H_{FF}^{-W} at t_1 and with $H_{\text{FF}}^{-W+E_g}$ at t_2 , and the time between t_1 and t_2 corresponds to resonance with diabatic potentials correlating with surface states. Single-photon absorption from a low-power CW HF laser will populate surface states over a third of the way up the band gap, with a significant increase in the neutralization rate.

D. Partial pressure and surface coverage

In this section, we shall investigate the partial pressure of selectivity-excited adspecies in a multicomponent system by combining the generalized Langmuir kinetic theory and the laser rate equation.¹⁵⁰ We first calculate the total desorption rate in terms of the laser-induced and thermal-excitation-induced rates and the steady-state partial pressure produced by the desorption of excited adspecies. The possible mechanism for laser-stimulated desorption will then be discussed.

Employing the Langmuir equation for the laser-stimulated rate, we may express the steady-state partial pressure of the desorbed species as follows:^{150,151}

$$p = (k_T + k_L) z^{1-y} \theta^x / (1-\theta)^y, \quad (3.31)$$

where z is the number of unoccupied nearest-neighbor sites; x and y are the kinetic order and occupancy order, e.g., $(x,y) = (1,2)$ and $(2,2)$ are the associative dual-site and the dissociative dual-site occupancy, respectively; θ is the fractional coverage of the selectively-excited adspecies; and k_T and k_L are the thermally-induced and laser-induced desorption rates. The thermal desorption rate may be expressed by an Arrhenius form^{126,151}

$$k_T = k_0 \exp\left[-E_d^*/k_B T_s\right], \quad (3.32)$$

where k_0 is a preexponential factor, k_B the Boltzmann factor, T_s the surface temperature and $E_d^* = E_d - F(\theta)$, E_d being an activation energy at low coverage and $F(\theta)$ a coverage-dependent correction factor due to the adspecies-adspecies inter-

action. The laser-stimulated desorption rate k_L may be calculated from the master equation for the energy population [Eq. (2.49)]. The results show a power law $k_L \propto I^p$, where I is the laser intensity and p is the power factor $\frac{1}{3} \leq p \leq 1$ as discussed in a previous section.¹⁵⁰

In Eq. (3.31) we assumed that the total desorption rate is simply the sum of k_T and k_L and ignored the interference between the incoherent thermal excitation and the coherent laser excitation. A more rigorous treatment including this interference effect shows that both k_T and k_L are influenced by changing the temperature of the laser-heated surface, whereby the adspecies is pumped to higher vibrational states by the coherent laser field and finally desorbed from the laser-heated surface via a thermal excitation channel. We note that a previous 1D Morse potential model without these interference effects results in an unrealistically high laser intensity, $I \approx 10^{14}$ W/cm², for laser desorption. In fact, the intensity required for desorption should be significantly lower than the above estimate, if coherent laser excitation pumps the adspecies to some higher vibrational state with subsequent excitation to the desorption state via laser-induced thermal phonons. We note that a much lower laser intensity suffices for the initial coherent excitation compared to that in the 1D Morse model, where an extremely high laser intensity is needed to overcome the anharmonicity near the desorption region.^{74,103} A new model including the aforementioned interference effects and thereby providing a nonequilibrium total desorption rate takes the form^{100,152}

$$k_D(t) = \int_0^\infty d\epsilon \sum_n W_{n\epsilon}(t) P_n(t) , \quad (3.33)$$

where $P_n(t)$ is the probability that the adspecies is in the bound vibrational state $|n\rangle$, given by, e.g., a Poisson function [Eq. (2.77)]. $W_{n\epsilon}(t)$ is a thermal transition rate from the bound state $|n\rangle$ to the continuum state $|\epsilon\rangle$ given by

$$W_{n\epsilon}(t) = k_0 \exp\left[-(\epsilon - E_n)/k_B T_s(t)\right] , \quad (3.34)$$

where E_n is the energy of the n -th vibrational state. The laser-induced surface temperature can be calculated from a heat diffusion equation¹⁰⁰

$$\frac{\partial T}{\partial t} = \vec{\nabla} \cdot (D \vec{\nabla} T) + \frac{\theta}{C_v} W_R(T) , \quad (3.35)$$

where T is the laser-induced transient temperature of the system with diffusivity D and heat capacity C_v , and heat diffuses according to the gradient, $\vec{\nabla}$, in the direction of energy flow; θ is a coverage factor defined in Eq. (3.31); $W_R(T)$ is a temperature-dependent nonequilibrium energy relaxation rate of the pumped adspecies via multiphonon processes and can be calculated from the correlation function of

the active mode-bath mode interaction Hamiltonian H_{AB} [Eq. (2.81b)].¹⁰⁰

Knowing the total desorption rate $k_D(t)$, we may calculate the dynamical partial pressure of the desorbed species from the desorption rate equation for the coverage,¹⁵³

$$-\frac{d\theta(t)}{dt} = k_D(t)\theta^n(t) \quad , \quad (3.36)$$

where n is the desorption order. For first-order kinetics, $n=1$, the formal solution of Eqs. (3.33) - (3.36) is readily deduced, with an initial coverage θ_0 , as

$$\theta(t) = \theta_0 \exp \left\{ - \int_0^t dt' \int_0^\infty d\varepsilon k_0 \exp \left[-(\varepsilon - E_n)/k_B T_S(t') \right] \right\} . \quad (3.37)$$

The above discussion suggests some possible desorption mechanisms: (i) Direct bond breaking characterized by the laser desorption rate k_L if the laser pumping rate is faster than the intramolecular vibrational relaxation rate (IVR). (ii) Indirect bond breaking via fast anharmonic IVR where the thermal desorption rate k_T dominates the processes. (iii) Indirect bond breaking via bound-continuum coupling. Consider, for example, the system CO-Ni in which $\omega_{CO} \gg \omega_{CNi}$, and excitation of the CO bond causes rupture of the CNi bond. This process may be referred to as "autodesorption" in analogy with Fano's "autopredissociation" for a system governed by configuration coupling.¹⁵⁴ (iv) Migration-induced reactive desorption in which the absorption of photon energy causes the adspecies to change its state from a strongly-bound chemisorbed state to a weakly-bound physisorbed state. The resulting high mobility may lead to migration-induced desorption via reactive collisions with other adspecies. This type of desorption can be investigated by combining the migration rate governed by the Hamiltonian in Eq. (2.256) and the desorption rate given in Eq. (3.33).¹⁵³

4. Surface Waves

Surface waves (SW) or surface polaritons have recently received considerable attention.¹⁵⁵⁻¹⁵⁷ For an electromagnetic wave propagating along an interface, the electric and magnetic fields decay exponentially as one moves away from the interface. The dispersion of the propagation wave vector, assumed to be in the x -direction, may be expressed as

$$k_x(\omega) = \frac{\omega}{c} \left[\frac{\varepsilon_g(\omega)\varepsilon_m(\omega)}{\varepsilon_g(\omega) + \varepsilon_m(\omega)} \right]^{\frac{1}{2}} \quad , \quad (4.1)$$

where ω and c are the frequency and speed of light in air for a metal-air interface system and $\varepsilon_g(\omega)$ and $\varepsilon_m(\omega)$ are the dielectric functions. In general, the metal

has a complex dielectric function, and for SW to exist we require

$$\operatorname{Re}\epsilon_m(\omega) < -\operatorname{Re}\epsilon_g(\omega) \quad (4.2)$$

It is seen that under the above condition, $k_x(\omega)$ is a complex function whose imaginary part tells us how fast the SW decays when it propagates along the interface. We note that SW may propagate several centimeters at a wavelength of $10 \mu\text{m}$, since most of the energy in the SW is in the air above the metal.

For a short pulse propagating in a dilute gas medium, the electric field of the pulse may be described by an optical Bloch equation, neglecting damping rates.¹³⁰ This lossless system provides us with a coherent pulse which is area- and shape-stable in its propagation and has a hyperbolic secant amplitude. Combining this result from a Bloch equation with a Maxwell equation and imposing the usual boundary condition, we can investigate the propagation of SW along the interface between a dilute gas medium and a metal.¹⁵⁸ To demonstrate the exponential decay of SW propagating along the interface, we present amplitude profiles in Fig. 26. It is seen that SW decays faster in the metal than in the air.

5. Annealing

Laser-matter interactions have interesting applications in materials processing.¹⁵⁹⁻¹⁶¹ Areas such as laser-assisted crystal regrowth and annealing of ion-implantation damage have provided an economically competitive alternative to conventional methods. We shall study the fundamental physical phenomena that

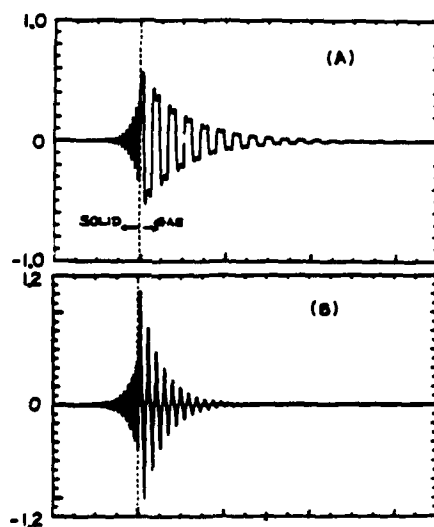


Fig. 26. Propagation of SW along a metal-air interface at $z=0$ for (A) strong damping in the metal with $\operatorname{Re}\epsilon_m = -10$ and (B) weak damping with $\operatorname{Re}\epsilon_m = -5$. The dielectric function for the air is $\operatorname{Re}\epsilon_g \approx -1$.

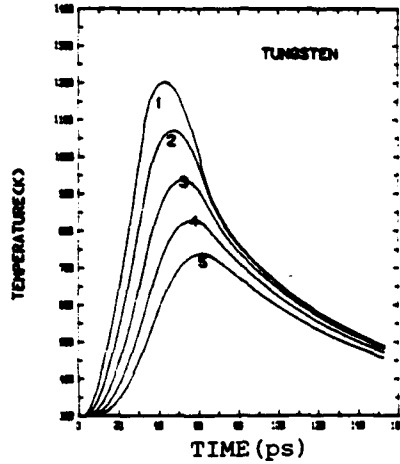


Fig. 27. Temperature profiles for laser-heated tungsten at different depths: $z = 20n$ (\AA), $n=0,5,10,15$ and 20 for curves 1 to 5, respectively, Here a Gaussian pulse has been approximated by an isosceles triangle with $\text{FWHM}=30$ ps and intensity $I = 5 \text{ GW/cm}^2$.¹⁶⁵

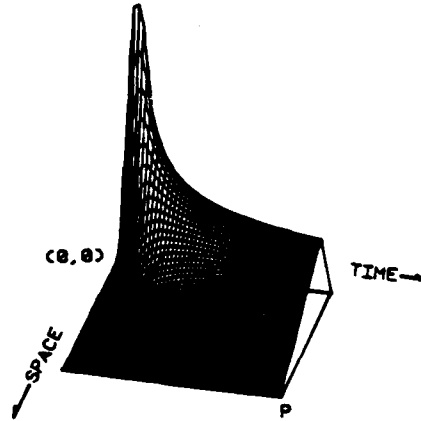


Fig. 28. 3D temperature profiles corresponding to Fig. 27, where the point is $p = (350 \text{ ps}, 5000 \text{ \AA})$.¹⁶⁵

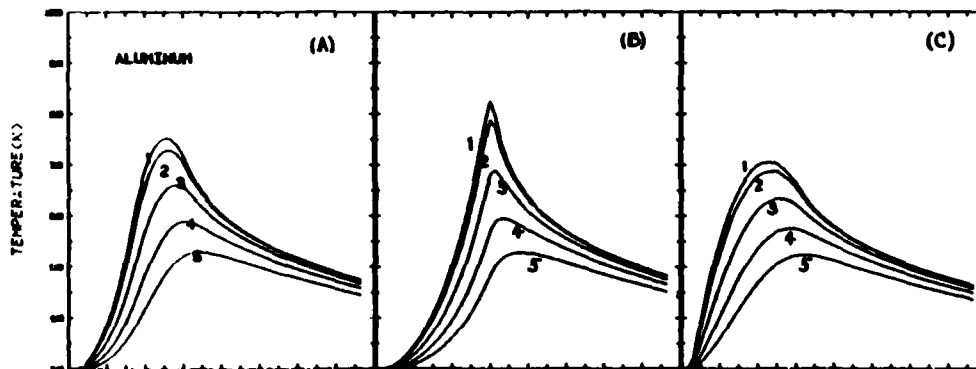


Fig. 29. Temperature profiles for laser-heated aluminum with a temperature-dependent absorptivity for different pulse shapes as defined in Eq. (2.406) for triangular temporal dependence with laser intensity peaked at a and $\text{FWHM (ps)} = (a+b)/2$ for (A) $(a,b)=(30,30)$, (B) $(a,b)=(55,5)$ and (C) $(a,b)=(5,55)$. Here a laser peak intensity $I = 1 \text{ GW/cm}^2$ has been used. Curves 1 to 5 are for different depths as shown in Fig. 27.¹⁶⁵ As in Fig. 27, each abscissa ranges from 0 to 160 ps.

underlie laser material processing in which the laser-generated temperature increase of the material plays an essential role. The absorption of photon energy occurs primarily through its interaction with electrons which rapidly give up their energy via collision processes, on a time scale of a picosecond or less. The absorbed energy is then transformed into lattice phonon energy, i.e., heat. Within the transient laser heating region, most of the photon energy is deposited within a range of $1/\alpha$, where α is the absorption coefficient, and decreases monotonically with depth. For metals, typical values of α are in the range of $10^4 - 10^5 \text{ cm}^{-1}$, so that the laser energy (heat) is deposited in a thin layer of $10^{-5} - 10^{-4} \text{ cm}$.

Laser annealing can be accomplished by either a CW laser or a pulsed laser and involves solid-state and liquid-state regrowth of the ion-implanted layers. One point of view is that pulsed-laser annealing involves heating and melting of the surface,¹⁶² while another suggests nonthermal processes to occur due to the presence of a dense plasma of free carriers excited by the laser radiation.¹⁶³ In the latter case, the electron temperature in the plasma is assumed to be much higher than the lattice temperature. In this section, we shall present a thermal model in which a heat diffusion equation is solved to obtain the laser-generated transient temperature of the material. In the previous section, we assumed a constant absorptivity $A \equiv 1-R$ to calculate the thermionic current emitted from a tungsten surface, and only the surface temperature was shown. To demonstrate the temperature increase of the laser-heated tungsten on the surface and in the bulk, we solve the heat diffusion equation [Eq. (2.403)] numerically. The results for the temperature profiles are shown in Fig. 27 for the 2D case and in Fig. 28 for the 3D case.

In general, most metals have a temperature-dependent absorptivity which can lead to a positive feedback and thereby a considerable increase in the laser-generated temperature compared to the case of constant absorptivity. For the case of aluminum, the absorptivity is¹⁶⁴

$$A = A_0 + A_1 T, \quad (5.1)$$

with $A_0 = 4.67 \times 10^{-3}$ and $A_1 = 3.05 \times 10^{-5}/\text{K}$. The results are shown in Fig. 29 for 2D.¹⁶⁵

Acknowledgments

This research was supported in part by the Office of Naval Research, the Air Force Office of Scientific Research (AFSC), United States Air Force, under Grant AFOSR-82-0046, the National Science Foundation under Grant CHE-8022874 and the U.S. Army Research Office. The United States Government is authorized to reproduce and distribute reprints for governmental purposes notwithstanding any copyright nota-

tion hereon. TFG acknowledges the Camille and Henry Dreyfus Foundation for a Teacher-Scholar Award (1975-84) and the John Simon Guggenheim Memorial Foundation for a Fellowship (1983-84). Special thanks go to June M. Rouse for her extreme patience, accuracy and dedication in typing this manuscript.

References

1. T. F. George, A. C. Beri, K. S. Lam and J. Lin, in Laser Applications, Vol. 5, R. K. Erf and J. F. Ready, eds., Academic Press, New York, in press.
2. T. F. George, J. Phys. Chem., **86**, 10 (1982).
3. T. F. George, Opt. Eng., **18**, 167 (1979).
4. T. F. George, ed., Special Issue on "Laser Applications to Chemistry", Opt. Eng., **19**, 1-112 (1980).
5. A. H. Zewail, V. S. Letokhov, R. N. Zare, R. B. Bernstein, Y. T. Lee and Y. R. Shen, in A Special Issue on "Laser Chemistry", Physics Today, **33** (11), 25-59 (1980).
6. R. M. Osgood, Jr. and S. R. J. Brueck, eds., Laser Diagnostics and Photochemical Processing for Semiconductor Devices, Elsevier, New York, in press.
7. D. H. Auston, W. L. Brown and G. K. Celler, Bell Laboratories Record (July/August, 1979), pp. 187-191.
8. D. J. Ehrlich, R. M. Osgood, Jr. and T. F. Deutsch, IEEE J. Quantum Electron., **QE-12**, 1233 (1980).
9. S. D. Allen and M. Bass, J. Vac. Sci. Technol., **16**, 431 (1979).
10. J. I. Steinfeld, T. G. Anderson, C. Reiser, B. R. Denison, L. D. Hartsough and J. R. Hollahan, J. Electrochem. Soc., **127**, 514 (1980).
11. M. S. Djidjoev, R. V. Khokhlov, A. V. Kiselev, V. A. Namiot, A. I. Osipov, V. I. Panchenko and B. I. Provotorov, in Tunable Lasers and Applications, A. Mooradian, T. Jaeger and P. Stokseth, eds., Springer, Berlin (1976), pp. 100-107.
12. F. Schwirzke, L. Oren, S. Talmadge and R. J. Taylor, Phys. Rev. Lett., **40**, 1181 (1978); G. Ertl and M. Neumann, Z. Naturforschung, **27a**, 1607 (1972); J. P. Cowin, D. J. Auerbach, C. Becker and L. Wharton, Surface Sci., **78**, 545 (1978).
13. R. Viswanathan, D. R. Burgess, Jr., P. C. Stair and E. Weitz, J. Vac. Sci. Technol., **20**, 605 (1982).
14. T. J. Chuang and H. Seki, Phys. Rev. Lett., **49**, 382 (1982); J. Heidberg, H. Stein and E. Riehl, Phys. Rev. Lett., **49**, 666 (1982).
15. For a review of photodesorption using incoherent light sources, see D. Lichtman and Y. Shapiro, CRC Crit. Rev. Solid State Sci., **8**, 93 (1978).
16. N. V. Karlov and A. M. Prokhorov, Sov. Phys. Usp., **20**, 721 (1977).
17. A. V. Khmelev, V. V. Apollonov, V. D. Borman, B. J. Nikolaev, A. A. Sazykin, V. I. Troyan, K. N. Firsov and B. A. Frolov, Sov. J. Quantum Electron., **7**, 1302 (1977); M. S. Dzhidzhoev, A. J. Osipov, V. Ya. Panchenko, V. T. Platonenko, R. V. Khokhlov and K. V. Shahtan, Sov. Phys. JETP, **47**, 684 (1978).
18. M. E. Umstead and M. C. Lin, J. Phys. Chem., **82**, 2047 (1978); M. E. Umstead, L. D. Talley, D. E. Tevault and M. C. Lin, Opt. Eng., **19**, 94 (1980); G. S. Selwyn and M. C. Lin, in Lasers as Reactants and Probes in Chemistry, W. M. Jackson and A. B. Harvey, eds., Howard University Press, Washington, D. C. (1983), in press.
19. D. R. Betteridge and J. T. Yardley, Chem. Phys. Lett., **62**, 570 (1979).
20. T. J. Chuang, J. Chem. Phys., **74**, 1461 (1981); T. J. Chuang and F. A. Houle, J. Vac. Sci. Technol., **20**, 603 (1982).
21. V. I. Goldanskii, V. A. Namiot and R. V. Khokhlov, Sov. Phys. JETP, **43**, 1226 (1976).
22. M. Wautelat, Surface Sci., **95**, 299 (1980).

23. J. R. Rios Leite and C. B. de Araujo, Chem. Phys. Lett., 73, 71 (1980).
24. H. J. Kreuzer and D. N. Lowy, Chem. Phys. Lett., 78, 50 (1981).
25. C. Jedrzejek, K. F. Freed, S. Efrima and H. Metiu, Surface Sci., 109, 191 (1981).
26. F. O. Goodman, Surface Sci., 109, 341 (1981).
27. G. Korzeniewski, E. Hood and H. Metiu, J. Vac. Sci. Technol., 20, 594 (1982).
28. A. Nitzan and L. E. Brus, J. Chem. Phys., 75, 2205 (1981).
29. T. F. George, J. Lin, K. S. Lam and C. Chang, Opt. Eng., 19, 100 (1980).
30. J. Lin and T. F. George, J. Chem. Phys., 72, 2554 (1980).
31. J. Lin, A. C. Beri, M. Hutchinson, W. C. Murphy and T. F. George, Phys. Lett., 79A, 233 (1980).
32. J. Lin and T. F. George, Surface Sci., 100, 381 (1980).
33. J. Lin and T. F. George, J. Phys. Chem., 84, 2957 (1980).
34. J. Lin, X. Y. Huang and T. F. George, Z. Phys. B, 48, 355 (1982).
35. J. Lin and T. F. George, J. Chem. Phys., 78, 5197 (1983).
36. W. H. Louisell, Quantum Statistical Properties of Radiation, Wiley, New York, (1973).
37. N. N. Bogoliubov and Y. A. Mitropolsky, Asymptotic Methods in the Theory of Nonlinear Oscillators, Gordon and Breach, New York, (1961).
38. J. Lin and T. F. George, Surface Sci., 117, 587 (1982).
39. J. Lin, Phys. Lett., 70A, 195 (1979).
40. J. Lin and T. F. George, Phys. Lett., 80A, 296 (1980).
41. J. Lin and T. F. George, Surface Sci., 108, 340 (1981).
42. J. Lin, Ph.D. Thesis, University of Rochester (1980).
43. J. Lin and T. F. George, Phys. Rev. B, 24, 65 (1981).
44. R. Kubo, Rep. Prog. Phys., 29, 225 (1966).
45. L. M. Narducci and J. M. Yuan, Phys. Rev. A, 22, 261 (1980).
46. A. Tsuchida, Surface Sci., 14, 375 (1969); H. Chow and E. D. Thompson, Surface Sci., 59, 225 (1976); M. W. Cole and D. R. Frankl, Surface Sci., 70, 585 (1978).
47. F. Ricca, C. Pisani and E. Garrone, J. Chem. Phys., 51, 4079 (1969); F. J. Milford and A. D. Novaco, Phys. Rev. A, 4, 1136 (1971).
48. J. L. Beeby, CRC Crit. Rev. Solid State Mater. Sci., 7, 153 (1978); D. A. King, ibid. 7, 167 (1978); F. O. Goodman, Surface Sci., 24, 667 (1971); D. Menzel, in Interactions on Metal Surfaces, R. Gomer, ed., Springer, Berlin (1975), pp. 102-143.
49. F. O. Goodman, CRC Crit. Rev. Solid State Mater. Sci., 6, 33 (1977); J. C. Tully, Ann. Rev. Phys. Chem., 31, 319 (1980).
50. B. Bendow and S.-C. Ying, Phys. Rev. B, 7, 622 (1973); S.-C. Ying and B. Bendow, ibid. 637 (1973).
51. Z. W. Gortel, H. J. Kreuzer and D. Spaner, J. Chem. Phys., 72, 234 (1980); E. Goldys, Z. W. Gortel and H. J. Kreuzer, Surface Sci., 116, 33 (1982).
52. F. O. Goodman and I. Romero, J. Chem. Phys., 69, 1086 (1978).
53. S. A. Cohen and J. G. King, Phys. Rev. Lett., 31, 703 (1973).
54. S. A. Adelman and J. D. Doll, J. Chem. Phys., 61, 4242 (1974); 62, 2518 (1975); D. J. Deistler and R. S. Wilson, ibid. 62, 1572 (1975); S. A. Adelman, ibid. 64, 124 (1976).
55. J. D. Doll, L. E. Myers and S. A. Adelman, J. Chem. Phys., 63, 4908 (1975).
56. J. D. Doll, J. Chem. Phys., 68, 3158 (1978); C. L. Brooks III, M. Berkowitz and S. A. Adelman, ibid. 73, 4353 (1980).
57. S. A. Adelman and J. D. Doll, J. Chem. Phys., 64, 2375 (1976); S. A. Adelman and B. J. Garrison, ibid. 65, 3751 (1976).
58. H. Mori, Prog. Theoret. Phys., 33, 423 (1965); 34, 399 (1965).
59. R. Zwanzig, in Lectures in Theoretical Physics (Boulder) III, Interscience, New York (1960), p. 106; Ann. Rev. Phys. Chem., 16, 67 (1965).
60. M. Shugard, J. C. Tully and A. Nitzan, J. Chem. Phys., 66, 2534 (1977).
61. J. C. Tully, G. H. Gilmer and M. Shugard, J. Chem. Phys., 71, 1630 (1979).

62. J. H. McCreery and G. Wolken, Jr., J. Chem. Phys., 63, 2340 (1975); 64, 2845 (1976); 65, 1310 (1976); 67, 2551 (1977).
63. G. Wolken, Jr., J. Chem. Phys., 60, 2210 (1976); Y.-W. Lin and G. Wolken, Jr., ibid. 65, 2634 (1976); 65, 3729 (1976).
64. A. C. Diebold and G. Wolken, Jr., Surface Sci., 82, 245 (1979).
65. W. E. Carlos, G. Derry and D. R. Frankl, Phys. Rev. B, 19, 3258 (1979); W. E. Carlos and M. Cole, Phys. Rev. B, 21, 3713 (1980).
66. D. R. Frankl, D. Wesner, S. V. Krishnaswamy, G. Derry and T. O'Gorman, Phys. Rev. Lett., 41, 60 (1978).
67. C. E. Harvie and J. H. Weare, Phys. Rev. Lett., 40, 87 (1978); K. L. Wolfe and J. H. Weare, Surface Sci., 94, 581 (1980); J. H. Weare, in Potential Energy Surfaces and Dynamics Calculations, D. G. Truhlar, ed., Plenum, New York (1981), p. 817.
68. A. D. Novaco and F. J. Milford, Phys. Rev. A, 5, 783 (1972); see also References 47 and 65.
69. R. I. Masel, R. P. Merrill and W. H. Miller, J. Chem. Phys., 64, 45 (1976); 65, 2690 (1976).
70. H. Metiu, J. Chem. Phys., 67, 5456 (1977).
71. K. Kitahara, H. Metiu, J. Ross and R. Silbey, J. Chem. Phys., 65, 2871 (1976).
72. S. Efrima and H. Metiu, J. Chem. Phys., 69, 2286 (1978).
73. S. Efrima, K. F. Freed, C. Jedrzejek and H. Metiu, Chem. Phys. Lett., 74, 43 (1980).
74. C. Jedrzejek, K. F. Freed, S. Efrima and H. Metiu, Chem. Phys. Lett., 79, 227 (1981).
75. Z. W. Gortel and H. J. Kreuzer, Chem. Phys. Lett., 67, 197 (1979); H. J. Kreuzer, Surface Sci., 100, 178 (1980); Z. W. Gortel, H. J. Kreuzer and R. Teshima, Phys. Rev. B, 22, 512 (1980); H. J. Kreuzer and Z. W. Gortel, Chem. Phys. Lett., 73, 365 (1980); Z. W. Gortel, H. J. Kreuzer and R. Teshima, Phys. Rev. B, 22, 5655 (1980).
76. H. J. Kreuzer and P. Summerside, Surface Sci., 111, 102 (1981)
77. Z. W. Gortel, H. J. Kreuzer, R. Teshima and L. A. Turski, Phys. Rev. B, 24, 4456 (1981); H. J. Kreuzer and R. Teshima, ibid. 24, 4470 (1981).
78. M. R. Baklanov, I. M. Beterov, S. M. Repinski, A. V. Rzhano, V. P. Chebotaev and N. I. Yurshina, Sov. Phys. Dokl., 19, 312 (1974); R. V. Ambartsumyan, Yu. A. Gorokhov, G. N. Makarov, A. A. Pureskii and N. P. Furzikov, JETP Lett., 24, 256 (1976); J. C. Moulder and A. F. Clark, Chem. Phys. Lett., 49, 471 (1977); R. Gauthier and P. Pinard, Phys. Stat. Sol. A, 38, 85 (1976); R. Gauthier and C. Guittard, ibid. 38, 477 (1976); R. Gauthier, M. Babout and C. Guittard, ibid. 48, 459 (1978); I. M. Beterov, V. P. Chebotaev, N. I. Yurshina and B. Ya. Yurshin, Sov. J. Quant. Electron., 8, 1310 (1978); T. Kawai and T. Sakata, Chem. Phys. Lett., 69, 33 (1980); T. J. Chuang, J. Chem. Phys., 72, 6303 (1980).
79. C. T. Lin and T. D. Z. Atvars, J. Chem. Phys., 68, 4233 (1978); J. T. Yates, Jr., J. J. Zinck, S. Sneed and W. H. Weinberg, J. Chem. Phys., 70, 2266 (1979).
80. T. F. Deutsch, D. J. Ehrlich and R. M. Osgood, Jr., Appl. Phys. Lett., 35, 175 (1979); D. J. Ehrlich, R. M. Osgood, Jr., and T. F. Deutsch, Appl. Phys. Lett., 36, 698 (1980); 36, 916 (1980); 38, 946 (1981); D. J. Ehrlich and R. M. Osgood, Jr., Chem. Phys. Lett., 79, 381 (1981); P. K. Boyer, G. A. Roche, W. H. Ritchie and G. J. Collins, Appl. Phys. Lett., 40, 716 (1982).
81. A. C. Beri and T. F. George, J. Chem. Phys., 78, 4288 (1983).
82. J. W. Gadzuk and H. Metiu, Phys. Rev. B, 22, 2603 (1980); H. Metiu and J. W. Gadzuk, J. Chem. Phys., 74, 2641 (1981); J. W. Gadzuk and H. Metiu, in Vibrations at Surfaces, R. Caudano, J. M. Giles and A. A. Lucas, eds., Plenum, New York (1982); see also Reference 27.
83. G. Herzberg, Molecular Spectra and Molecular Structure, Vol. I, 2nd ed., Van Nostrand, Princeton (1950).
84. W. E. Carlos and M. W. Cole, Phys. Rev. Lett., 43, 697 (1979). Surface Sci., 91, 339 (1980).

85. A. A. Maradudin, E. W. Montroll, G. H. Weiss and I. P. Ipatova, Theory of Lattice Dynamics in the Harmonic Approximation, Academic, New York (1971).
86. N. Cabrera, V. Celli, F. O. Goodman and R. Manson, Surface Sci., 19, 67 (1970); F. O. Goodman, ibid. 19, 93 (1970); F. O. Goodman and W.-K. Tan, J. Chem. Phys., 59, 1805 (1973).
87. N. Garcia, F. O. Goodman, V. Celli and N. R. Hill, Phys. Rev. B, 19, 1808 (1979).
88. K. F. Wojciechowski, Prog. Surface Sci., 1, 65 (1971); J. W. Gadzuk, Surface Sci., 43, 44 (1974); A. M. Brodskiy and M. I. Urbakh, Prog. Surface Sci., 8, 103 (1977); J. P. Muscat and D. M. Newns, ibid. 9, 1 (1978).
89. W. Magnus, Commun. Pure Appl. Math., VII, 649 (1954); P. Pechukas and J. C. Light, J. Chem. Phys., 44, 3897 (1966).
90. A. S. Davydov, Quantum Mechanics, 2nd ed., Pergamon, Oxford (1976).
91. C. B. Duke and G. E. Laramore, Phys. Rev. B, 2, 4765 (1970); G. E. Laramore and C. B. Duke, ibid. 2, 4783 (1970).
92. A. Messiah, Quantum Mechanics, Vol. I. Wiley, New York (1958), Chap. XII.
93. C. Kittel, Quantum Theory of Solids, Wiley, New York (1963).
94. L. Van Hove, Phys. Rev., 95, 249 (1954).
95. M. S. Slutsky and T. F. George, Chem. Phys. Lett., 57, 474 (1978).
96. D. Lucas and G. Ewing, Chem. Phys., 58, 385 (1981).
97. E. W. Montroll and K. E. Shuler, Adv. Chem. Phys., 1, 361 (1958).
98. W. C. Murphy and T. F. George, Surface Sci., 102, L46 (1981).
99. J. Lin and T. F. George, Surface Sci., 115, 569 (1982).
100. J. Lin and T. F. George, Phys. Rev. B, in press.
101. J. Lin, unpublished results.
102. S. Lundqvist, in Surface Science, Vol. 1, International Atomic Energy Agency, Vienna (1975), p. 331 ff.
103. W. C. Murphy and T. F. George, Surface Sci., 114, 189 (1982).
104. W. C. Murphy and T. F. George, J. Phys. Chem., 86, 4481 (1982).
105. D. P. Woodruff, M. M. Traum, H. H. Farrell, N. V. Smith, P. D. Johnson, D. A. King, R. I. Benbow and Z. Hurych, Phys. Rev. B, 21, 5642 (1980); R. Jaeger, J. Feldhaus, J. Haase, J. Stöhr, Z. Hussain, D. Menzel and D. Norman, Phys. Rev. Lett., 45, 1870 (1980).
106. M. L. Knotek and P. J. Feibelman, Phys. Rev. Lett., 40, 964 (1978).
107. C. R. Pidgeon, E. S. Wherrett, A. M. Johnston, J. Dempsey and A. Miller, Phys. Rev. Lett., 42, 1785 (1979); C. C. Lee and H. Y. Fan, Phys. Rev. B, 9, 3502 (1974).
108. See, e.g., J. M. Ziman, Principles of the Theory of Solids, Cambridge University, London, (1965).
109. See, e.g., V. Heine, in Solid State Physics, Vol. 24, Academic, New York (1970), p. 30.
110. See, e.g., J. Callaway, Quantum Theory of the Solid State, Academic, New York (1976).
111. C. Kittel, Introduction to Solid State Physics, 4th ed., Wiley, New York (1971).
112. J. Van Laer and J. Scheer, Philips Res. Rept., 17, 101 (1962).
113. D. M. Newns, Phys. Rev. B, 1, 3304 (1970); E. Gerlach, in Molecular Processes on Solid Surfaces, E. Drauglis, R. Gretz and R. Jaffee, eds., McGraw-Hill, New York (1969), p. 181 ff.
114. K. Mednick and L. Kleinman, Phys. Rev. B, 22, 5768 (1980); M. Posternak, H. Krakauer, A. J. Freeman and D. D. Koelling, Phys. Rev. B, 21, 5601 (1980).
115. W. C. Murphy, A. C. Beri, T. F. George and J. Lin, in Laser Diagnostics and Photochemical Processing for Semiconductor Devices, R. M. Osgood, Jr. and S. R. J. Brueck, eds., Elsevier, New York, in press.
116. N. F. Mott and H. Jones, The Theory of the Properties of Metals and Alloys, Dover, New York (1958), p. 220.
117. M. P. Das and J. Mahanty, Chem. Phys. Lett., 67, 142 (1979).
118. See, e.g., Ref. 83, Chapt. VII.

119. D. K. Bhattacharyya, J. Lin and T. F. George, Surface Sci., **116**, 423 (1982).
120. D. K. Bhattacharyya, K. S. Lam and T. F. George, J. Chem. Phys., **75**, 203 (1981).
121. W. H. Miller, Adv. Chem. Phys., **30**, 77 (1975).
122. J. M. Yuan and T. F. George, J. Chem. Phys., **68**, 3040 (1978).
123. K. S. Lam and T. F. George, in Semiclassical Methods in Molecular Scattering and Spectroscopy, M. S. Child, ed., Reidel, Dordrecht (1980), pp. 179-261.
124. J. Lin and T. F. George, Surface Sci., **107**, 417 (1981).
125. R. H. Fowler, Phys. Rev., **38**, 45 (1931).
126. J. Lin and T. F. George, J. Appl. Phys., **54**, 382 (1983).
127. H. S. Carslaw and J. C. Jaeger, Conduction of Heat in Solids, 2nd ed., Oxford University, London (1959).
128. J. F. Ready, Effects of High Power Laser Radiation, Academic, New York (1971).
129. R. K. Pathria, Statistical Mechanics, Pergamon, New York (1972).
130. L. Allen and J. H. Eberly, Optical Resonance and Two-Level Atoms, Wiley, New York (1975).
131. P. L. Knight and P. W. Milonni, Phys. Rep., **66**, 21 (1980).
132. J. Lin, X. Y. Huang and T. F. George, Solid State Commun., in press.
133. J. Lin, unpublished results.
134. R. R. Chance, A. Prock and R. Silbey, Adv. Chem. Phys., **38**, 1 (1978).
135. H. W. Lee and T. F. George, J. Chem. Phys., **70**, 3685 (1979).
136. H. W. Lee and T. F. George, Theoret. Chim. Acta (Berl.), **53**, 193 (1979).
137. R. B. Gerber, A. T. Yinnon and J. N. Murrell, Chem. Phys., **31**, 1 (1978).
138. A. T. Yinnon, S. Bosanac, R. B. Gerber and J. N. Murrell, Chem. Phys. Lett., **58**, 364 (1978).
139. H. W. Lee and T. F. George, J. Chem. Phys., **70**, 4220 (1979).
140. W. H. Weinberg, Adv. Colloid Interface Sci., **4**, 301 (1975).
141. L. B. Thomas, in Rarefied Gas Dynamics, Vol. I, C. L. Brundin, ed., Academic, New York (1967), p. 155 ff.
142. H. Conrad, G. Ertl, J. Küppers, S.-W. Wang, K. Gérard and H. Haberland, Phys. Rev. Lett., **42**, 1082 (1979).
143. S.-W. Wang, J. Vac. Sci. Technol., **20**, 600 (1982).
144. J. C. Bellum, K. S. Lam and T. F. George, J. Chem. Phys., **69**, 1781 (1978); J. C. Bellum and T. F. George, J. Chem. Phys., **70**, 5059 (1979).
145. K. S. Lam and T. F. George, Z. Phys. B, submitted.
146. N. H. Tolk, J. C. Tully, W. Heiland and C. W. White, eds., Inelastic Ion-Surface Collisions, Academic, New York (1977).
147. J. C. Tully, Phys. Rev. B, **16**, 4324 (1977).
148. H. D. Hagstrum, Phys. Rev., **122**, 83 (1961).
149. H. W. Lee, W. C. Murphy and T. F. George, Chem. Phys. Lett., **93**, 221 (1982).
150. J. Lin and T. F. George, Chem. Phys. Lett., **66**, 5 (1979).
151. F. C. Tompkins, Chemisorption of Gases on Metals, Academic, New York (1978).
152. J. Lin, unpublished results.
153. J. Lin and T. F. George, unpublished results.
154. U. Fano, Phys. Rev., **124**, 1866 (1961).
155. A. Otto, Z. Physik, **216**, 398 (1968).
156. G. Borstel and H. F. Falge, Appl. Phys., **16**, 211 (1978).
157. K. Bhasin, D. Bryan, R. W. Alexander and R. J. Bell, J. Chem. Phys., **64**, 5019 (1976).
158. X. Y. Huang, J. Lin and T. F. George, Z. Phys. B, **50**, 181 (1983).
159. S. D. Ferris, H. J. Leamy and J. M. Poate, eds., Laser-Solid Interactions and Laser Processing, American Institute of Physics, New York (1979).
160. C. W. White and P. S. Peercy, eds., Laser and Electron Beam Processing of Materials, Academic, New York (1980).
161. J. F. Gibbons, L. D. Hess and T. W. Sigmon, eds., Laser and Electron Beam Solid Interactions and Materials Processing, Elsevier, New York (1981).

162. J. C. Wang, R. F. Wood and P. P. Pronko, Appl. Phys. Lett., 33, 455 (1978).
163. J. A. Van Vechten, R. Tsu and F. W. Saris, Phys. Lett., 74A, 422 (1979);
74A, 417 (1979).
164. M. Sparks and E. Loh, J. Opt. Soc. Amer., 69, 859 (1979).
165. C. M. Tang and J. Lin, unpublished results.

TECHNICAL REPORT DISTRIBUTION LIST, 056

	<u>No.</u> <u>Copies</u>		<u>No.</u> <u>Copies</u>
Dr. Robert Gomer Department of Chemistry James Franck Institute 5640 Ellis Avenue Chicago, Illinois 60637	1	Dr. K. G. Spears Chemistry Department Northwestern University Evanston, Illinois 60201	1
Dr. R. G. Wallis Department of Physics University of California, Irvine Irvine, California 92664	1	Dr. R. W. Plummer University of Pennsylvania Department of Physics Philadelphia, Pennsylvania 19104	1
Dr. D. Ramaker Chemistry Department George Washington University Washington, D.C. 20052	1	Dr. E. Yeager Department of Chemistry Case Western Reserve University Cleveland, Ohio 41106	1
Dr. P. Hansma Physics Department University of California, Santa Barbara Santa Barbara, California 93106	1	Professor D. Hercules University of Pittsburgh Chemistry Department Pittsburgh, Pennsylvania 15260	1
Dr. J. C. Hemminger Chemistry Department University of California, Irvine Irvine, California 92717	1	Professor N. Winograd The Pennsylvania State University Department of Chemistry University Park, Pennsylvania 16802	1
Dr. Martin Fleischmann Department of Chemistry Southampton University Southampton SO9 5NH Hampshire, England	1	Professor T. F. George The University of Rochester Chemistry Department Rochester, New York 14627	1
Dr. G. Rubloff IBM Thomas J. Watson Research Center P. O. Box 218 Yorktown Heights, New York 10598	1	Professor Dudley R. Herschbach Harvard College Office for Research Contracts 1350 Massachusetts Avenue Cambridge, Massachusetts 02138	1
Dr. J. A. Gardner Department of Physics Oregon State University Corvallis, Oregon 97331	1	Professor Horia Metiu University of California, Santa Barbara Chemistry Department Santa Barbara, California 93106	1
Dr. G. D. Stein Mechanical Engineering Department Northwestern University Evanston, Illinois 60201	1	Professor A. Steckl Rensselaer Polytechnic Institute Department of Electrical and Systems Engineering Integrated Circuits Laboratories Troy, New York 12181	1

TECHNICAL REPORT DISTRIBUTION LIST, 056

	<u>No.</u> <u>Copies</u>	<u>No.</u> <u>Copies</u>
Dr. John T. Yates Department of Chemistry University of Pittsburgh Pittsburgh, Pennsylvania 15260	1	
Professor G. H. Morrison Department of Chemistry Cornell University Ithaca, New York 14853	1	
Captain Lee Myers AFOSR/NC Bolling AFB Washington, D.C. 20332	1	
Dr. David Squire Army Research Office P. O. Box 12211 Research Triangle Park, NC 27709	1	
Professor Ronald Hoffman Department of Chemistry Cornell University Ithaca, New York 14853	1	

TECHNICAL REPORT DISTRIBUTION LIST, GEN

	<u>No. Copies</u>		<u>No. Copies</u>
Office of Naval Research Attn: Code 413 800 North Quincy Street Arlington, Virginia 22217	2	Naval Ocean Systems Center Attn: Mr. Joe McCartney San Diego, California 92152	1
ONR Pasadena Detachment Attn: Dr. R. J. Marcus 1030 East Green Street Pasadena, California 91106	1	Naval Weapons Center Attn: Dr. A. B. Amster, Chemistry Division China Lake, California 93555	1
Commander, Naval Air Systems Command Attn: Code 310C (H. Rosenwasser) Department of the Navy Washington, D.C. 20360	1	Naval Civil Engineering Laboratory Attn: Dr. R. W. Drisko Port Hueneme, California 93401	1
Defense Technical Information Center Building 5, Cameron Station Alexandria, Virginia 22314	12	Dean William Tolles Naval Postgraduate School Monterey, California 93940	1
Dr. Fred Saalfeld Chemistry Division, Code 6100 Naval Research Laboratory Washington, D.C. 20375	1	Scientific Advisor Commandant of the Marine Corps (Code RD-1) Washington, D.C. 20380	1
U.S. Army Research Office Attn: CRD-AA-IP P. O. Box 12211 Research Triangle Park, N.C. 27709	1	Naval Ship Research and Development Center Attn: Dr. G. Bosmajian, Applied Chemistry Division Annapolis, Maryland 21401	1
Mr. Vincent Schaper DTNSRDC Code 2803 Annapolis, Maryland 21402	1	Mr. John Boyle Materials Branch Naval Ship Engineering Center Philadelphia, Pennsylvania 19112	1
Naval Ocean Systems Center Attn: Dr. S. Yamamoto Marine Sciences Division San Diego, California 91232	1	Mr. A. M. Anzalone Administrative Librarian PLASTEC/ARRADCOM Bldg 3401 Dover, New Jersey 07801	1
Dr. David L. Nelson Chemistry Program Office of Naval Research 800 North Quincy Street Arlington, Virginia 22217	1		

TECHNICAL REPORT DISTRIBUTION LIST, 056

	<u>No.</u> <u>Copies</u>		<u>No.</u> <u>Copies</u>
Dr. G. A. Somorjai Department of Chemistry University of California Berkeley, California 94720	1	Dr. W. Kohn Department of Physics University of California (San Diego) La Jolla, California 92037	1
Dr. J. Murday Naval Research Laboratory Surface Chemistry Division (6170) 455 Overlook Avenue, S.W. Washington, D.C. 20375	1	Dr. R. L. Park Director, Center of Materials Research University of Maryland College Park, Maryland 20742	1
Dr. J. B. Hudson Materials Division Rensselaer Polytechnic Institute Troy, New York 12181	1	Dr. W. T. Peria Electrical Engineering Department University of Minnesota Minneapolis, Minnesota 55455	1
Dr. Theodore E. Madey Surface Chemistry Section Department of Commerce National Bureau of Standards Washington, D.C. 20234	1	Dr. Chia-wei Woo Department of Physics Northwestern University Evanston, Illinois 60201	1
Dr. J. M. White Department of Chemistry University of Texas Austin, Texas 78712	1	Dr. Robert M. Hexter Department of Chemistry University of Minnesota Minneapolis, Minnesota 55455	1
Dr. Keith H. Johnson Department of Metallurgy and Materials Science Massachusetts Institute of Technology Cambridge, Massachusetts 02139	1	Dr. R. P. Van Duyne Chemistry Department Northwestern University Evanston, Illinois 60201	1
Dr. J. E. Demuth IBM Corporation Thomas J. Watson Research Center P. O. Box 218 Yorktown Heights, New York 10598	1	Dr. S. Sibener Department of Chemistry James Franck Institute 5640 Ellis Avenue Chicago, Illinois 60637	1
Dr. C. P. Flynn Department of Physics University of Illinois Urbana, Illinois 61801	1	Dr. M. G. Lagally Department of Metallurgical and Mining Engineering University of Wisconsin Madison, Wisconsin 53706	1

END

DATE
FILMED

6 - 83

DTIC